

FACILITY FORM 602

N 66 - 13641

(ACCESSION NUMBER)

96

(PAGES)

CP 68479

(NASA CR OR TMX OR AD NUMBER)

(THRU)

1

(CODE)

03

(CATEGORY)

GPO PRICE \$ _____

CFSTI PRICE(S) \$ _____

Hard copy (HC) 3.00

Microfiche (MF) .75

ff 653 July 65

FINAL REPORT

Design and Evaluation Study of Deployable Solar Array for

Spinning Satellites

HUGHES

NASA Contract NAS 5-3989

HUGHES AIRCRAFT COMPANY
SPACE SYSTEMS DIVISION

October 1964

FINAL REPORT

•

*Design
and
Evaluation Study
of
Deployable
Solar Array for*

Spinning Satellites

NASA Contract NAS 5-3989

HUGHES

HUGHES AIRCRAFT COMPANY
SPACE SYSTEMS DIVISION

SSD 4473R

FOREWORD

This report was prepared by Hughes Aircraft Company, Space Systems Division under NASA Contract No. NAS 5-3989. The work was administered under the direction of Goddard Space Flight Center with Joseph G. Haynos as technical director.

Key personnel contributing to this project include: K. A. Ray, Project Manager, L. B. Keller, Head,Plastics Section, and G.H. Syrov, Group Head, Mechanical Design.

ABSTRACT

13641

Solar cell array deployment systems are studied for application to spinning satellites. Systems which have the potential of more efficient packaging and deployment and offer increased performance in terms of specific power over a range of panel areas are studied in detail. The study includes the mechanical design, substrate properties, the evaluation and incorporation of chemical systems for space rigidization of flexible deployment systems, and cell assembly design and tests. The results of the study are presented on a chart listing the performance of seven deployment systems, four of which utilize flexible substrates and three utilize rigid substrates. The deployable systems based on flexible substrates and chemical rigidization offer the highest performance of 9.2 watts per pound and 383 watts per cubic foot of stowed volume.

Author

CONTENTS

	Page
1. INTRODUCTION	1-1
2. MECHANICAL DESIGN	
Study Approach	2-1
Governing Parameters and Assumptions	2-1
Selection of Candidate Systems	2-3
Description of Systems Studied	2-7
Structural and Vibrational Evaluation	2-30
Weights	2-37
Reliability Considerations	2-37
3. CHEMICAL RIGIDIZATION SYSTEM AND MATERIALS	
Chemical Rigidization System	3-1
Physical Properties of Substrate Materials	3-19
Thermal Radiative Properties	3-23
4. WIRE INTERCONNECTION TESTS	
Mechanical Analysis	4-1
Bending Tests	4-3
5. COMPARISON OF POLAR AND EQUATORIAL ORBITS	
Evaluation of Semi-Oriented (1 Degree of Freedom) Arrays	5-7
6. SYSTEM COMPARISON	
Comparison Chart	6-1
Conclusions	6-3
7. RECOMMENDATIONS	
System 3	7-1
APPENDICES	
A. Structural Analysis	A-1
B. Solar Array Thermal Analysis	B-1
C. Calculation of Stowed Diameter of Any Number of Flexible Panels Rolled Around a Cylinder	C-1

ILLUSTRATIONS

	Page
2-1 Preliminary Concepts for Deployable Solar Array Study	2-5
2-2 System 1 - Four Flexible Panels - Cruciform Configuration	2-9
2-3 System 3 - Three Flexible Panels - Drum Stowed	2-11
2-4 Retaining Hoop - Flexible Solar Panels Systems	2-17
2-5 System Comparison Chart	2-19
2-6 System 2 - Three Flexible Panels - Body Stowed	2-21
2-7 System 4 - Tri-Nodal Configuration	2-25
2-8 System 5 - Rigid Panel - Multiple Fold Configuration	2-27
2-9 System 6 - Expanding Rigid Panels	2-31
2-10 System 7 - Rigid Telescoping Panels	2-33
2-11 Power-to-Weight Ratio versus Length of Panel for Two Different Width Panels	2-36
3-1 Cross Section of Rigidized Tube After Deployment	3-2
3-2 Tensile Test Specimens Made from Braided Fiberglass Sleeving Space-Rigidized with Polyurethane	3-7
3-3 Elongation of Polyurethane Test Tube During Tensile Test	3-7
3-4 Failure of Polyurethane Tube During Compression Test	3-7
3-5 Flexural Specimen of Rigidized Tubing Fitted for Test as Cantilever Beam	3-8
3-6 Setup for Flexural Testing of Short Tubes as Cantilever Beams Prior to Starting Test	3-8
3-7 Load Deflection Curve for 1-Inch Diameter Braided Tube Impregnated with Gelatin	3-10
3-8 Vacuum Test Setup for Determining Effect of Rigidization Component Outgassing on Solar Cell Efficiency	3-14
3-9 Closeup of Vacuum Test Chamber	3-14
3-10 Tensile Shear Test of TFE Glass Cloth to Glass Specimen	3-25
3-11 Tensile Shear Test of H Film (FEP Coated) to Glass Specimen	3-25
3-12 Peel Test of TFE Glass Cloth to Glass Specimen	3-26
3-13 Peel Test of H Film (FEP Coated) to Glass Specimen	3-26
4-1 Cell Assembly - Copper Wire Reversed Loops	4-2
4-2 Cell Assembly - Coarse Mesh	4-2
4-3 Cell Assembly - Copper Foil	4-2
4-4 Cell Assembly Binding Test Apparatus	4-4
4-5 Cell Assembly - Copper Wire	4-4
4-6 Cell Assembly - Fine Mesh	4-4

5-1	Satellite Attitude	5-3
5-2	Satellite Geometry	5-3
5-3	Earth Orbit Geometry	5-3
5-4	Satellite Orbit Geometry	5-4
5-5	Satellite Eclipse Geometry	5-4
5-6	$\cos \beta_e$ versus Time after Injection	5-6
5-7	Average $\cos \beta_p$ Initial Right Ascension of Ascending Node	5-6
5-8	$\cos \beta_p$ Time After Injection for $\Omega_0 = 10$ Degrees	5-6
5-9	Spinning Satellite	5-9
5-10	Deployable Solar Cell Array	5-9
5-11	Deployable Solar Cell Array Mounted on Movable Supports	5-9
5-12	Aavg versus γ for Values of β	5-11
5-13	γ_{opt} versus β	5-11
5-14	Aavg versus β for $\gamma = 0$	5-12
5-15	Aavg versus β for $\gamma = \gamma_{opt}$	5-13

TABLES

	<u>Page</u>
2-1 Description of Preliminary Concepts for Deployable Solar Array Study Shown on Figure 2-1	2-4
3-1 Comparison of Properties of Space-Rigidized Systems	3-5
3-2 Flexural Properties of Impregnated Braided Tubes	3-11
3-3 Tensile and Compressive Properties of Impregnated Braided Tubes	3-12
3-4 Flexural Test of 6-Foot Polyester Tubes	3-13
3-5 Test Results	3-16
3-6 Tensile Strength (ASTM D 882) of Flexible Substrate Materials	3-21
3-7 Physical Properties of Types of Honeycomb Suitable for Substrate	3-22
3-8 Physical Properties of Low Density Honeycomb Sandwiches Suitable for Substrate	3-22
3-9 Physical Properties of Flexible Substrate Materials Bonded to Glass	3-26
4-1 Wire Interconnection Evaluation	4-5
5-1 Reduced Data	5-8
5-2 Aavg at $\gamma = 8$ Degrees for Various β	5-14
5-3 Aavg at $\gamma = 1$ Degree for Various β	5-14
5-4 Polar Orbit	5-15
6-1 System Rating Method	6-4
B-1 Temperatures for Systems 1 through 7	B-3

1. INTRODUCTION

The need for additional power as larger and more advanced spacecraft are developed cannot always be met by a simple increase in the solar cell panel area based on conventional solar panel design. The volume between the spacecraft and launch vehicle shroud as well as the basic size of the spacecraft are fundamental constraints on increasing panel area. The complexity and weight penalty are undesirable results of solar panels that are hinged and folded.

On 1 July 1964 the Space Systems Division of Hughes Aircraft Company under NASA, GSFC Contract NAS 5-3989, initiated a 3-month study program to investigate deployable solar array designs for spinning satellites. The goals of the program were to conduct material and design studies leading to devices which would:

- 1) Utilize to the maximum the volume between spacecraft and shroud
- 2) Provide a means of deployment and rigidization in space that would be compatible with spin stabilization of the spacecraft
- 3) Be compatible with present day solar cell mounting techniques
- 4) Provide large area lightweight solar arrays

The study covered deployment systems that were mechanical, pneumatic, chemical, and a combination thereof; solar cell interconnection design; substrates; and a comparison of polar and equatorial orbits with nonoriented and 1-degree-of-freedom arrays.

This report presents the results of the deployment system selection process described in the mechanical design section, data and test results of three chemical systems for space rigidization, substrate properties and wire connection test results, potential advantages of 1-degree-of-freedom orientation in a polar orbit, and the overall evaluation of seven deployment systems on a comparison chart.

2. MECHANICAL DESIGN

STUDY APPROACH

At the start of the program, outline drawings and descriptions of 14 different systems were prepared. Some of the systems did not conform to the suggested stowed configuration of 13 inches wide by 25 inches long by 4 inches deep, but merited further consideration. It was decided to package the solar panels in the optimum manner for each individual system. Of the fourteen systems shown on Figure 2-1, six were selected for further study. An additional system was subsequently added. Deployment systems were eliminated by considering the relative complexity of the deployment mechanism, the difficulty in achieving and maintaining the required rigidity, and the amount of satellite surface masked by the deployed array. Layout drawings were prepared for the seven systems. In order to make a valid comparison of the seven candidate systems, an effort was made to keep the deployed area approximately the same for each system. Two of the systems (4 and 6) are limited in size due to their geometry and therefore their deployed area is smaller. Of the seven systems, four (1, 2, 3, and 4) have flexible substrates and three (5, 6, and 7) are of conventional aluminum honeycomb type construction. Due to their advantage in weight, stowed volume, and growth potential, the four flexible systems were selected for detailed study.

GOVERNING PARAMETERS AND ASSUMPTIONS

The following are some basic parameters and assumptions that formulated the basis of the design study:

- 1) The satellite shall be cylindrical, 36 inches in diameter and 24 inches long and in an equatorial earth orbit at 600 n.mi.
- 2) The deployment mechanism shall be capable of maintaining a rigid configuration in the earth's gravitational field.
- 3) The array shall be capable of positive deployment and of maintaining dimensional integrity while attached to the body of a spacecraft spinning at an initial rate (before deployment) of 80 to 160 revolutions per minute and a final rate (after deployment) of 20 to 40 revolutions per minute.

- 4) The deployment mechanism, wiring interconnections, and solar cells with attached 6-mil glass slips shall be included in the total weight.
- 5) The deployment mechanism shall be capable of reliable operation in the hard vacuum of space.
- 6) The packaged array shall be capable of withstanding shock, vibration, and accelerations such as might be experienced by arrays during launch.

A typical vibration schedule and input accelerations at the spacecraft interface will be as follows:

a) Sinusoidal tests:

<u>Frequency, cps</u>	<u>Acceleration, g</u>	
	<u>Thrust Axis, z</u>	<u>Transverse Axis, x and y</u>
5 to 50	2.3	0.9
50 to 500	10.7	2.1
500 to 2000	21.0	4.2
2000 to 3000	54.0	17.0
3000 to 5000	21.0	17.0

Constant sweep rate of 2 octaves per minute.

b) Random test (each axis):

<u>Frequency Range, cps</u>	<u>PSD, g²/cps</u>	<u>Amplitude, g-rms</u>	<u>Duration, minutes</u>
20 to 2000	0.07	11.5	4.0

- c) The above vibration levels are typical inputs to the spacecraft and are not necessarily the levels of acceleration that the solar cell assemblies will experience while mounted to the spacecraft. The actual level of acceleration is a function of the spacecraft structural response as well as input acceleration. Past experience indicates that amplifications of approximately 4 to 1 are possible within a frequency range of 50 to 200 cps.

- 7) All materials shall be nonmagnetic.

- 8) Materials shall be capable of withstanding humidity (up to 95 per-cent RH at 30° C for 24 hours).
- 9) The packaged arrays shall be capable of long-term (100 days) storage at temperatures which may vary from -20° to 60° C.
- 10) Materials shall be capable of withstanding radiations (including both ultraviolet and hard particles) experienced in space.
- 11) Materials shall be capable of withstanding hard vacuum conditions for extended periods (1 to 5 years) without excessive deterioration.
- 12) The extended array shall be capable of withstanding thermal cycling test at 10^{-7} Torr pressure from -70° to 70° C for 1000 cycles at a nominal rate of 2 hours per cycle.
- 13) Structure shall be capable of meeting the above conditions without degrading the performance of the attached cells.

SELECTION OF CANDIDATE SYSTEMS

In order to consider all possible candidates for a deployable solar array system, a large number of configurations was postulated and analyzed in the early phases of this study. From these a promising group was selected for a more detailed study. Figure 2-1 and Table 2-1 describe the fourteen different concepts that were considered. From this the seven systems selected for study in more depth are as follows:

<u>System</u>	
1	Drum stowed concept — derived from concept No. 9
2	Three flexible panels body stowed — concept No. 11
3	Three panel common drum stowed — derived from concept No. 9
4	Tri-nodal configuration — variation of concept No. 6
5	Rigid multifold panels — concept No. 13
6	Rigid curved foldout panels (an added concept to Figure 2-1)
7	Rigid telescoping panels — concept No. 12

The first four systems were studied in more detail since they showed the most favorable power-to-weight ratio, a favorable stowed volume configuration, good reliability, and favorable growth potential.

TABLE 2-1. DESCRIPTION OF PRELIMINARY CONCEPTS FOR DEPLOYABLE SOLAR ARRAY STUDY SHOWN ON FIGURE 2-1

Concept Number	Description	Comment
1	Cylindrical solar panels that telescope from satellite body	Adverse effect on moment of inertia
2	Folded flexible solar panels	Difficult to deploy
3	Solar panels that unfold to form larger cylinder	Inhibits installation of instrumentation on cylindrical surface of satellite
4	Same as concept 3 except smaller segmented panels	Same as concept 3
5	Flexible unrolling solar panels	Same as concept 3
6	Folded flexible solar panels	Modified and chosen for study; becomes system 4
7	Solar panels that fold from cylindrical surface of satellite then rotate into position	Limited to polar orbit and complex deployment
8	Solar panels that open similar to petals of a flower	Same as concept 7
9	Drum stowed flexible panels	Chosen for study; becomes system 3; a variation of this becomes system 1
10	Triangular solar panels that are folded closed and wrapped around the satellite when stowed	Requires change of angle between panels during orbit
11	Flexible solar panels that are wrapped around the satellite; deployed by pressurizing and rigidizing fiberglass tubes	Chosen for study; becomes system 2
12	Rigid telescoping solar panels	Chosen for study; becomes system 7
13	Foldout rigid solar panels; mechanical linked support beams	Chosen for study; becomes system 5
14	Foldout rigid solar panels; chemically rigid support beams	Variation of concept 13

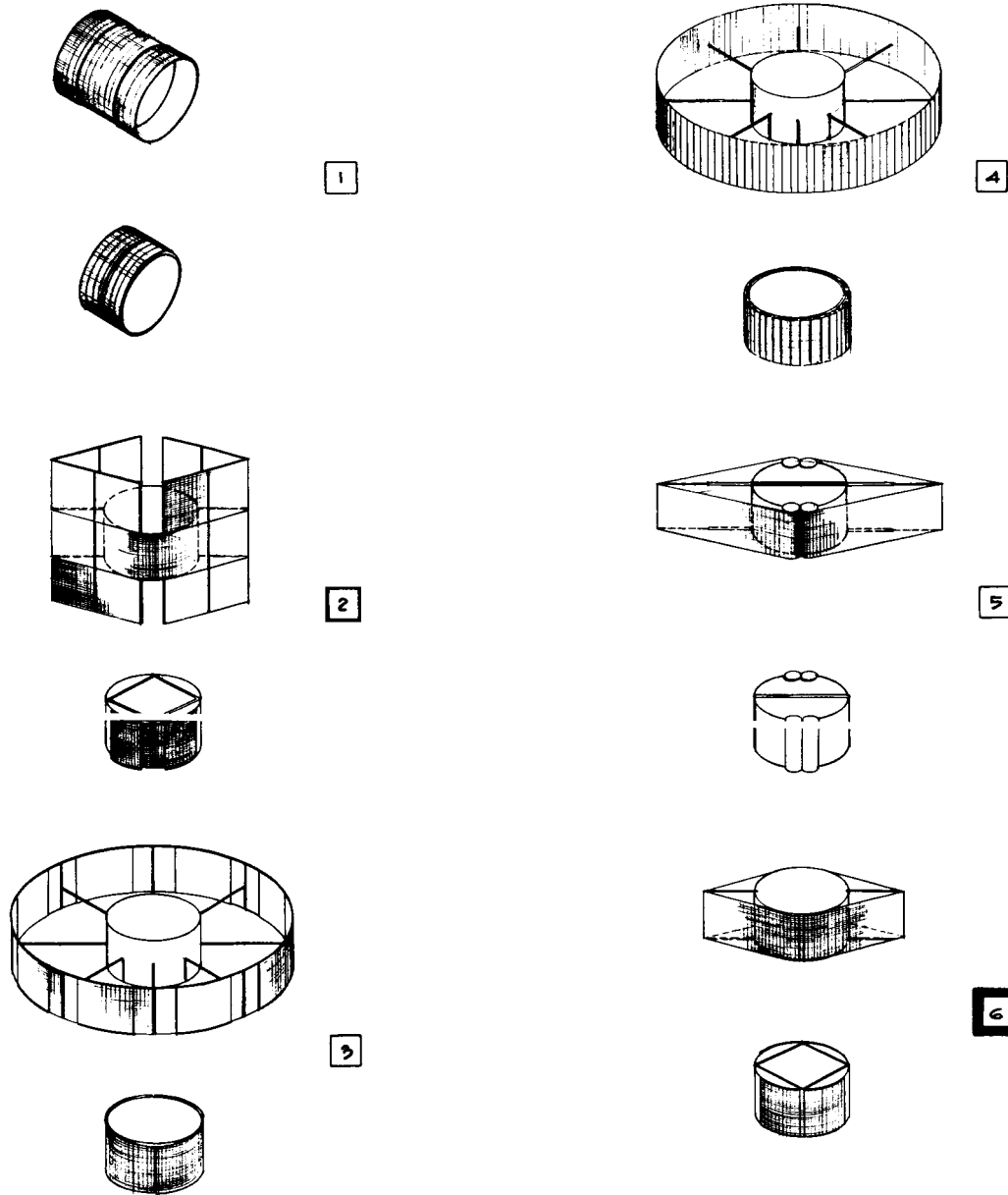
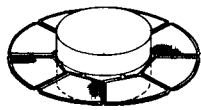
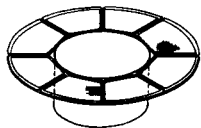
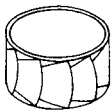


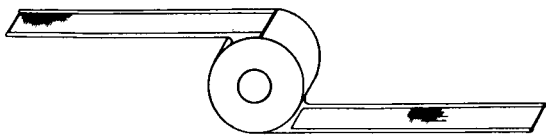
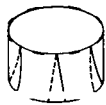
Figure 2-1. Preliminary Concepts for Deployable Solar Array Study



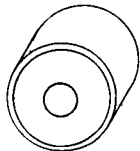
7



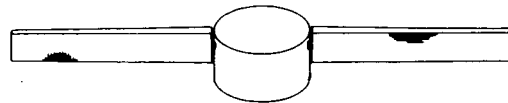
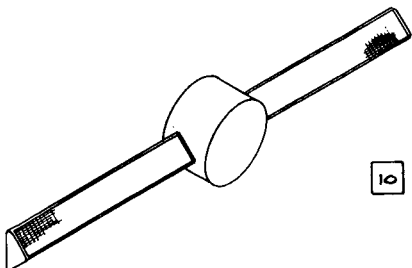
8



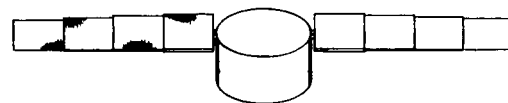
9



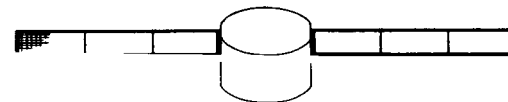
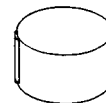
10



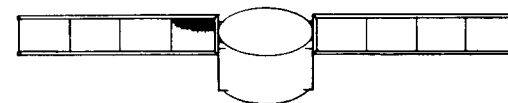
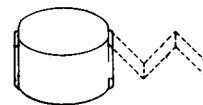
11



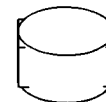
12



13



14



DESCRIPTION OF SYSTEMS STUDIED

System 1 - Four-Panel Cruciform Configuration

This design consists of four panels, 78 by 22 inches, arranged as shown in Figure 2-2. The substrate material is 0.0012-inch thick teflon impregnated fiberglass with solar cells attached to both sides of the substrate on an area measuring 58 by 18 inches. The solar panel, when deployed, is supported with chemically rigidized type E fiberglass tubes of 1-inch diameter and 0.015-inch wall attached to the two edges of the substrate. These panels, when in the stowed condition, are wrapped around the two 6-inch diameter drums located on the spin axis of the spacecraft - i.e., one drum at each end. A typical drum design is shown in Figure 2-3c. When deployed, the two panels on each drum are 180 degrees apart, with the panels on one end 90 degrees to those on the other. This design exhibits minimum power loss due to panel shadowing.

The panels are held in the stowed position by the retaining hoop shown in Figure 2-4. The hoop was designed to exert 1.0 psi pressure on the rolled-up solar panels. A pressure of 0.61 psi has been determined to be adequate to prevent relative motion between the panel layers during the shock and vibration loads that a typical spacecraft will receive during launch (see page 2-35). The retaining hoop consists of a 5/16-inch diameter aluminum alloy tube attached to one end of a sheet of 0.0012-inch thick teflon impregnated fiberglass. The fiberglass sheet is wrapped once around the solar panels and the ends of the sheet wrapped on the 5/16-inch diameter tube as shown in section B-B of Figure 2-4.

The hoop is then tightened by turning the ratchet assembly that is attached to the top of the 5/16-inch diameter tube. The ratchet assembly is turned against a stop attached to the storage drum. After torqueing the ratchet assembly to the required value, the ratchet assembly is safety-wired to the stop through a guillotine squib.

Upon a signal the guillotine squib severs the safety wire and releases the ratchet assembly, thus allowing the leaf spring, shown in the top view of Figure 2-4, to exert a torque and unspin the 5/16-inch diameter tube. This motion releases the retaining hoop permitting it to be thrown off by centrifugal force. It is possible to use a means not dependent on centrifugal force to assist deployment. Leaf springs can be built into the fiberglass hoop so that upon release the retaining hoop will straighten and fly away from the spacecraft.

The solar panel is similar to the panel shown in Figure 2-3b. The design of the panel is identical except for the size of the panel, which is 78 by 22 inches, instead of 88 by 24 inches. The storage drum is made of a plastic fiberglass reinforced shell with rigid polyurethane foam-filled very similar to that shown on Figure 2-3c except that the panel attachments are 180 degrees to each other. A 0.150-inch thick flexible polyurethane foam pad is used between the layers of stowed solar cell substrate as shown in Figure 2-2.

After jettisoning the retaining hoop, the panels are deployed by pressurizing the resin-impregnated fiberglass tubes shown at the top and bottom of the solar panels. After the panels have been deployed, the tubes are chemically rigidized by ultraviolet activation of polyester resin and support the solar panels in the correct position. The resin impregnated fiberglass tube rigidization is described in detail in Section 3 of this report.

The weight of this system is 22.6 pounds with detailed weights and materials shown in Figure 2-2. The specific power output would be about 8.0 watts per pound. More characteristics such as the projected area of solar array panel, power output, etc., are shown on the system comparison chart, Figure 2-5.

System 2 - Three Flexible Panels Body Stowed

This design has three solar panels, 75 inches long by 24 inches wide, mounted 120 degrees apart and attached directly to the cylindrical surface of the spacecraft as shown in Figure 2-6a and 2-6b. The substrate material is 0.0012-inch thick teflon impregnated fiberglass. Solar cells are mounted on both sides of this substrate on an area measuring 69.55 inches long by 20.18 inches wide. The solar panels are extended and supported with chemically rigidized fiberglass tubing (as in system 1) which is attached to the two edges of the substrate. A 1/4-inch diameter aluminum spreader bar tube is attached to the fiberglass tubes at the end away from the spacecraft forming essentially a picture frame structure.

When stowed, the solar panels are wrapped around the 36-inch diameter body of the spacecraft. At this time, the support tubes will be flexible and in a flattened configuration. Thin sheets (0.150-inch thick) of polyurethane foam between the panels will cushion the solar cells. These sheets will be jettisoned when the solar panels are deployed. The solar panels will be held in place with a retaining hoop utilizing a release mechanism similar to the one shown in Figure 2-4. This retaining hoop, made of the same material as the panel substrate, holds the solar panel in the stowed position and exerts a pressure of about 1 psi on the solar panels.

The first step in deployment of the solar panels will be to jettison the retaining hoop. This is accomplished by the sequence described previously. The deployment is shown in Figure 2-6a.

The solar panels are erected by pressurizing the support tubes, and chemically rigidizing them, as in system 1, to complete deployment of the solar panels. The mechanics of the chemical rigidization process and material are described in more detail in Section 3 of this report. The total weight of the system is about 20.0 pounds. The weight breakdown is shown in Figure 2-6a. This system has the highest specific power output (9.2 watts per pound) and the highest volumetric efficiency (383 watts per cubic foot). Additional pertinent data such as the projected area of the solar array panel power output, etc., are shown on the system comparison chart, Figure 2-5.

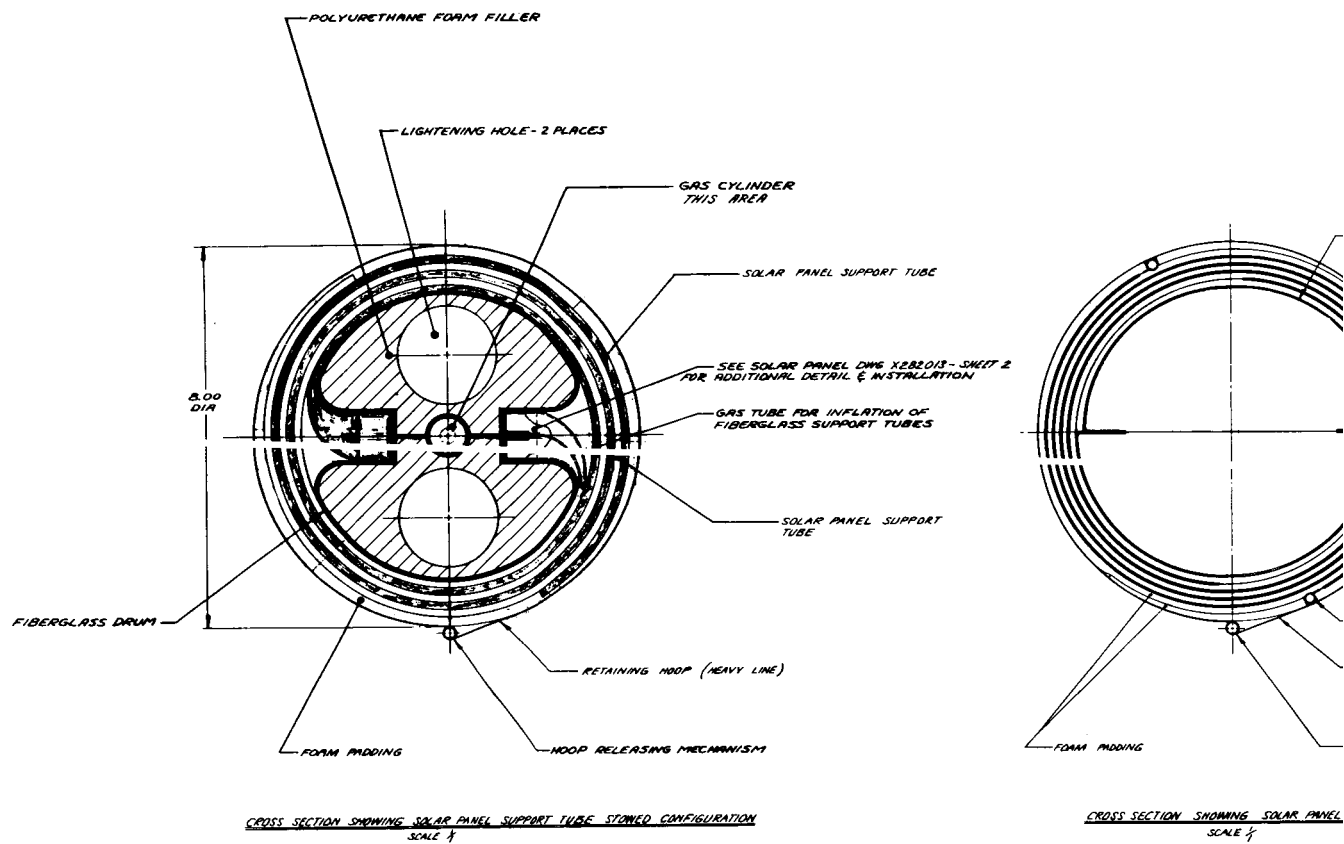
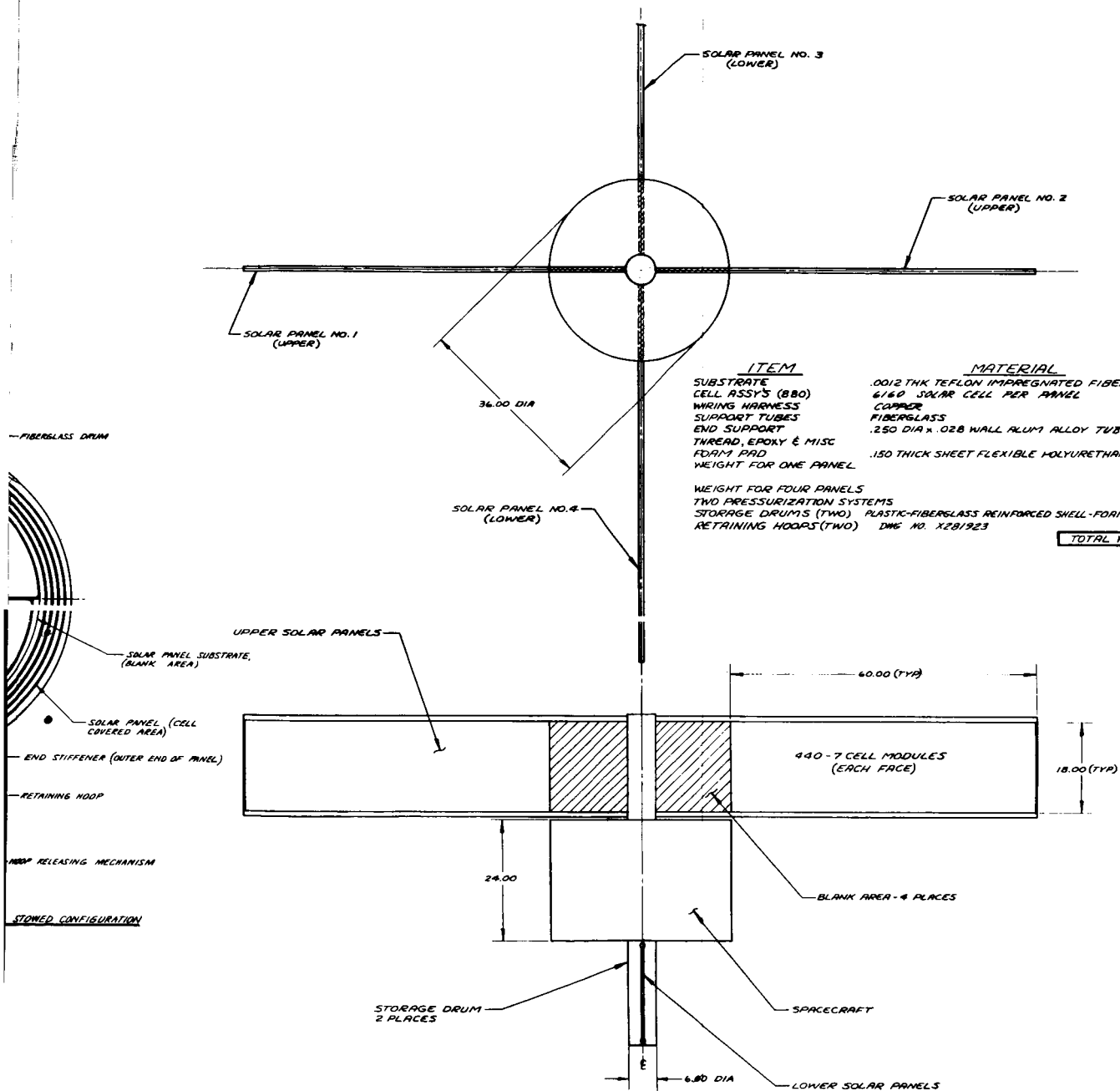


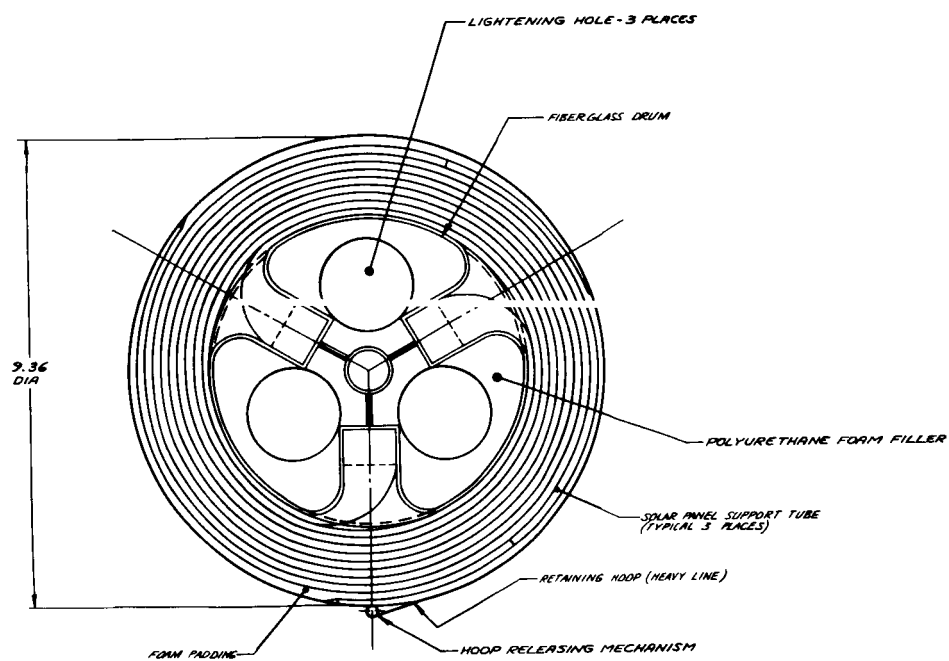
Figure 2-2. System 1 - Four Flexible Panels - Cruciform Configuration

2

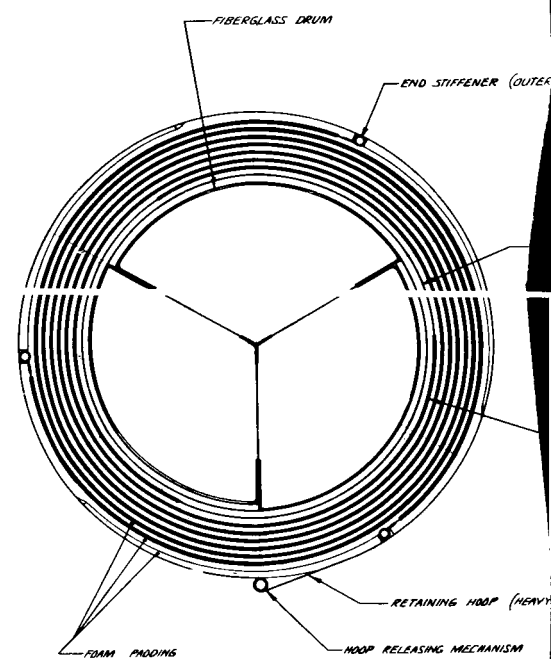


ITEM	MATERIAL	WT. LBS.
SUBSTRATE	.0012 THK TEFLON IMPREGNATED FIBERGLASS	.044
CELL ASSYS (880)	6160 SOLAR CELL PER PANEL	3.550
WIRING HARNESS	COPPER	.197
SUPPORT TUBES	FIBERGLASS	.780
END SUPPORT	.250 DIA X .028 WALL ALUM ALLOY TUBE	.045
THREAD, EPOXY & MISC		.010
FOAM PAD	.150 THICK SHEET FLEXIBLE POLYURETHANE FOAM	.360
WEIGHT FOR ONE PANEL		4.986
WEIGHT FOR FOUR PANELS		19.944
TWO PRESSURIZATION SYSTEMS		.300
STORAGE DRUMS (TWO)	PLASTIC-FIBERGLASS REINFORCED SHELL-FORM FILLER	2.000
RETAINING HOOPS (TWO)	DWG NO. X281923	.358
TOTAL WEIGHT		22.602

UNLESS OTHERWISE SPECIFIED DIMENSIONS ARE IN INCHES TOLERANCES ON		DATE OF JOURN	DATE	APPROVED	APPROVED
DECIMALS	FRACTIONS	DECIMALS	FRACTIONS	DATE	DATE
.001	.001	.001	.001	1/1/52	1/1/52
.010	.010	.010	.010	1/1/52	1/1/52
.031	.031	.031	.031	1/1/52	1/1/52
.062	.062	.062	.062	1/1/52	1/1/52
.125	.125	.125	.125	1/1/52	1/1/52
.250	.250	.250	.250	1/1/52	1/1/52
.500	.500	.500	.500	1/1/52	1/1/52
1.000	1.000	1.000	1.000	1/1/52	1/1/52
2.000	2.000	2.000	2.000	1/1/52	1/1/52
3.000	3.000	3.000	3.000	1/1/52	1/1/52
4.000	4.000	4.000	4.000	1/1/52	1/1/52
5.000	5.000	5.000	5.000	1/1/52	1/1/52
6.000	6.000	6.000	6.000	1/1/52	1/1/52
7.000	7.000	7.000	7.000	1/1/52	1/1/52
8.000	8.000	8.000	8.000	1/1/52	1/1/52
9.000	9.000	9.000	9.000	1/1/52	1/1/52
10.000	10.000	10.000	10.000	1/1/52	1/1/52
11.000	11.000	11.000	11.000	1/1/52	1/1/52
12.000	12.000	12.000	12.000	1/1/52	1/1/52
13.000	13.000	13.000	13.000	1/1/52	1/1/52
14.000	14.000	14.000	14.000	1/1/52	1/1/52
15.000	15.000	15.000	15.000	1/1/52	1/1/52
16.000	16.000	16.000	16.000	1/1/52	1/1/52
17.000	17.000	17.000	17.000	1/1/52	1/1/52
18.000	18.000	18.000	18.000	1/1/52	1/1/52
19.000	19.000	19.000	19.000	1/1/52	1/1/52
20.000	20.000	20.000	20.000	1/1/52	1/1/52
21.000	21.000	21.000	21.000	1/1/52	1/1/52
22.000	22.000	22.000	22.000	1/1/52	1/1/52
23.000	23.000	23.000	23.000	1/1/52	1/1/52
24.000	24.000	24.000	24.000	1/1/52	1/1/52
25.000	25.000	25.000	25.000	1/1/52	1/1/52
26.000	26.000	26.000	26.000	1/1/52	1/1/52
27.000	27.000	27.000	27.000	1/1/52	1/1/52
28.000	28.000	28.000	28.000	1/1/52	1/1/52
29.000	29.000	29.000	29.000	1/1/52	1/1/52
30.000	30.000	30.000	30.000	1/1/52	1/1/52
31.000	31.000	31.000	31.000	1/1/52	1/1/52
32.000	32.000	32.000	32.000	1/1/52	1/1/52
33.000	33.000	33.000	33.000	1/1/52	1/1/52
34.000	34.000	34.000	34.000	1/1/52	1/1/52
35.000	35.000	35.000	35.000	1/1/52	1/1/52
36.000	36.000	36.000	36.000	1/1/52	1/1/52
37.000	37.000	37.000	37.000	1/1/52	1/1/52
38.000	38.000	38.000	38.000	1/1/52	1/1/52
39.000	39.000	39.000	39.000	1/1/52	1/1/52
40.000	40.000	40.000	40.000	1/1/52	1/1/52
41.000	41.000	41.000	41.000	1/1/52	1/1/52
42.000	42.000	42.000	42.000	1/1/52	1/1/52
43.000	43.000	43.000	43.000	1/1/52	1/1/52
44.000	44.000	44.000	44.000	1/1/52	1/1/52
45.000	45.000	45.000	45.000	1/1/52	1/1/52
46.000	46.000	46.000	46.000	1/1/52	1/1/52
47.000	47.000	47.000	47.000	1/1/52	1/1/52
48.000	48.000	48.000	48.000	1/1/52	1/1/52
49.000	49.000	49.000	49.000	1/1/52	1/1/52
50.000	50.000	50.000	50.000	1/1/52	1/1/52
51.000	51.000	51.000	51.000	1/1/52	1/1/52
52.000	52.000	52.000	52.000	1/1/52	1/1/52
53.000	53.000	53.000	53.000	1/1/52	1/1/52
54.000	54.000	54.000	54.000	1/1/52	1/1/52
55.000	55.000	55.000	55.000	1/1/52	1/1/52
56.000	56.000	56.000	56.000	1/1/52	1/1/52
57.000	57.000	57.000	57.000	1/1/52	1/1/52
58.000	58.000	58.000	58.000	1/1/52	1/1/52
59.000	59.000	59.000	59.000	1/1/52	1/1/52
60.000	60.000	60.000	60.000	1/1/52	1/1/52
61.000	61.000	61.000	61.000	1/1/52	1/1/52
62.000	62.000	62.000	62.000	1/1/52	1/1/52
63.000	63.000	63.000	63.000	1/1/52	1/1/52
64.000	64.000	64.000	64.000	1/1/52	1/1/52
65.000	65.000	65.000	65.000	1/1/52	1/1/52
66.000	66.000	66.000	66.000	1/1/52	1/1/52
67.000	67.000	67.000	67.000	1/1/52	1/1/52
68.000	68.000	68.000	68.000	1/1/52	1/1/52
69.000	69.000	69.000	69.000	1/1/52	1/1/52
70.000	70.000	70.000	70.000	1/1/52	1/1/52
71.000	71.000	71.000	71.000	1/1/52	1/1/52
72.000	72.000	72.000	72.000	1/1/52	1/1/52
73.000	73.000	73.000	73.000	1/1/52	1/1/52
74.000	74.000	74.000	74.000	1/1/52	1/1/52
75.000	75.000	75.000	75.000	1/1/52	1/1/52
76.000	76.000	76.000	76.000	1/1/52	1/1/52
77.000	77.000	77.000	77.000	1/1/52	1/1/52
78.000	78.000	78.000	78.000	1/1/52	1/1/52
79.000	79.000	79.000	79.000	1/1/52	1/1/52
80.000	80.000	80.000	80.000	1/1/52	1/1/52
81.000	81.000	81.000	81.000	1/1/52	1/1/52
82.000	82.000	82.000	82.000	1/1/52	1/1/52
83.000	83.000	83.000	83.000	1/1/52	1/1/52
84.000	84.000	84.000	84.000	1/1/52	1/1/52
85.000	85.000	85.000	85.000	1/1/52	1/1/52
86.000	86.000	86.000	86.000	1/1/52	1/1/52
87.000	87.000	87.000	87.000	1/1/52	1/1/52
88.000	88.000	88.000	88.000	1/1/52	1/1/52
89.000	89.000	89.000	89.000	1/1/52	1/1/52
90.000	90.000	90.000	90.000	1/1/52	1/1/52
91.000	91.000	91.000	91.000	1/1/52	1/1/52
92.000	92.000	92.000	92.000	1/1/52	1/1/52
93.000	93.000	93.000	93.000	1/1/52	1/1/52
94.000	94.000	94.000	94.000	1/1/52	1/1/52
95.000	95.000	95.000	95.000	1/1/52	1/1/52
96.000	96.000	96.000	96.000	1/1/52	1/1/52
97.000	97.000	97.000	97.000	1/1/52	1/1/52
98.000	98.000	98.000	98.000	1/1/52	1/1/52
99.000	99.000	99.000	99.000	1/1/52	1/1/52
100.000	100.000	100.000	100.000	1/1/52	1/1/52



CROSS SECTION SHOWING SOLAR PANEL SUPPORT TUBE STOWED CONFIGURATION
SCALE $\frac{1}{2}$

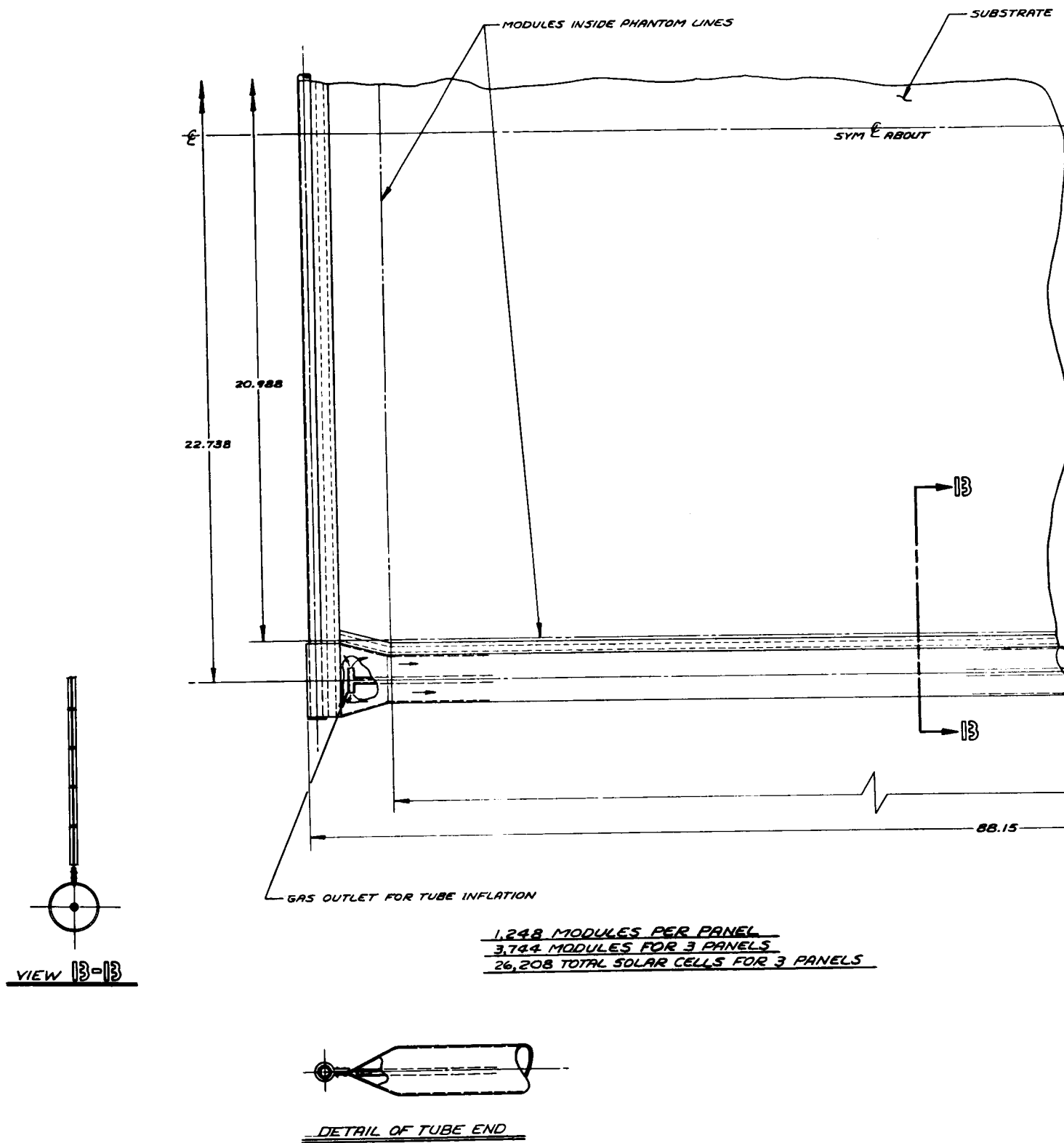


CROSS SECTION SHOWING SOLAR PANEL STOWED CONFIGURATION
SCALE $\frac{1}{2}$

a) Overall View

Figure 2-3. System 3 - Three Flexible Panels - Drum Stowed

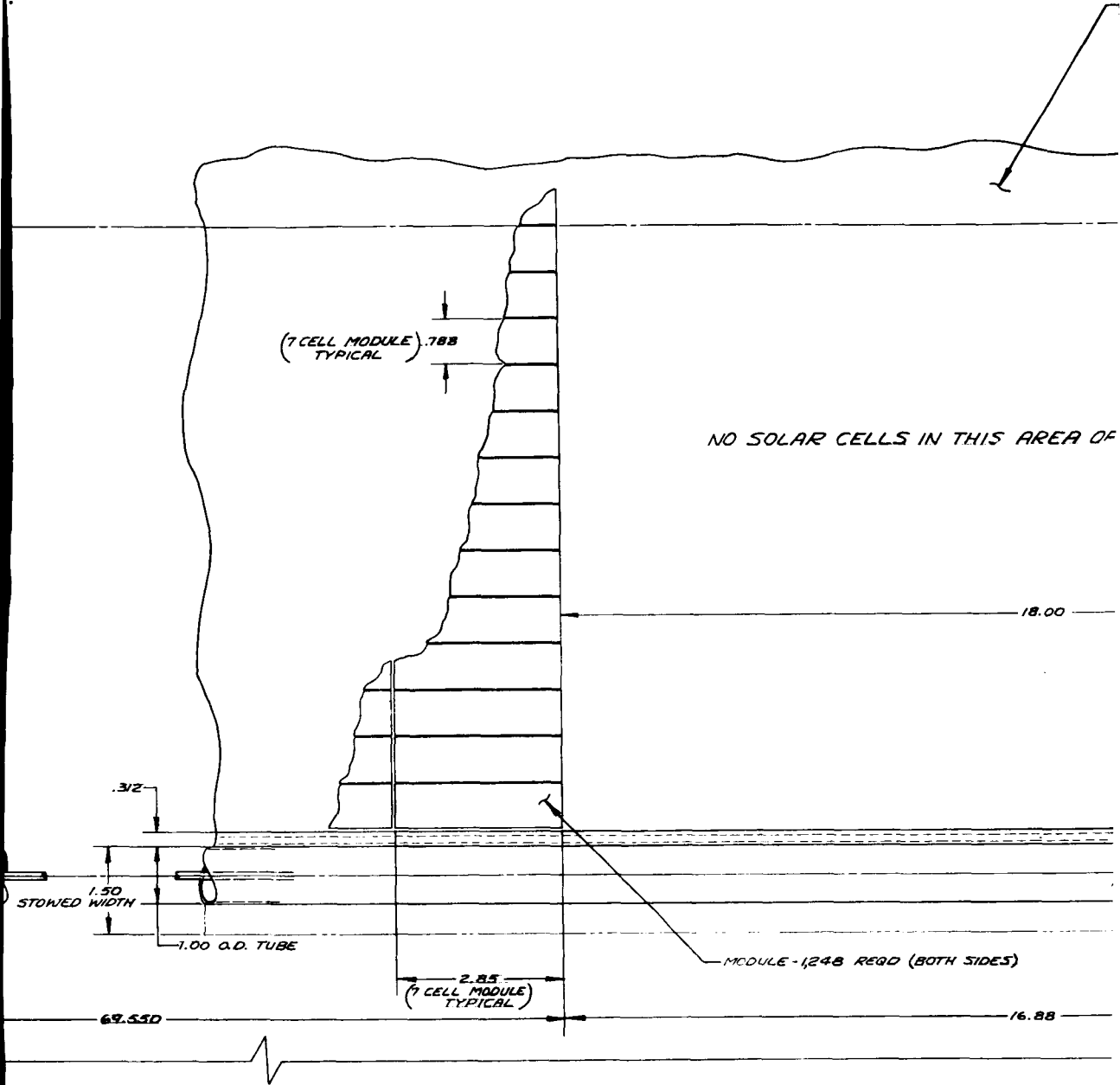
UNLESS OTHERWISE SPECIFIED:		NAME <i>as per</i>		DATE <i>26 AUG 64</i>	LIST OF MATERIALS		FORM NO.
DIMENSIONS ARE IN INCHES		CHECKED			HUGHES		HUGHES AIRCRAFT COMPANY
TOLERANCES ON DIMENSIONS		DRAWN <i>DeLong</i>		<i>26 SEP 64</i>	CULVER CITY, CALIF.		
JOE	JX				TITLE		
± .010	± .03				SYSTEM #3		
MATERIAL					THREE FLEXIBLE PANELS -		
		<i>Handwritten signature</i>		<i>9/2/64</i>	DRUM STOWED		
		<i>Handwritten signature</i>		<i>11/1/64</i>	CODE QUERY NO.		
		APPROVED			ISSUE	NUMBER	
					82557	J	X282013
					SCALE 1/8"	SHEET 1 OF 1	



b) Panel Details

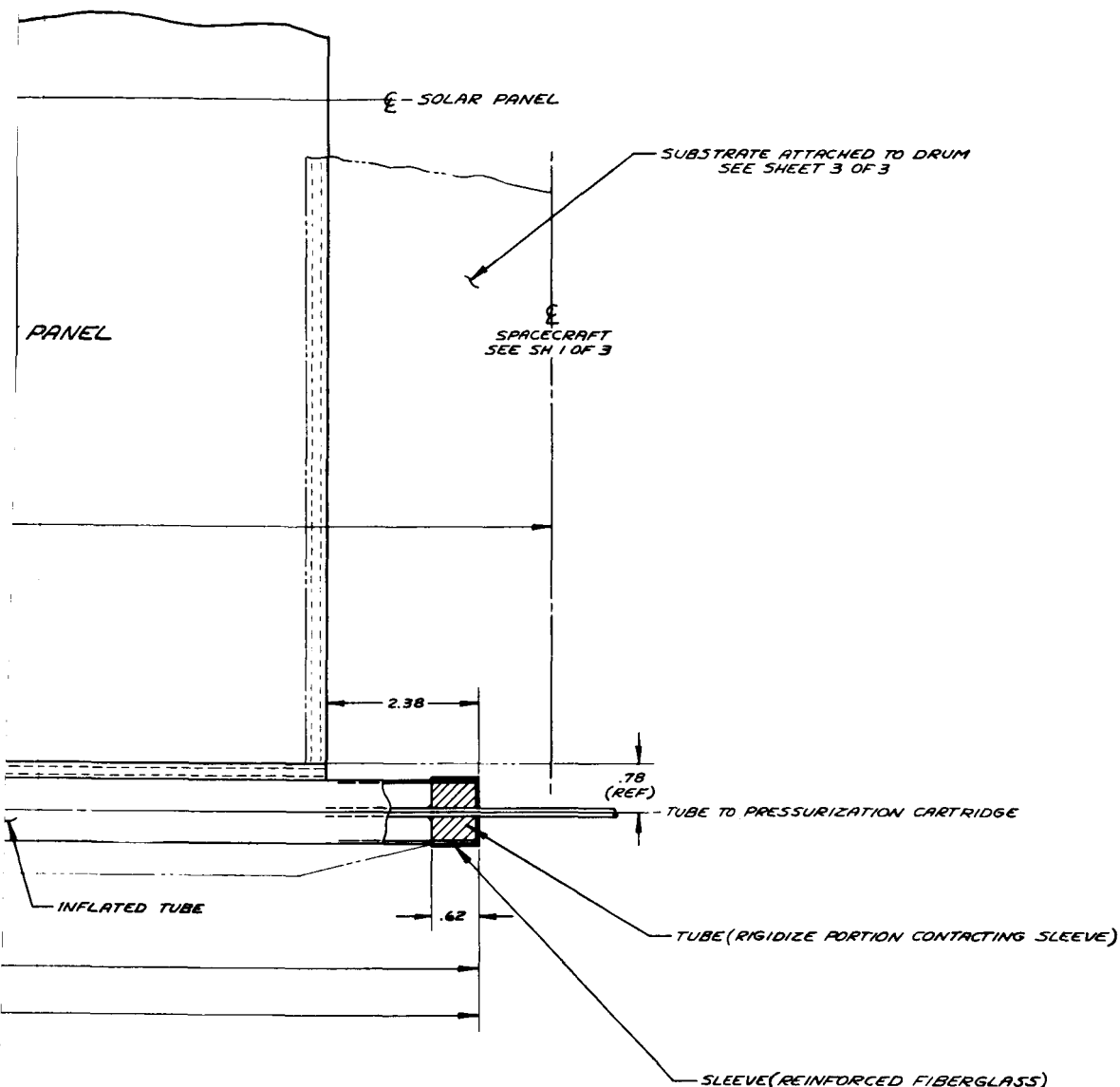
Figure 2-3 (continued). System 3 - Three Flexible Panels - Drum Stowed

2

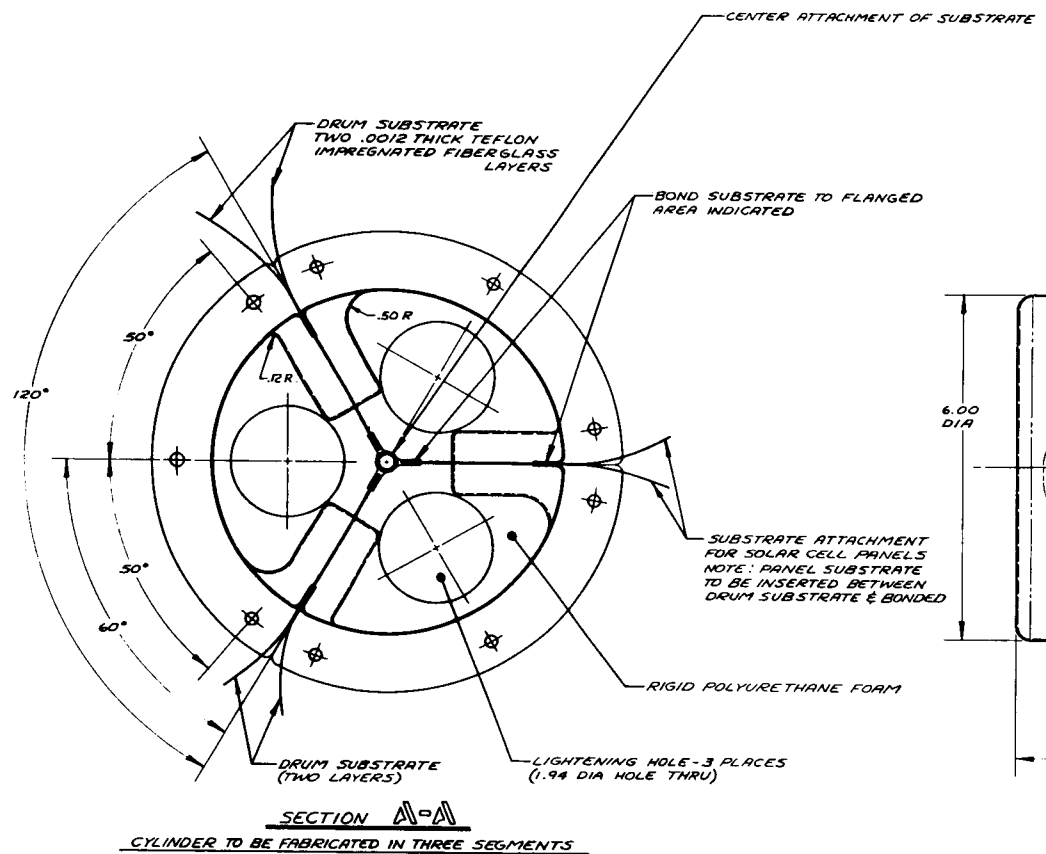


- SUBSTRATE .0012 THK TEFLON
IMPREGNATED FIBERGLASS

3



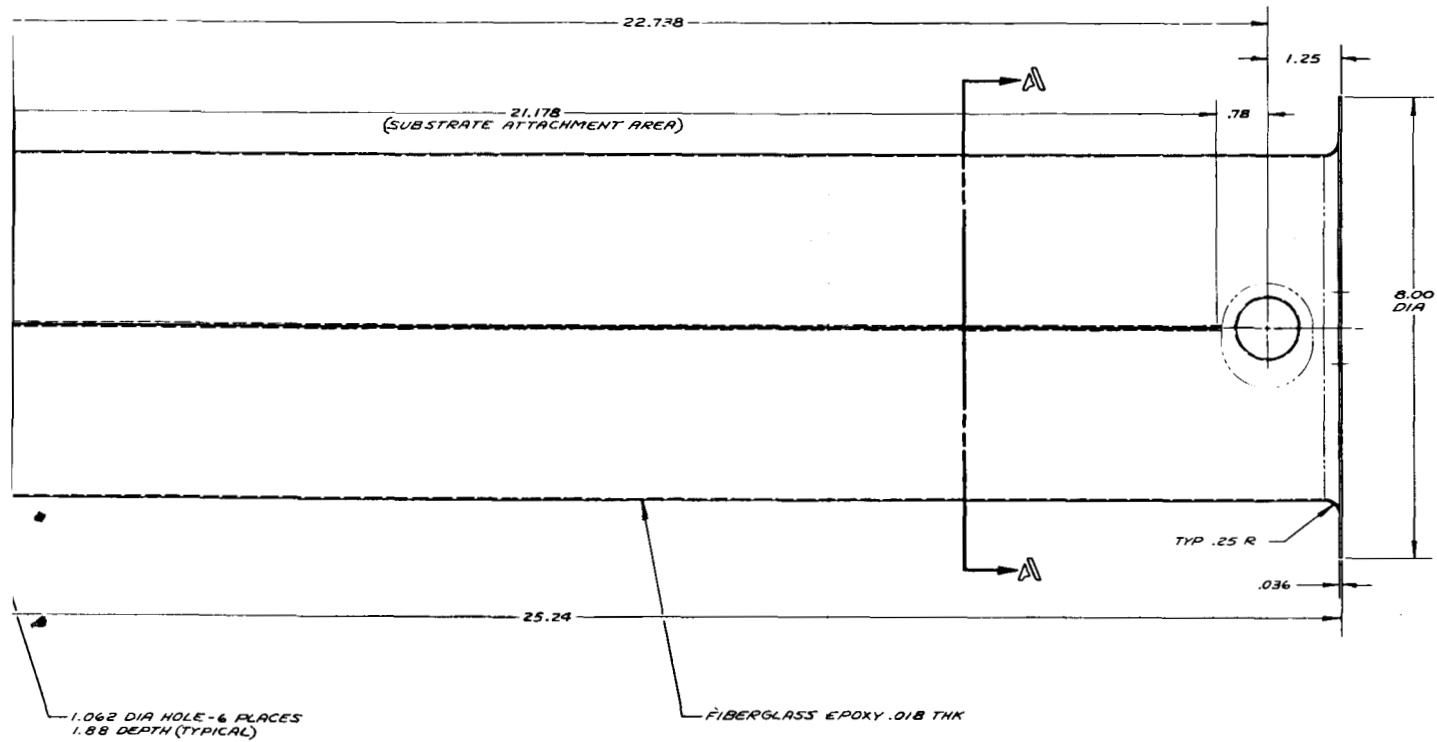
QTY REQD		PART OR IDENTIFYING NO.		NOMENCLATURE OR DESCRIPTION		ZONE NO.	
LIST OF MATERIALS							
UNLESS OTHERWISE SPECIFIED DIMENSIONS ARE IN INCHES TOLERANCES ON DECIMALS				DRAWN <i>Ol. Fair</i> DATE <i>26 AUG 66</i> CHECKED <i>Ol. Fair</i> DATE <i>26 AUG 66</i> MATERIAL <i>6/11/66</i> <i>9/29/66</i> APPROVED <i>2/2/67</i> <i>11/4/66</i>			
XXX ± .010 JXX ± .03 ANGLES ± 0° 30'				HUGHES HUGHES AIRCRAFT COMPANY CULVER CITY, CALIF. TITLE SYSTEM #3 THREE FLEXIBLE PANELS DRUM STOWED CODE IDENT NO. 82577 SIZE J NUMBER X282013 SCALE SHEET 2 OF 3			
NEXT ASSY		USED ON		APPLICATION			



c) Drum Details

Figure 2-3 (continued). System 3 - Three Flexible Panels - Drum Stowed

2



COMPLETE DRUM WEIGHT = APPROX 1.17 LBS.

QTY REQD		PART OR IDENTIFYING NO.		NOMENCLATURE OR DESCRIPTION		ZONE	ITEM NO.
UNLESS OTHERWISE SPECIFIED		DRAWN		DATE		LIST OF MATERIALS	
DIMENSIONS ARE IN INCHES		AL Jain		3 SEPT 66		HUGHES HUGHES AIRCRAFT COMPANY	
TOLERANCES ON		CHECKED				CULVER CITY, CALIF.	
XXX	XX	Only		2-5066		TITLE	
± .010	± .03					SYSTEM #3	
ANGLES						THREE FLEXIBLE PANELS	
± 0° 30'						DRUM STOWED	
MATERIAL		APPROVED		9/23/66		CODE IDENT NO.	
		T. H. Jain		4/6/67		SIZE	
						NUMBER	
						82577 H X282013	
						SCALE 1/1	
						SHEET 3 OF 3	
NEXT ASSY		USED ON					
APPLICATION							

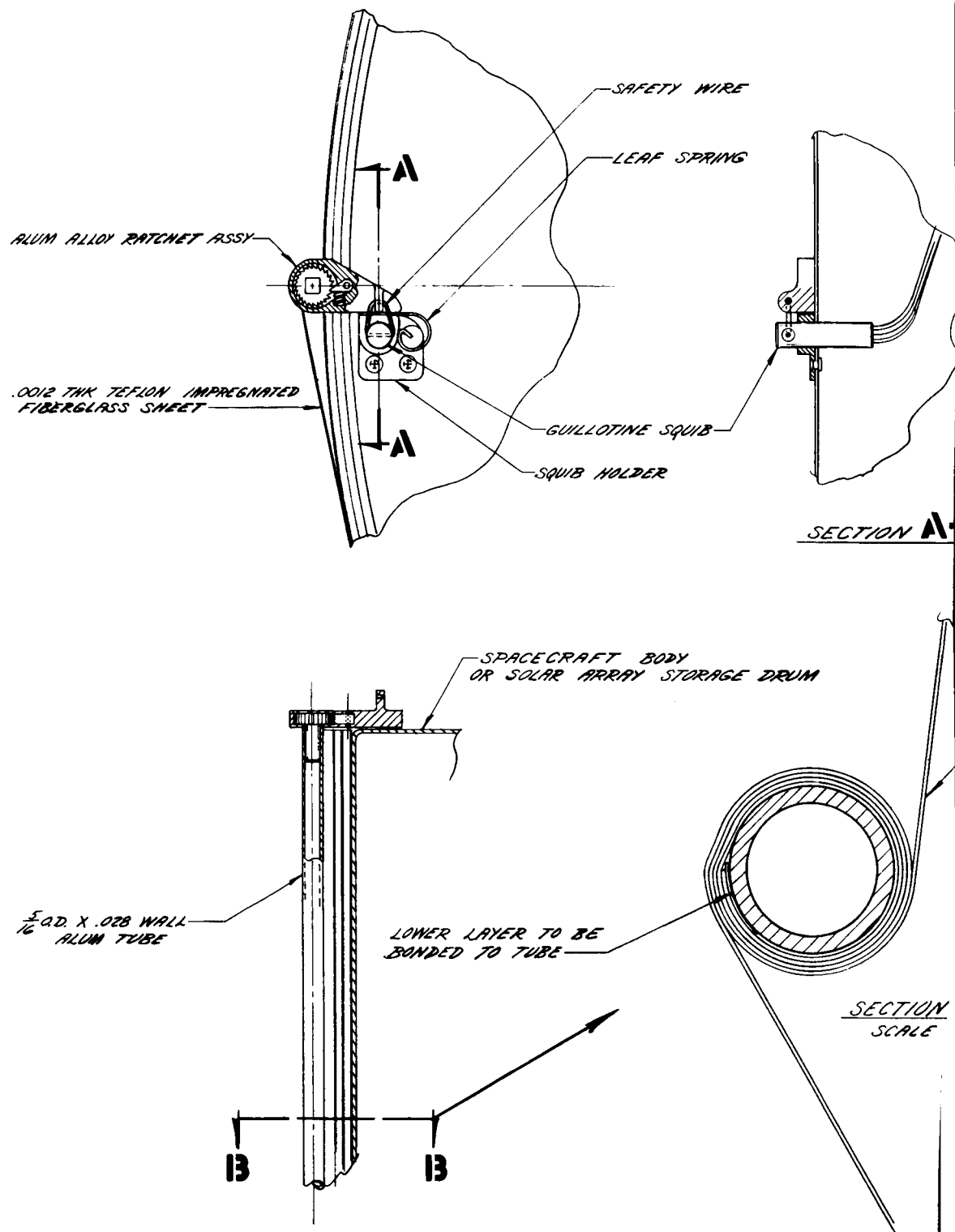


Figure 2-4. Retaining Hoop - Flexible Solar Panels Systems

2

WEIGHT - LBS

	<u>36 INCH DRUM</u>	<u>6 INCH DRUM</u>
$\frac{3}{16}$ DIA X .028 WALL ALUM TUBE	.058	.058
RATCHET ASSY (ALUM)	.030	.030
SQUIB	.055	.055
SQUIB HOLDER	.010	.010
SPRING, RIVETS, & SAFETY WIRE	.010	.010
RETAINING HOOP	.075	.016
TOTAL	.238 LBS	.179 LBS

.0012 THK (REF)
SHOWN OUT OF SCALE

13-13

QTY REQD		PART OR IDENTIFYING NO.		NOMENCLATURE OR DESCRIPTION		ZONE	ITEM NO.
LIST OF MATERIALS							
UNLESS OTHERWISE SPECIFIED		DRAWN A.B. Khan		DATE 1/26/64		HUGHES HUGHES AIRCRAFT COMPANY CULVER CITY, CALIF.	
DIMENSIONS ARE IN INCHES		CHECKED Bely		25 FEB 64		TITLE RETAINING HOOP-FLEXIBLE SOLAR PANELS SYSTEMS	
TOLERANCES ON							
DECIMALS		ANGLES					
XXX ± .010		XX ± .03		± 0° 30'			
MATERIAL		APPROVED H. H. Jerny		9/28/64		CODE IDENT NO. SIZE NUMBER 82577 D X281923	
NEXT ASSY		USED ON		APPROVED H. H. Jerny		SCALE 1/16" = 1" NOTED SHEET	
APPLICATION							

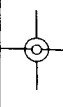
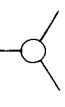


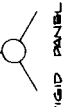


SYSTEM DESCRIPTION	DIMENSIONS & FT ³	TOTAL WEIGHT LBS	TOTAL DEPLOYED AREA FT ²	DUE TO ROTATION OF SATELLITE			AVERAGE PANEL OPERATING TEMP °C	WATTS PER FT ²	WATTS PER LB	WATTS PER FT ³ (STOWED VOLUME)	OVERALL SYSTEM RELIABILITY ESTIMATE	COST COMPARISON	GROWTH POTENTIAL	OVERALL RATING NUMBER
				MAX AVE MIN	PROJECTED AREA FT ²	ARRAY OUTPUT WATTS	P _{MAX} -P _{MIN} PWS							
SYSTEM #1 	4 PANELS, EACH = 76 x 22, 2 DRUMS, 600 DIA x 22 LONG STOWED DIA (WITH 0.150 CUSHION & RESTRAINING HOOP) TOTAL STOWED VOLUME = 1.290 FT ³	22.6	95.3	20.0 17.9 14.2	202 181 143	.325	54	1.9	8.0	140	HIGH	LOW	EXCELLENT	19.9
SYSTEM #2 	EACH PANEL = 79 x 24 (WITH TUBES) STOWED DIA (WITH 0.150 CUSHION & RESTRAINING HOOP) = 36.0 TOTAL STOWED VOLUME = 0.450 FT ³	20.0	75.0	18.5 17.1 15.2	199 184 163	.196	43	2.5	9.2	383	HIGH	LOW	EXCELLENT	33.7
SYSTEM #3 	EACH PANEL = 68 x 24 (WITH TUBES) STOWED DIA (WITH 0.150 CUSHION & RESTRAINING HOOP) = 9.3% TOTAL STOWED VOLUME = 0.9% FT ³	21.5	88.0	18.5 17.1 15.2	199 184 163	.196	43	2.1	8.6	192	HIGH	LOW	EXCELLENT	23.4
SYSTEM #4 	PANEL 5/16 = 20 x 24 STOWED 0.7 = 36.7 TUBES, 12 OF 3/4 DIA x 14 LONG TOTAL STOWED VOLUME = 0.98 FT ³	12.1	28.0	9.6 9.2 8.3	97 93 84	.139	54	3.3	7.7	158	FAIR	HIGH	LIMITED	22.0
TRI NODAL CONFIGURATION SYSTEM #5 	EACH PANEL CON-SISTS OF (9), 12 x 24 SEGMENTS STOWED VOLUME = 1.33 FT ³	26.1	60.0	17.5 16.3 14.4	189 176 156	.187	42	2.9	6.7	132	LOW	MODERATE	LIMITED	18.9
SYSTEM #6 	EACH PANEL CON-SISTS OF (6), 24 x 22 SEGMENTS, LENGTH = 36.7 STOWED DIA = 28 TOTAL STOWED VOLUME = 1.19 FT ³	28.1	66.1	13.9 13.2 12.1	158 151 137	.139	32	2.3	5.4	126	LOW	HIGH	LIMITED	16.1
SYSTEM #7 	EACH PANEL CON-SISTS OF (3), 12 x 24 SEGMENTS, TOTAL STOWED VOLUME = 2.65 FT ³	34.7	60.0	17.8 16.4 14.6	193 177 158	.198	42	3.0	5.1	61	LOW	HIGH	LIMITED	13.5

Figure 2-5. System Comparison Chart

System 3 – Three Panel Common Drum Stowed

This system, shown in Figure 2-3 is similar to system 1, except that it has three panels on one 6-inch diameter drum and mounted only on one end of the spacecraft. The panels measure 88 by 24 inches each and the area for mounting cells is 72 by 20 inches. The panels are retained, released and rigidized by the same method as described in system 1.

The total weight of this system is about 21.5 pounds, thus giving a specific power output of 8.6 watts per pound. The weight breakdown is also shown in Figure 2-3. Additional pertinent data such as the projected area of solar array, power output, etc., are shown in Figure 2-5.

System 4 – Tri-Nodal Configuration

This configuration, (Figure 2-7), consists of six flexible panels that will form a three-pointed star when deployed. It utilizes flexible substrates which are supported by two telescoping beryllium copper tubes. In the stowed position the substrate is folded once and held in place by means of a retaining hoop system similar to that shown in Figure 2-4. The substrate is 0.0012-inch teflon impregnated fiberglass with solar cells bonded to one side. Polyurethane foam padding, 0.150-inch thick, is used between layers of the solar array substrate and the spacecraft to protect the solar cell from any damage from the vibration conditions during launch. About 1 psi is exerted by the retaining hoop, which was explained previously.

To deploy the solar panel the retaining hoop would be cast off, allowing the tubes to swing out and extend to the deployed position. The rotation and telescoping motion is actuated by a spring but controlled by an escapement mechanism, thus maintaining a completely controlled deployment of the flexible solar array from a spin-stabilized spacecraft. When the tubes swing out to the normal position to the spacecraft, the first fold of substrate is unfurled and, on reaching this position, it triggers the release of a tuck holding the second fold and it is now free to unfold as the tube telescopes out to full deployed position.

The total weight of the system is about 12.1 pounds, thus giving a specific power output of 7.7 watts per pound. The weight breakdown is shown on Figure 2-7. Additional pertinent data such as the projected area of the solar array power output, etc., are shown in Figure 2-5.

System 5 – Multifold Rigid Panel Configuration

This system, in the deployed position, consists of three rigid segmented solar panels located 120 degrees apart on the spacecraft. Each panel contains six hinged segments that unfold from the spacecraft, with an accordion-type movement, as shown in Figure 2-8. This movement is controlled by pneumatically operated telescoping tubes. The telescoping tubes are attached to a pressurization manifold located at the spin-axis of the spacecraft.

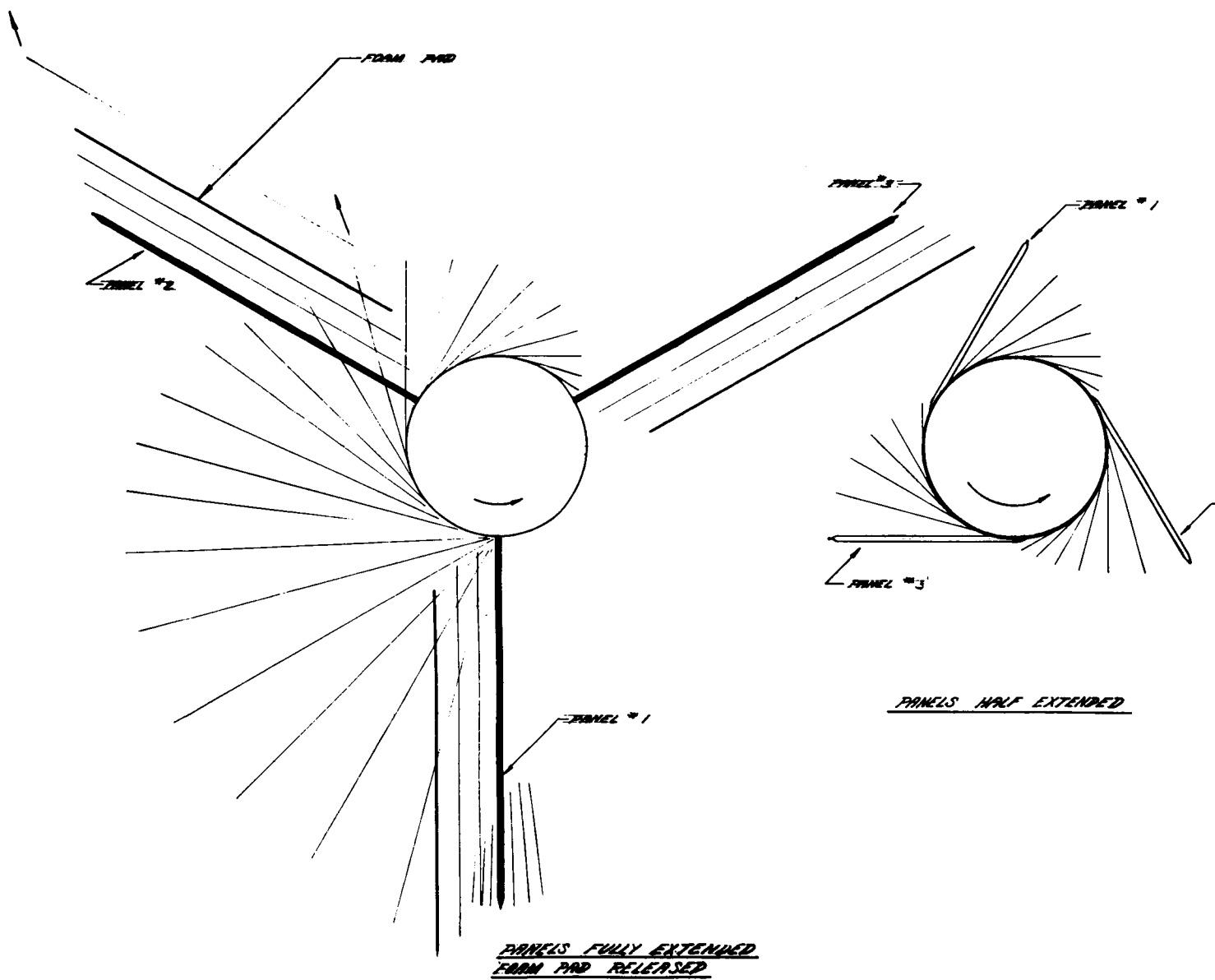
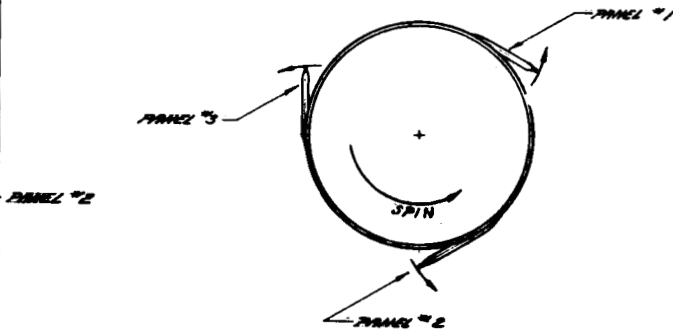
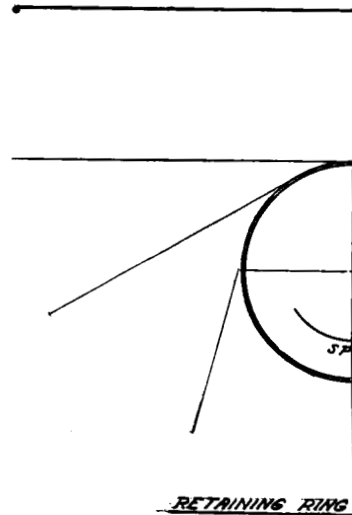


Figure 2-6. System 2 - Three Flexible Panels - Body Stowed

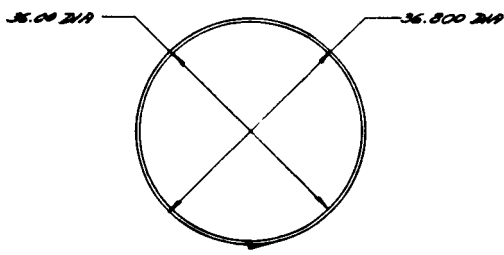
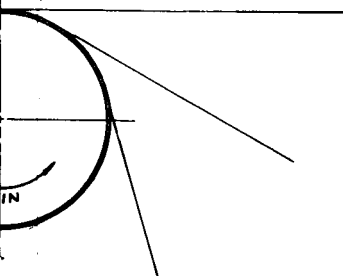


INFLATE SUPPORT TUBES



3

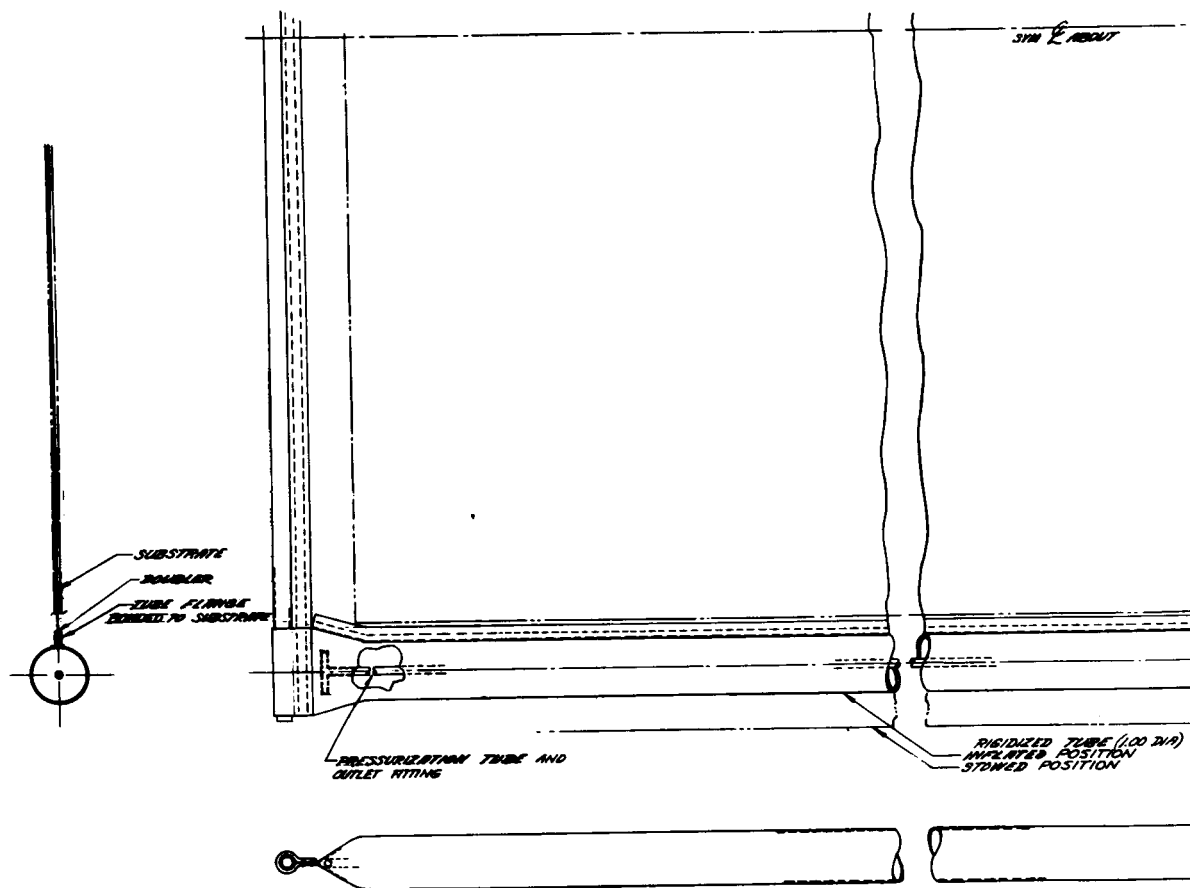
ITEM	MATERIAL	WT/LBS
SUBSTRATE	.0012 THK TEFLON IMPREGNATED FIBERGLASS	.051
CELL ASSY'S	1,200 SEVEN CELL MODULES	4.842
WIRING HARNESS	COPPER	.176
SUPPORT TUBES	.250 DIA x .028 WALL ALUM ALLOY	.750
END SUPPORT	FIBERGLASS	.045
BASE ATTACHMENT	ALUM ALLOY	.250
FOAM SHEET	FLEXIBLE POLYURETHANE FOAM .150 THK	.360
RIVETS, THREADS, EPOXY AND MISC		.020
WEIGHT ONE PANEL		6.624
WEIGHT THREE PANELS		19.872
TUBE PRESSURIZATION SYSTEM		.300
RETRAINING HOOP (DWG NO. X281923)		.728
TOTAL WEIGHT 19.990		



RELEASED

PANELS STOWED

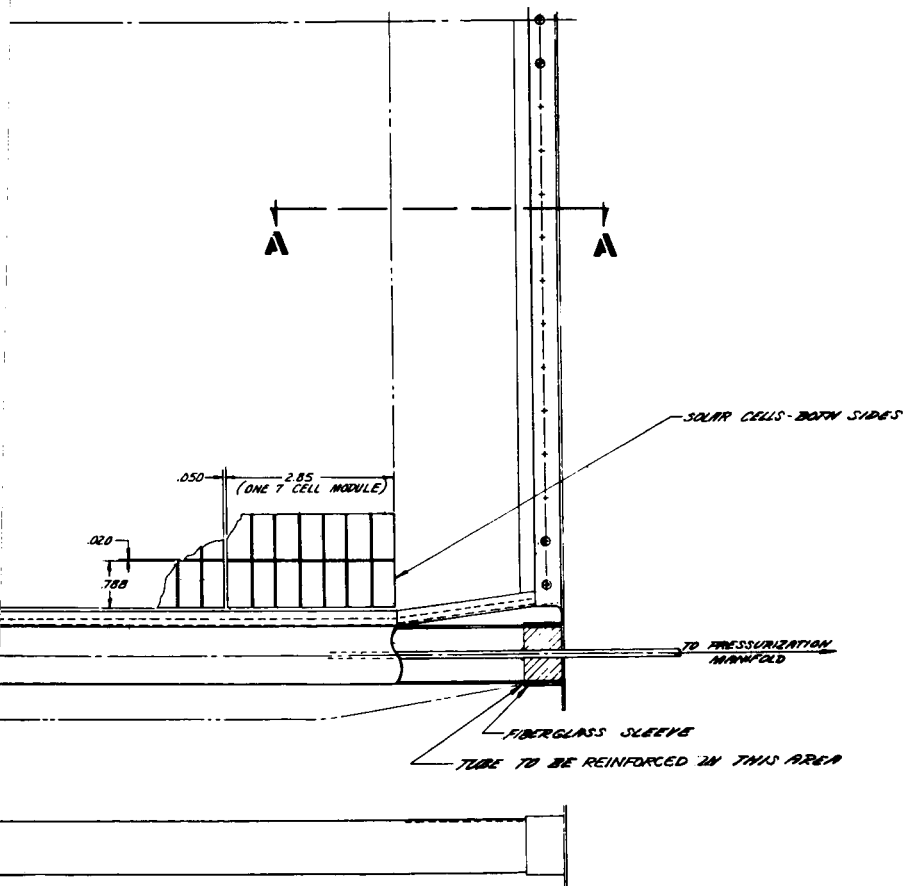
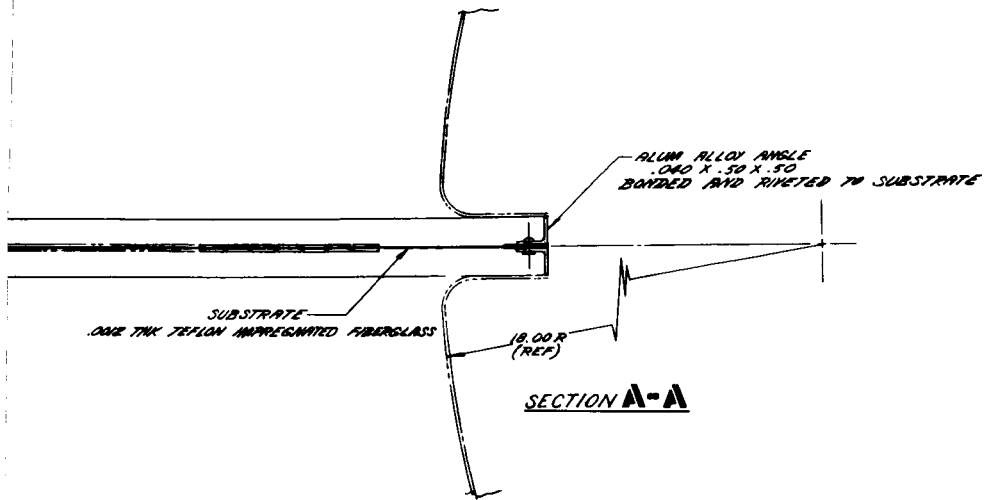
UNLESS OTHERWISE SPECIFIED DIMENSIONS ARE IN INCHES TOLERANCES ON DECIMALS JXX ±.010 JXX ±.03 ±.0° 30'		DATE 1/14/66 BY [Signature]		DATE 1/14/66 BY [Signature]		LIST OF MATERIALS HUGHES HUGHES AIRCRAFT COMPANY CULVER CITY, CALIF.		TITLE SYSTEM #2 THREE FLEXIBLE PANELS SPACECRAFT BODY STOWED	
MATERIAL		CODE IDENT NO.		82577		H		X282024	
NEXT ASSY		USED ON		SCALE 1/4"				SHEET 1 OF 2	
APPLICATION									



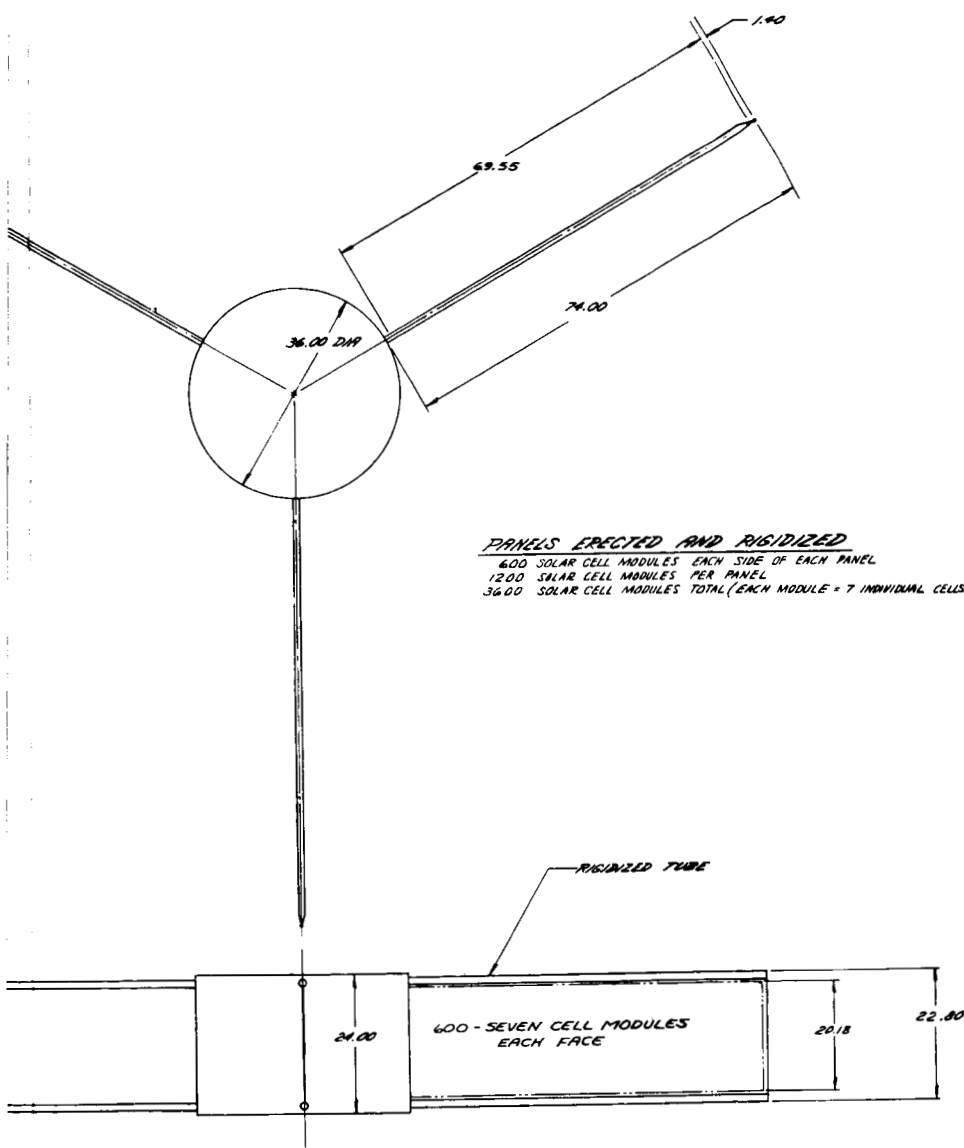
b) Panel Details

Figure 2-6 (continued). System 2 - Three Flexible Panels - Body Stowed

2



3



PANELS ERECTED AND RIGIDIZED
 600 SOLAR CELL MODULES EACH SIDE OF EACH PANEL
 1200 SOLAR CELL MODULES PER PANEL
 3600 SOLAR CELL MODULES TOTAL (EACH MODULE = 7 INDIVIDUAL CELLS)

QTY REQD		PART OR IDENTIFYING NO.		HOMOLOGATION OR DESCRIPTION		ZONE	ITEM NO.
UNLESS OTHERWISE SPECIFIED DIMENSIONS ARE IN INCHES TOLERANCES ON DECIMALS				LIST OF MATERIALS			
XXX = .010		XX = .03		DATE 10/1/64		HUGHES HUGHES AIRCRAFT COMPANY CULVER CITY, CALIF.	
ANGLES = 0° 30'		DRAWN J. S. JONES		CHECKED B. J. JONES		TITLE SYSTEM #2 THREE FLEXIBLE PANELS SPACECRAFT BODY STOWED	
MATERIAL		APPROVED [Signature]		APPROVED [Signature]		CODE IDENT NO. 82577 H	
NEXT ASSY		USED ON		APPROVED [Signature]		NUMBER X282024	
APPLICATION				SCALE 1/16" = 1"		SHEET 2 OF 2	

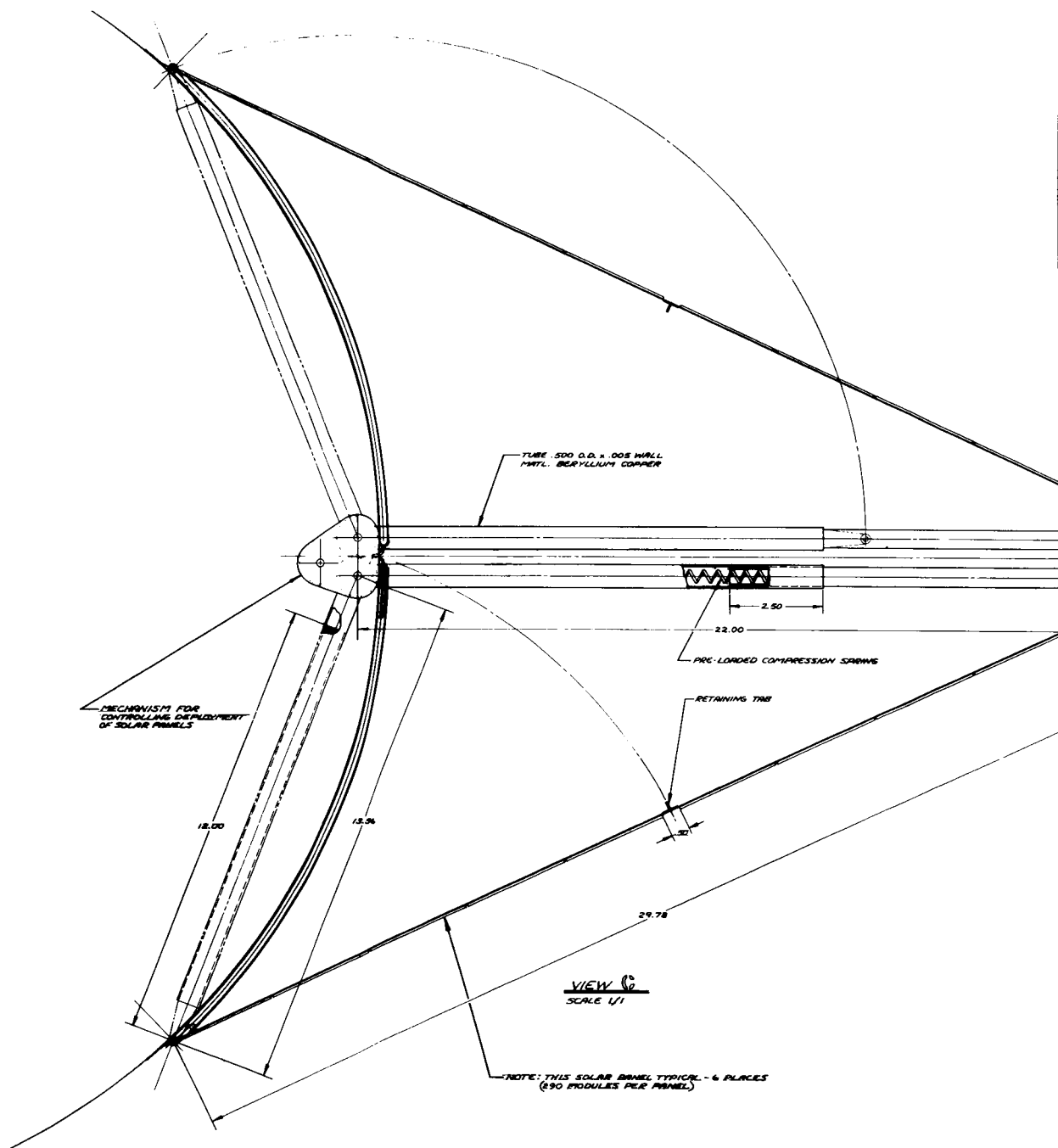
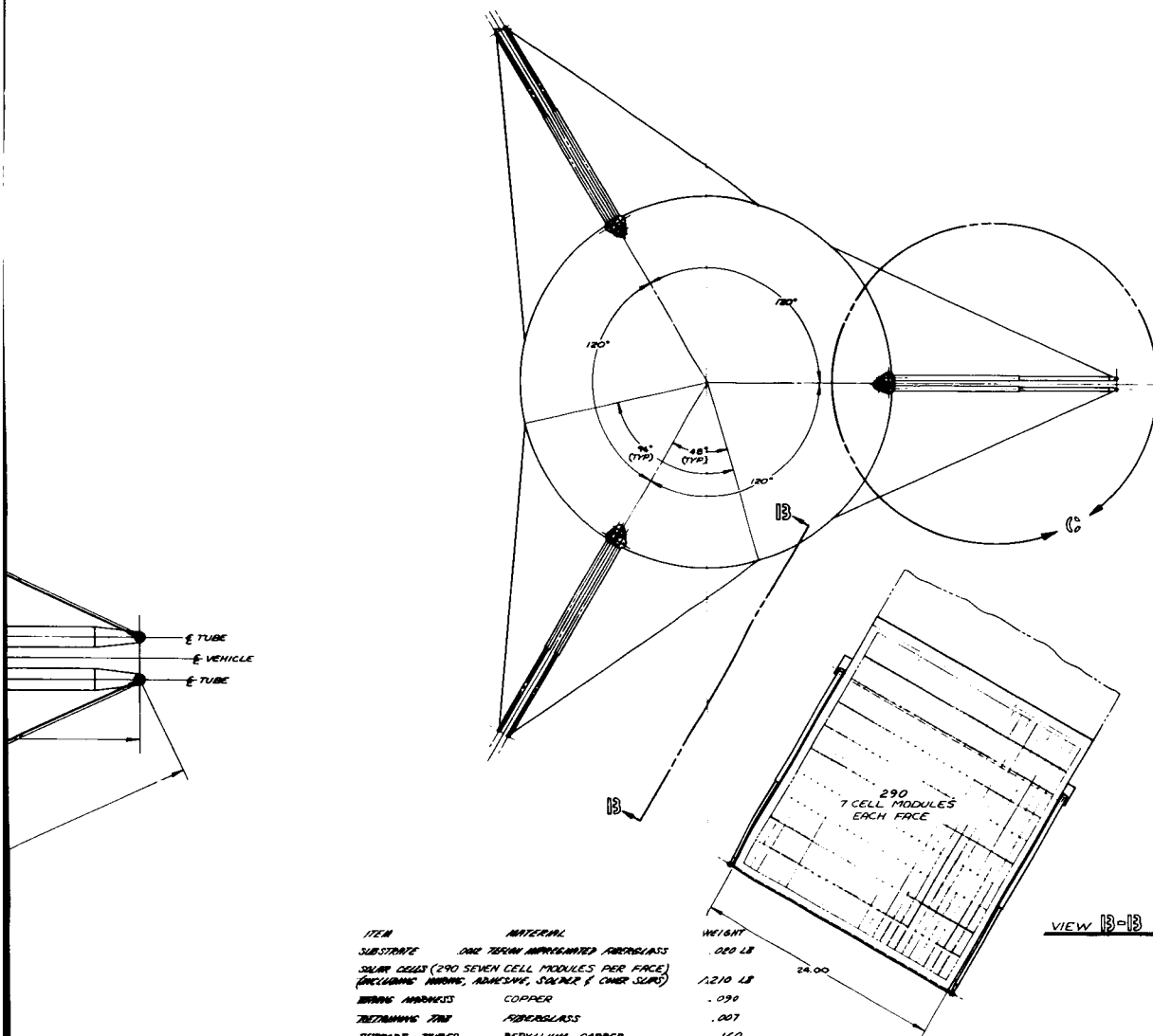


Figure 2-7. System 4 - Tri-Nodal Configuration

2



ITEM	MATERIAL	WEIGHT
SUBSTRATE	ONE TERN IMPREGNATED FIBERGLASS	.020 LB
SOLAR CELLS (290 SEVEN CELL MODULES PER FACE) (INCLUDING WIRING, ADHESIVE, SOLDER & OTHER SUPS)		12.10 LB
WIRING MARKINGS	COPPER	.099
RETAINING FILM	FIBERGLASS	.007
SEMPART TUBES	BERYLLIUM COPPER	.160
COMPRESSION SPRINGS	ONE IN. INSULATED BRONZE	.075
1 SEAL & TUBE FITTINGS	ALUM	.212
FIBER SHEET	POLYURETHANE	.120
TOTAL WEIGHT FOR 1 MODULE		13.894 LBS
6 MODULES		11.364
DEPLOYMENT CONTROL MECH (3) ALUM		.406
RETAINING ARM (ONE IN. X 2.00 IN)		.238
TOTAL WEIGHT		12.088 LBS

UNLESS OTHERWISE SPECIFIED DIMENSIONS ARE IN INCHES TOLERANCES ON DIMENSIONS		DRAWN BY: J. A. J. JR. CHECKED BY: J. A. J. JR. DATE: 10/1/64		HUGHES AIRCRAFT COMPANY CULVER CITY, CALIF.	
LIST OF MATERIALS		TITLE SYSTEM #4 TRI-NODAL CONFIGURATION		CODE 82577 J	
MATERIAL		QUANTITY		NUMBER	
NEXT REV. USED ON APPLICATION		SCALE 1/4"		SHEET	

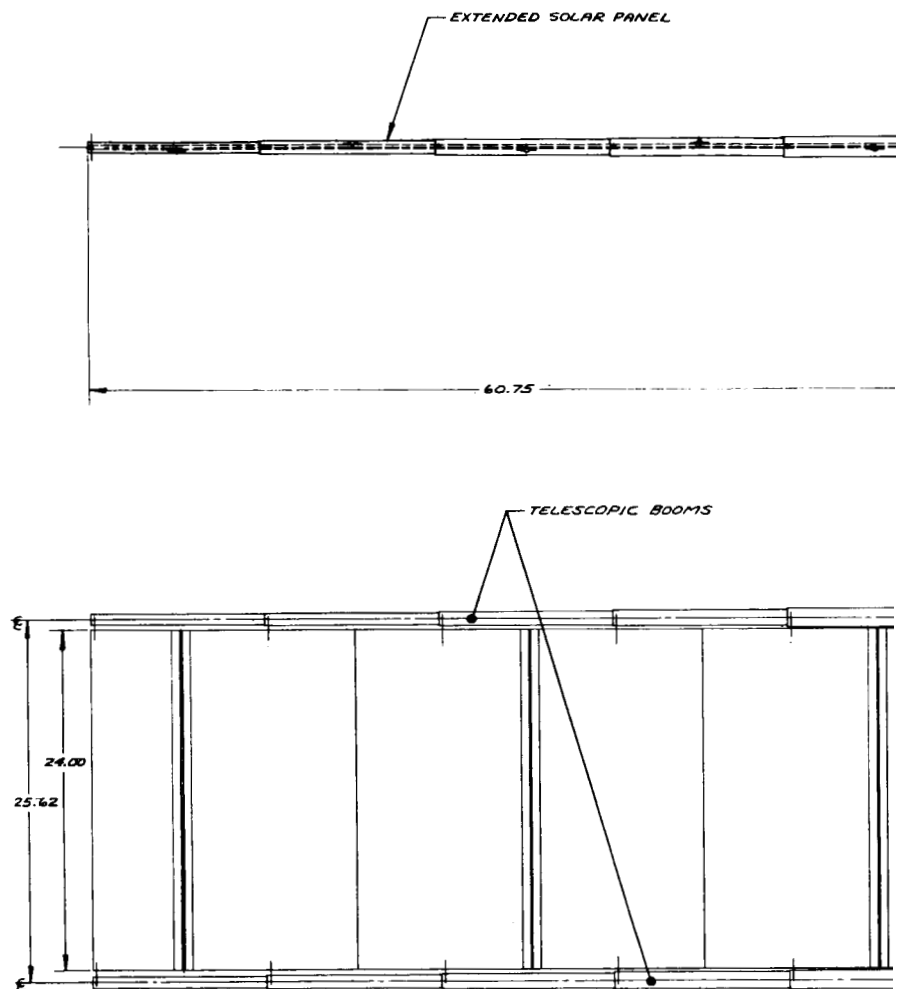
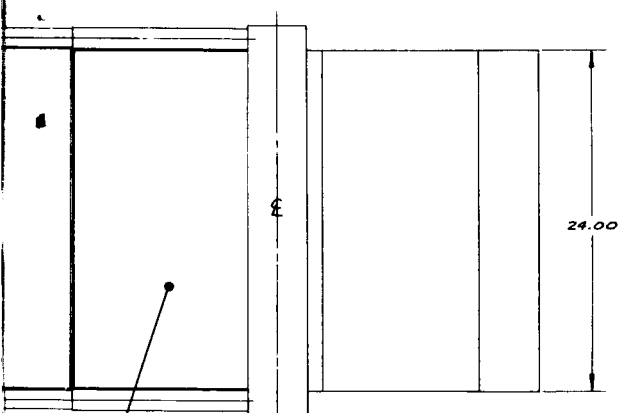
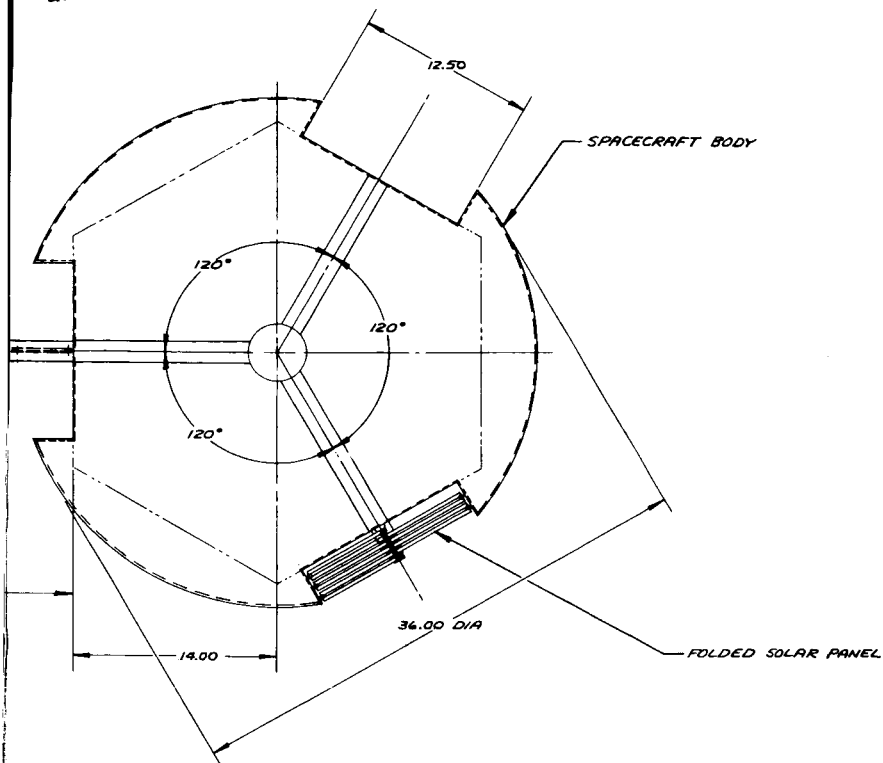


Figure 2-8. System 5 - Rigid Panel - Multiple Fold Configuration

2



QTY		PART OR IDENTIFYING NO.		NOMENCLATURE OR DESCRIPTION		ZONE		ITEM NO.	
UNLESS OTHERWISE SPECIFIED		DESIGN		DATE		LIST OF MATERIALS			
DIMENSIONS ARE IN INCHES		CHECKED		11 AUG 60		HUGHES HUGHES AIRCRAFT COMPANY			
TOLERANCES ON		BY		25 SEP 66		SULVER CITY, CALIF.			
DECIMALS		ANGLES				TITLE			
.001		.01		.001		SYSTEM #3			
.010		.03		.001		RIGID PANEL-MULTIPLE			
		.001		.001		FOLD CONFIGURATION			
MATERIAL		APPROVED		DATE		CODE IDENT NO.		NUMBER	
		11/1/60		11/1/60		82577		E X282030	
NEXT ASBY		USED ON		SCALE 1/4"		SHEET			
APPLICATION									

The individual panel segments are made up of 1/4-inch thick rigid aluminum honeycomb. Solar cells are bonded to both sides of the substrate and protected in the stowed condition by spacers located at the hinge points of the panel segments. The folded panel assembly would be firmly clamped in the stowed position so as to prevent damage during launch. Past experience from Surveyor solar panel vibration tests indicates that 3/16-inch spacing of the 12 by 24-inch panel is adequate.

When deployed, each panel is 2 feet wide by 5 feet long and 5/16-inch thick. The stowed volume is 1 foot by 2 feet by 3 inches and is presently shown recessed into the spacecraft. The panels may be moved to the outside, if required.

The total weight of the system is 26.1 pounds, thus giving a specific power output of 6.7 watts per pound. Additional pertinent data such as the projected solar array area, power output, etc., are shown in Figure 2-5.

System 6 - Expanding Rigid Panel

System 6 utilizes a series of curved rigid solar panels curved to the contour of the spacecraft and, when deployed, resemble a three-pointed star as shown in Figure 2-9. Each point of the star contains six curved solar panels hinged together and attached to the cylindrical surface of the spacecraft. The center joint of the solar panel is attached to a fiberglass tube which is pressurized and chemically rigidized so as to hold the solar array panels in the deployed position. When pressurized, the center joint moves away from the spacecraft and pulls the panels into position. The hinges are spring-loaded to prevent a snapping action.

As in system 5, aluminum honeycomb is used for the substrate material. Solar cells are bonded to one side of the substrate and spacers attached to the panels protect the cells in the stowed condition. The panels are curved to fit the side of the spacecraft so as to minimize stowed volume space. Prior to deployment, the panels are held in place and released by a retaining ring similar to that shown in Figure 2-4. This is accomplished similarly to system 1.

These panels are very similar in size and shape as those used on the Syncom communication satellite system, where experience has shown that launch vibration presents no problem.

The weight of the system is about 28.1 pounds, which gives a specific power output of 5.4 watts per pound. Additional pertinent data such as projected solar array area power output, etc., are shown in Figure 2-5.

System 7 - Rigid Telescoping Panels

System 7 consists of three sets of rigid, slide-out panels spaced 120 degrees apart on the cylindrical surface of the spacecraft. The deployment mechanism consists of an electrical actuator and a telescoping pneumatic

tube for each panel as shown in Figure 2-10. Each panel consists of nine segments; the segments are slid side by side into a pack when the panels are stowed. The panel clamping during the launch cycle is very similar to that of system 5. The electrical actuator is used to turn this pack away from the spacecraft. The panel is then erected with the telescoping tube. As in systems 5 and 6, the substrate is aluminum honeycomb. Solar cells are bonded to both sides of the center segment and one side of the remaining segments. This system is the heaviest with a total weight of 34.7 pounds and has a specific power output of 5.1 watts per pound. Additional pertinent data such as the projected area, power output, etc., are given in Figure 2-5.

STRUCTURAL AND VIBRATIONAL EVALUATION

The types of solar panel array structures studied represent tradeoffs with respect to weight, simplicity, thermal aspects, compact stowed volume and, of course, compatible with the spin-stabilized spacecraft. Consideration was given to the effects of launch loads and vibration in the stowed position, as well as the dynamic loads during deployment and after full deployment and rigidization.

Detailed stress studies were made only on the flexible solar array systems as these systems show the greatest promise, having the best power-to-weight ratio, best stowed volume configuration, greater reliability, and the most favorable growth potential.

Structural calculations checked the solar array panel designs for structural adequacy when deployed from the spinning spacecraft in the 0-g environment. In principle, the flexible teflon impregnated fiberglass substrate carried the centrifugal load of the rotating solar array panel, whereas the chemically rigidized tubes provided a beam structure to resist bending. The spreader bar at the outer extremity of the solar array panel formed a picture frame structure and provided a means of distributing the panel load. A 1-g loading was used as the criteria in the design of the structures. Sample detail calculations are included in Appendix A of this report.

The margins of safety in all cases appear quite adequate as can be seen from the sample calculations. For a 74-inch flexible substrate panel, the tensile stress caused by the centrifugal force load is such that the margin of safety of about 1.6 is maintained. This is at the worst possible condition where the spin-stabilized spacecraft would be rotating at 160 rpm.

As mentioned, the solar panels are normally designed so that the teflon-impregnated fiberglass substrate carries the entire centrifugal force load leaving the support tubes unstressed. However, in the event that the full centrifugal load is transferred to the support tubes, they can very easily carry the entire load intension with a very high margin of safety; i.e., about 12.5. The retaining hoop, made of 0.0012-inch thick teflon impregnated fiberglass, is stretched on the 36-inch diameter drums such as used in system 2, so as to produce a 1 psi pressure on the stowed solar substrate.

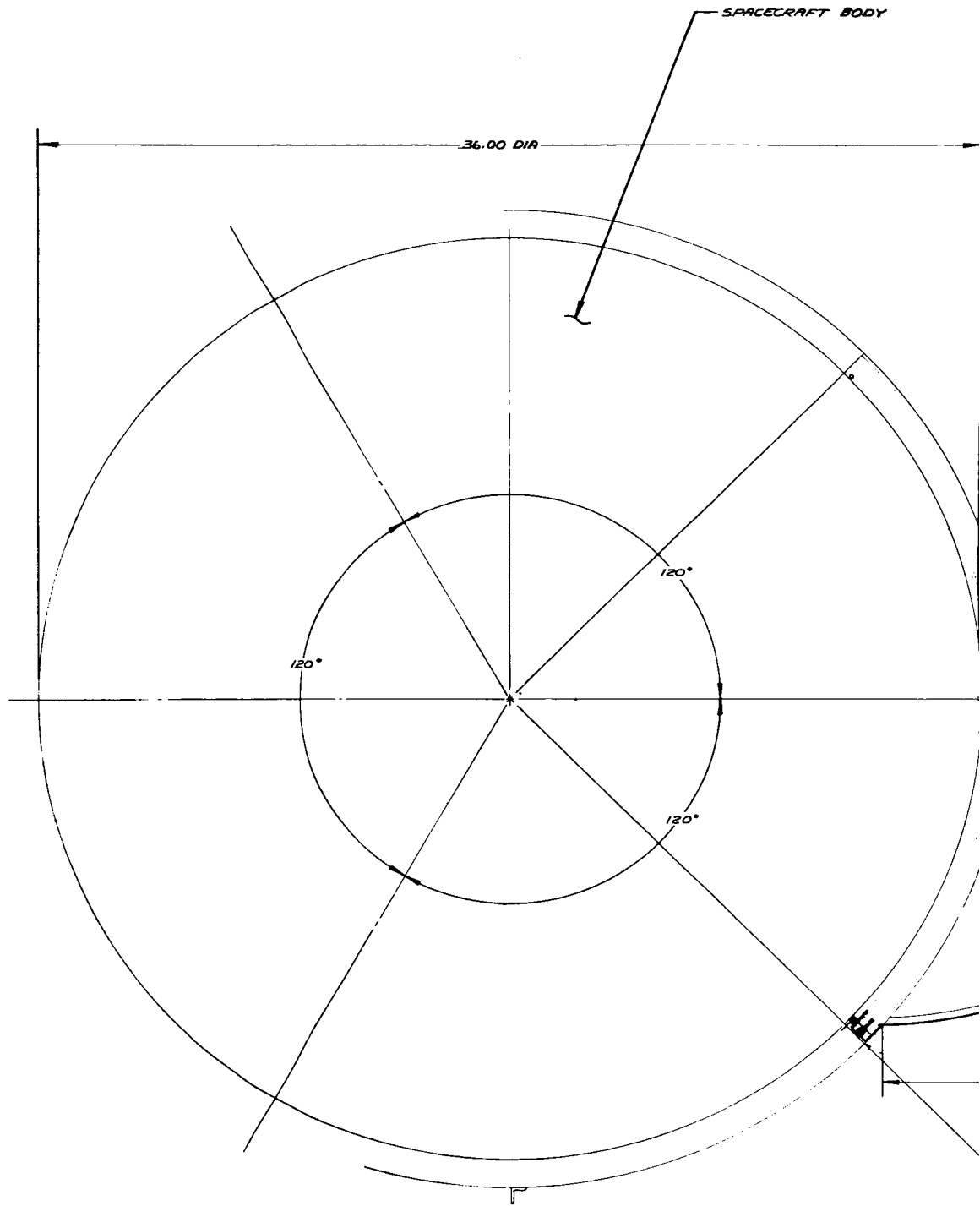
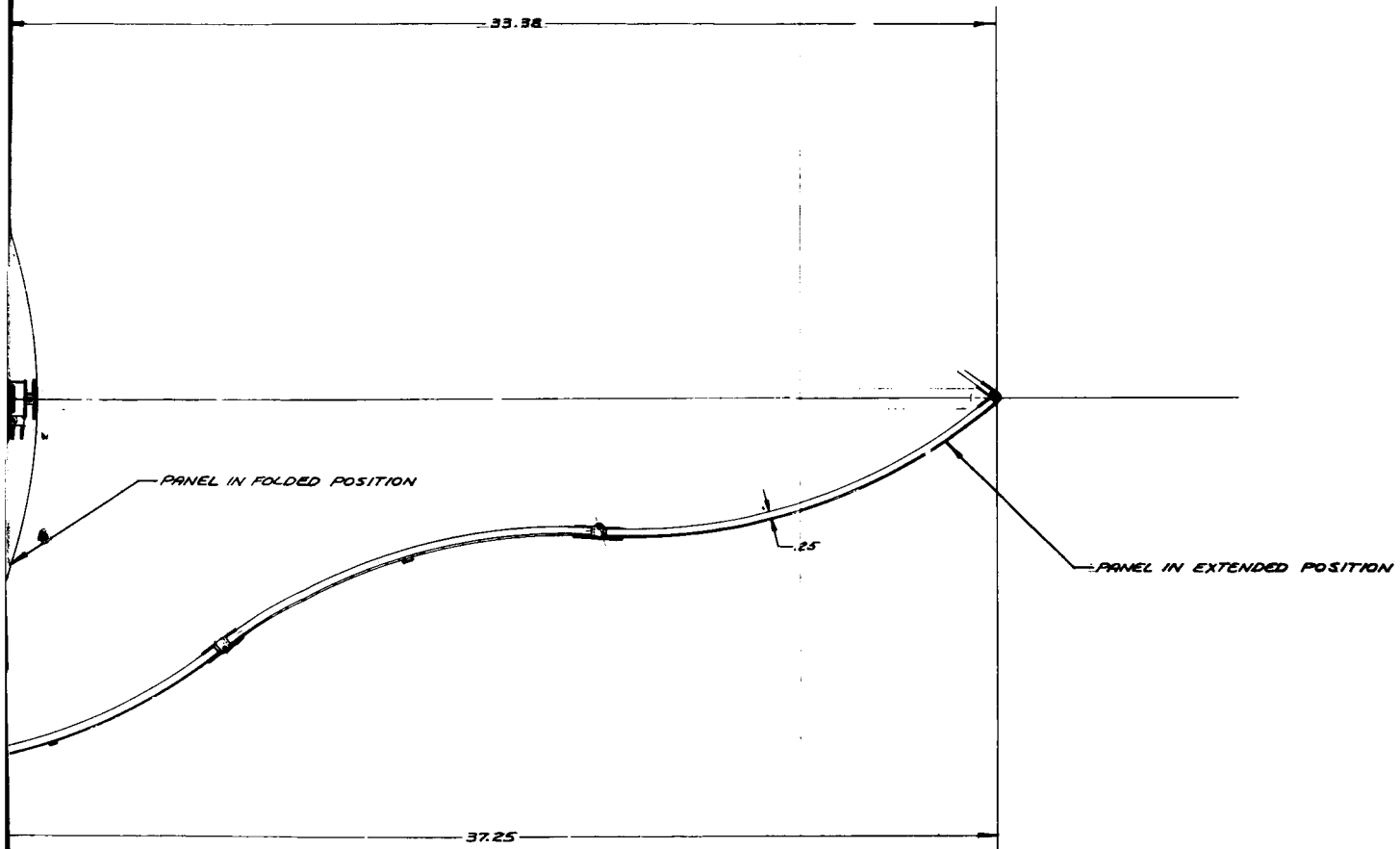


Figure 2-9. System 6 - Expanding Rigid Panels

2



QTY		PART OR IDENTIFYING NO.		MANUFACTURE OR DESCRIPTION		DATE	REVISION
UNLESS OTHERWISE SPECIFIED		DRAWN		DATE		LIST OF MATERIALS	
DIMENSIONS ARE IN INCHES		3-11-64		3 SEPT 64		HUGHES	
TOLERANCES ON DECIMALS		CHECKED		Bulley		HUGHES AIRCRAFT COMPANY CULVER CITY, CALIF.	
.001		.01		.001		TITLE	
.010		.03		.001		SYSTEM #6	
.03		.001		.001		EXPANDING RIDGID PANELS	
.001		.001		.001		CODE IDENT NO.	
.001		.001		.001		82577	
.001		.001		.001		X282032	
.001		.001		.001		SCALE 1/2	
.001		.001		.001		SHEET	
.001		.001		.001		1000 10 1000 10	

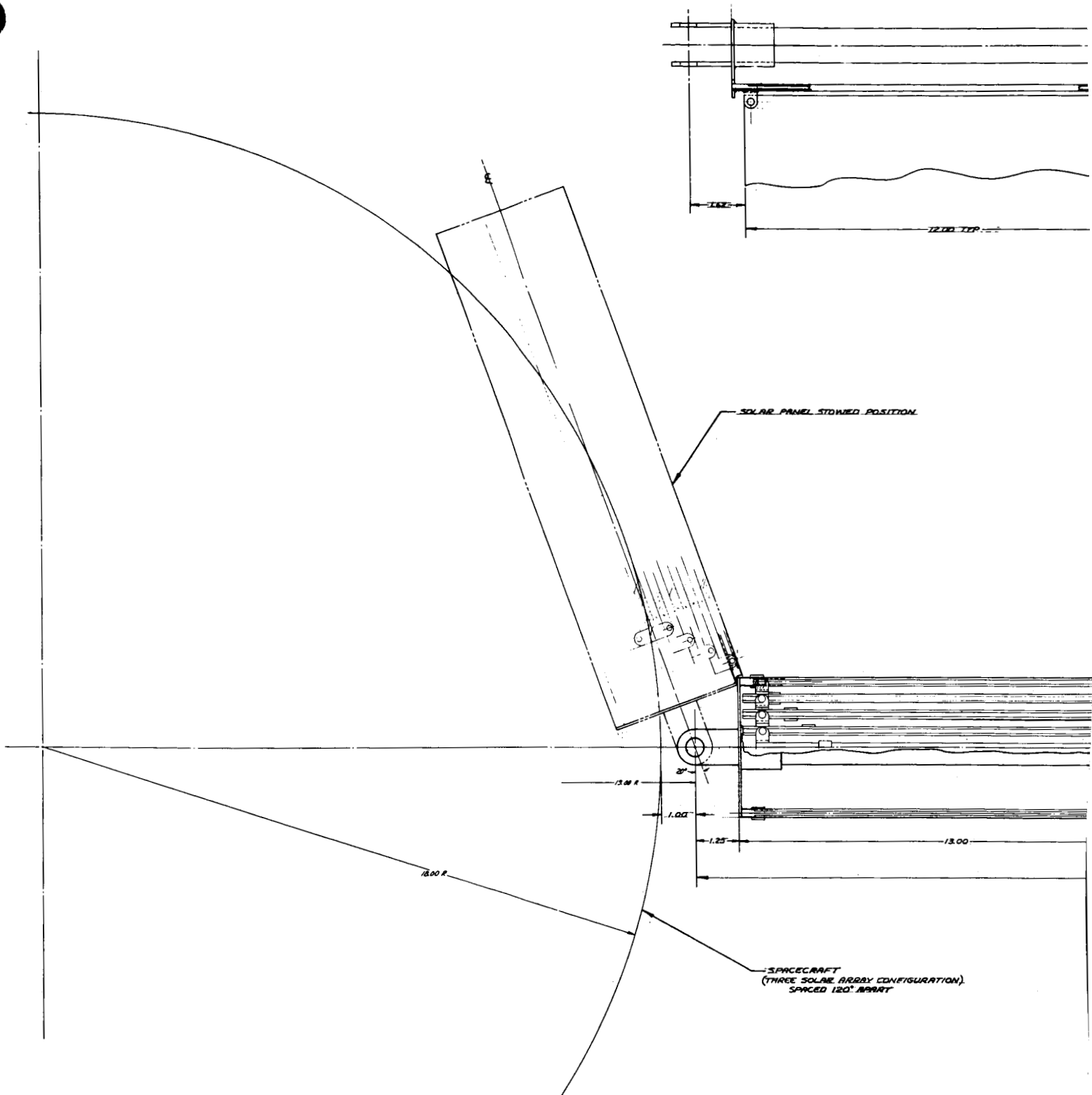
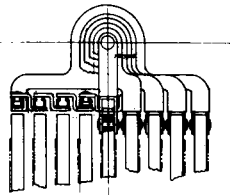
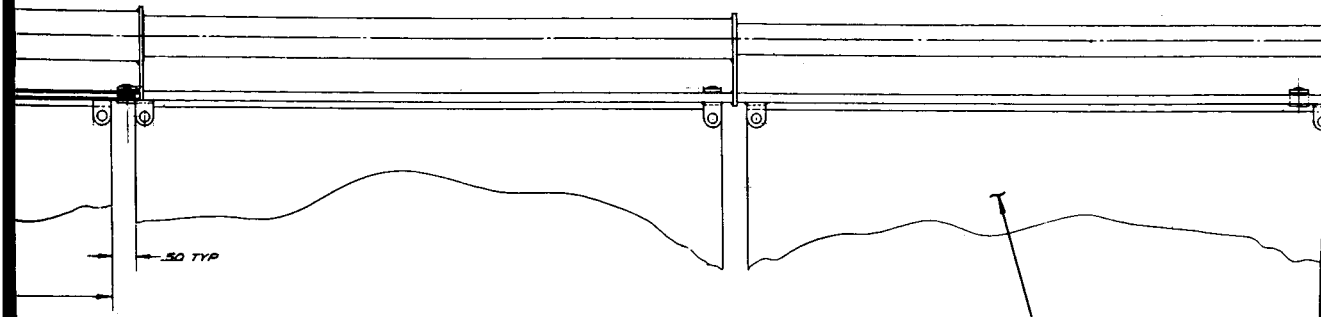
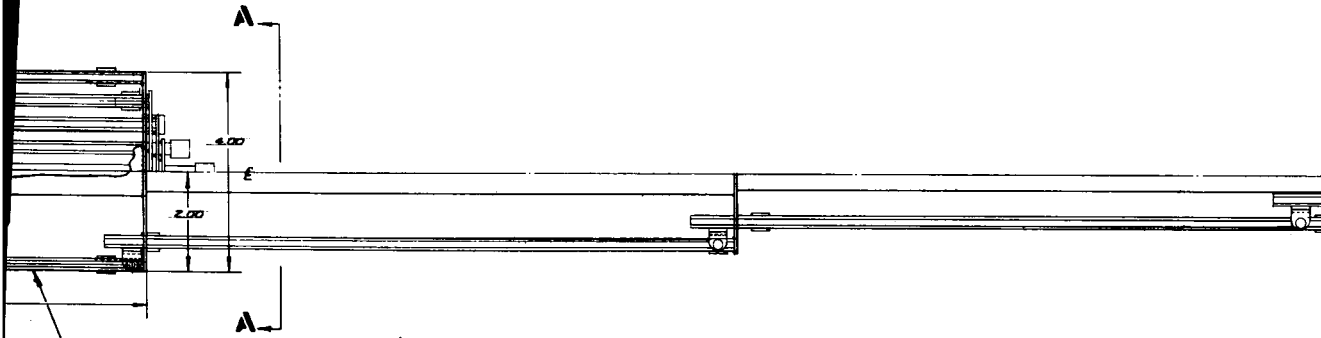


Figure 2-10. System 7 - Rigid Telescoping Panels

2

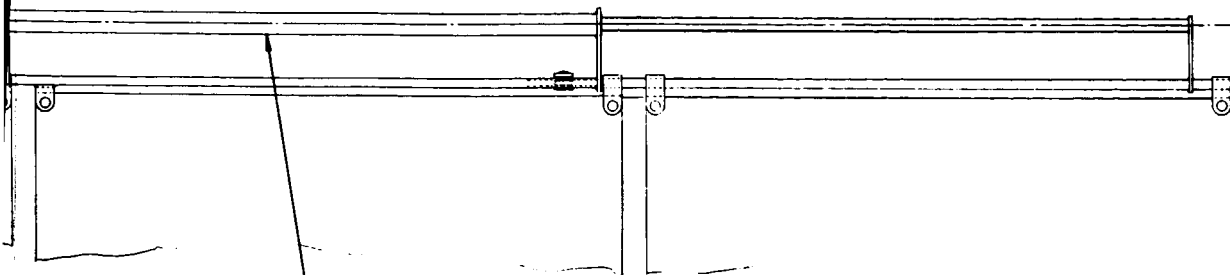


AA (ROTATED 30°)

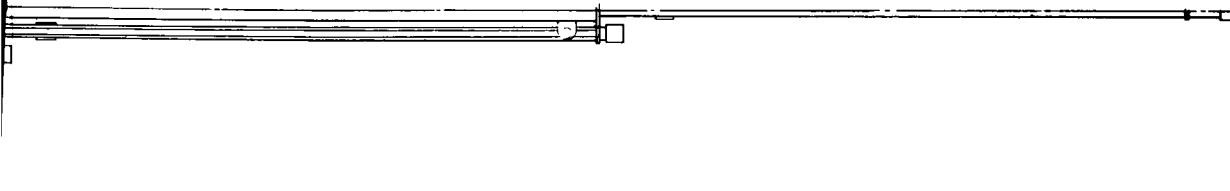


63.62

3



TELESCOPIC TUBE SUPPORT - 2 PLACES



UNLESS OTHERWISE SPECIFIED DIMENSIONS ARE IN INCHES TOLERANCES ON FRACTIONS		QUANTITY DESCRIPTION NO.		REVISIONS DESCRIPTION		DATE BY	
FRACTIONS		DECIMALS		FRACTIONS		DECIMALS	
.001		.005		.001		.005	
.010		.020		.010		.020	
.030		.040		.030		.040	
.050		.060		.050		.060	
.070		.080		.070		.080	
.090		.100		.090		.100	
.120		.140		.120		.140	
.160		.180		.160		.180	
.200		.220		.200		.220	
.250		.280		.250		.280	
.300		.320		.300		.320	
.350		.380		.350		.380	
.400		.420		.400		.420	
.450		.480		.450		.480	
.500		.520		.500		.520	
.550		.580		.550		.580	
.600		.620		.600		.620	
.650		.680		.650		.680	
.700		.720		.700		.720	
.750		.780		.750		.780	
.800		.820		.800		.820	
.850		.880		.850		.880	
.900		.920		.900		.920	
.950		.980		.950		.980	
1.000		1.020		1.000		1.020	
1.050		1.080		1.050		1.080	
1.100		1.120		1.100		1.120	
1.150		1.180		1.150		1.180	
1.200		1.220		1.200		1.220	
1.250		1.280		1.250		1.280	
1.300		1.320		1.300		1.320	
1.350		1.380		1.350		1.380	
1.400		1.420		1.400		1.420	
1.450		1.480		1.450		1.480	
1.500		1.520		1.500		1.520	
1.550		1.580		1.550		1.580	
1.600		1.620		1.600		1.620	
1.650		1.680		1.650		1.680	
1.700		1.720		1.700		1.720	
1.750		1.780		1.750		1.780	
1.800		1.820		1.800		1.820	
1.850		1.880		1.850		1.880	
1.900		1.920		1.900		1.920	
1.950		1.980		1.950		1.980	
2.000		2.020		2.000		2.020	
2.050		2.080		2.050		2.080	
2.100		2.120		2.100		2.120	
2.150		2.180		2.150		2.180	
2.200		2.220		2.200		2.220	
2.250		2.280		2.250		2.280	
2.300		2.320		2.300		2.320	
2.350		2.380		2.350		2.380	
2.400		2.420		2.400		2.420	
2.450		2.480		2.450		2.480	
2.500		2.520		2.500		2.520	
2.550		2.580		2.550		2.580	
2.600		2.620		2.600		2.620	
2.650		2.680		2.650		2.680	
2.700		2.720		2.700		2.720	
2.750		2.780		2.750		2.780	
2.800		2.820		2.800		2.820	
2.850		2.880		2.850		2.880	
2.900		2.920		2.900		2.920	
2.950		2.980		2.950		2.980	
3.000		3.020		3.000		3.020	
3.050		3.080		3.050		3.080	
3.100		3.120		3.100		3.120	
3.150		3.180		3.150		3.180	
3.200		3.220		3.200		3.220	
3.250		3.280		3.250		3.280	
3.300		3.320		3.300		3.320	
3.350		3.380		3.350		3.380	
3.400		3.420		3.400		3.420	
3.450		3.480		3.450		3.480	
3.500		3.520		3.500		3.520	
3.550		3.580		3.550		3.580	
3.600		3.620		3.600		3.620	
3.650		3.680		3.650		3.680	
3.700		3.720		3.700		3.720	
3.750		3.780		3.750		3.780	
3.800		3.820		3.800		3.820	
3.850		3.880		3.850		3.880	
3.900		3.920		3.900		3.920	
3.950		3.980		3.950		3.980	
4.000		4.020		4.000		4.020	
4.050		4.080		4.050		4.080	
4.100		4.120		4.100		4.120	
4.150		4.180		4.150		4.180	
4.200		4.220		4.200		4.220	
4.250		4.280		4.250		4.280	
4.300		4.320		4.300		4.320	
4.350		4.380		4.350		4.380	
4.400		4.420		4.400		4.420	
4.450		4.480		4.450		4.480	
4.500		4.520		4.500		4.520	
4.550		4.580		4.550		4.580	
4.600		4.620		4.600		4.620	
4.650		4.680		4.650		4.680	
4.700		4.720		4.700		4.720	
4.750		4.780		4.750		4.780	
4.800		4.820		4.800		4.820	
4.850		4.880		4.850		4.880	
4.900		4.920		4.900		4.920	
4.950		4.980		4.950		4.980	
5.000		5.020		5.000		5.020	
5.050		5.080		5.050		5.080	
5.100		5.120		5.100		5.120	
5.150		5.180		5.150		5.180	
5.200		5.220		5.200		5.220	
5.250		5.280		5.250		5.280	
5.300		5.320		5.300		5.320	
5.350		5.380		5.350		5.380	
5.400		5.420		5.400		5.420	
5.450		5.480		5.450		5.480	
5.500		5.520		5.500		5.520	
5.550		5.580		5.550		5.580	
5.600		5.620		5.600		5.620	
5.650		5.680		5.650		5.680	
5.700		5.720		5.700		5.720	
5.750		5.780		5.750		5.780	
5.800		5.820		5.800		5.820	
5.850		5.880		5.850		5.880	
5.900		5.920		5.900		5.920	
5.950		5.980		5.950		5.980	
6.000		6.020		6.000		6.020	
6.050		6.080		6.050		6.080	
6.100		6.120		6.100		6.120	
6.150		6.180		6.150		6.180	
6.200		6.220		6.200		6.220	
6.250		6.280		6.250		6.280	
6.300		6.320		6.300		6.320	
6.350		6.380		6.350		6.380	
6.400		6.420		6.400		6.420	
6.450		6.480		6.450		6.480	
6.500		6.520		6.500		6.520	
6.550		6.580		6.550		6.580	
6.600		6.620		6.600		6.620	
6.650		6.680		6.650		6.680	
6.700		6.720		6.700		6.720	
6.750		6.780		6.750		6.780	
6.800		6.820		6.800		6.820	
6.850		6.880		6.850		6.880	
6.900		6.920		6.900		6.920	
6.950		6.980		6.950		6.980	
7.000		7.020		7.000		7.020	
7.050		7.080		7.050		7.080	
7.100		7.120		7.100		7.120	
7.150		7.180		7.150		7.180	
7.200		7.220		7.200		7.220	
7.250		7.280		7.250		7.280	
7.300		7.320		7.300		7.320	
7.350		7.380		7.350		7.380	
7.400		7.420		7.400		7.420	
7.450		7.480		7.450		7.480	
7.500		7.520		7.500		7.520	
7.550		7.580		7.550		7.580	
7.600		7.620		7.600		7.620	
7.650		7.680		7.650		7.680	
7.700		7.720		7.700		7.720	
7.750		7.780		7.750		7.780	
7.800		7.820		7.800		7.820	
7.850		7.880		7.850		7.880	
7.900		7.920		7.900		7.920	
7.950		7.980		7.950		7.980	
8.000		8.020		8.000		8.020	
8.050		8.080		8.050		8.080	
8.100		8.120		8.100		8.120	
8.150		8.180		8.150		8.180	
8.200		8.220		8.200		8.220	
8.250		8.280		8.250		8.280	
8.300		8.320		8.300		8.320	
8.350		8.380		8.350		8.380	
8.400		8.420		8.400		8.420	
8.450		8.480		8.450		8.480	
8.500		8.520		8.500		8.520	
8.550		8.580		8.550		8.580	
8.600		8.620		8.600		8.620	
8.650		8.680		8.650		8.680	
8.700		8.720		8.700		8.720	
8.750		8.780		8.750		8.780	
8.800		8.820		8.800		8.820	
8.850		8.880		8.850		8.880	
8.900		8.920		8.900		8.920	
8.950		8.980		8.950		8.980	
9.000		9.020		9.000		9.020	
9.050		9.080		9.050		9.080	
9.100		9.120		9.100		9.120	
9.150		9.180		9.150		9.180	
9.200		9.220		9.200		9.220	
9.250		9.280		9.250		9.280	
9.300		9.320		9.300		9.320	
9.350		9.380		9.350			

At this design condition, the margin of safety is 0.65. For the small diameter drums, such as in systems 1 and 3 and using a similar 0.0012-inch thick retaining hoop, the stresses would be much lower and, consequently, a much greater margin of safety would result.

The basic study compared seven different configurations. In order to compare them fairly, all systems were based on a deployed solar array about 60 square feet and used panels about 2 feet wide. Consequently, these do not represent the maximum capability of these configurations. Panel dimensions can be varied resulting in longer panels as well as different widths. Figure 2-11 shows the watts-per-pound ratio plotted against deployed length of panel for a drum stowed configuration, system 1. Two panel widths, 12 and 22 inches, are shown on this curve. Both of the curves peak at an optimum panel length indicating that there is an optimum aspect ratio for different panel widths. However, large narrow panels are feasible with some sacrifice in the power-weight ratios.

The vibrational analysis made was to determine a method of packaging the flexible solar array in its stowed conditions during the launch cycle. In the stowed condition the flexible solar panels are protected from damage with a 0.15-inch thick open-cell polyurethane pad wrapped between each layer of solar panel. This assembly is compressed with sufficient pressure to prevent relative motion of the rolled-up layers during the vibration and acceleration of launching.

In order to determine this pressure, it was assumed that the force preventing relative motion of the rolled-up panel and cushion layers is due solely to the friction between the layers. The force that tends to cause any layer to move relative to the cushion adjacent to it due to an acceleration in the direction of the inner cylinder axis is:

$$F_m = G_L W p_p l \quad (2-1)$$

where l is the length of the layer, p_p is the weight per unit area of the layer, G_L is the launch acceleration in g , and W is the panel width.

The frictional force resisting movement of the layer relative to its adjacent cushion is

$$F_f = \mu l W P \quad (2-2)$$

where μ is the coefficient of static friction between the layer and cushion and P is the radial, uniformly distributed pressure on the layer applied by the outer cylindrical shell.

The condition for zero relative movement is F_f equal to F_m , so that

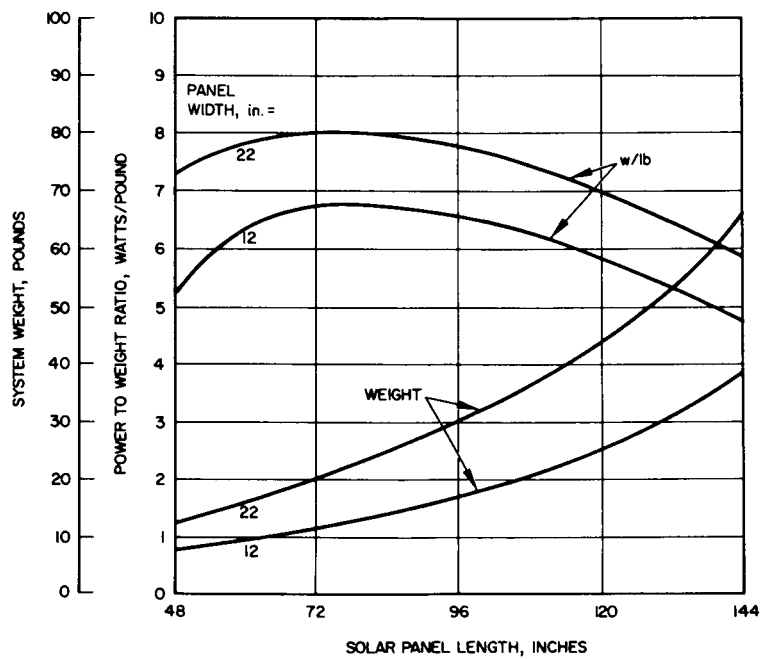


Figure 2-11. Power-to-Weight Ratio versus Length of Panel for Two Different Width Panels

System 1

$$P = \frac{p_p G_L}{\mu} \quad (2-3)$$

A value measured at Hughes for μ between a teflon film and an open-cell polyurethane foam cushion is 0.244. This value has been used to determine P , ignoring the added frictional resistance of the solar cells and wiring, to give an upper limit for the necessary pressure. A value of p_p , also measured at Hughes, including the weight of substrate, solar cells, 0.006-inch coverglass solder, adhesive, and wiring is 0.00229 psi. Using these values, Equation 2-3 shows that the pressure that must be applied by the outer shell to prevent relative motion during launch accelerations of 65 g is less than 0.61 psi.

WEIGHTS

The weight of the seven systems studied is summarized in Figure 2-5. Systems 1 through 4 were studied in more detail and, consequently, reflect more accurate weight analysis. The flexible-substrate chemically-rigidized systems appear to have the most favorable weight-to-power ratios. The rigid panel systems have much more mechanism and thus are heavier with poorer power-to-weight ratios. The weight of the different systems is shown in Figure 2-5.

RELIABILITY CONSIDERATIONS

The reliability of the systems studied can be analyzed only on a relative basis with the information available. These can be grouped in about three groups; i. e., group I — the chemically rigidized systems having essentially no moving parts and categorized by systems 1, 2, and 3; group II — the combination flexible panel with minimum mechanical actions categorized by system 4; and group III — the all-mechanical systems categorized by systems 5, 6, and 7. It would appear that group I, the flexible substrate system utilizing simple mechanical motion and mechanism, would be rated second. Group III, having the maximum of mechanism and mechanical motion, would be rated the poorest.

3. CHEMICAL RIGIDIZATION SYSTEM AND MATERIALS

CHEMICAL RIGIDIZATION SYSTEM

Chemical rigidization systems may be used to deploy a planar array and to maintain the solar array in the extended position. It is possible to deploy single and multiple tubular structures from a tight compact package to form a rigid frame. This frame would be more than adequate to support a solar array mounted on one of the flexible substrates previously described.

The basis of the chemical rigidization systems is the pre-impregnation of a plastic resin into a woven or sewn shape made of fiberglass or other woven cloth. The resin is stabilized in a highly viscous liquid condition so that the structure may be folded, compressed, wrapped, and otherwise packaged conveniently in a small volume. The structure is then deployed, usually by the inflation of lightweight internal tubes of polyethylene, and the curing of the resin is initiated and continued until a rigid reinforced plastic structure is formed.

The simplest example of this technique is the erection and rigidization of a circular tube. These may be produced from braided fiberglass sleeving or by sewing from standard fiberglass cloth. If sewn, the tubes may be tapered, have local reinforcement where required, and be constructed from multiple layers. Since there is a great variety of standard fiberglass weaves, many of which are designed with anisotropic strength properties, the designer can design tubular structures of great structural efficiency and low weight.

The use of a circular tube as an edge stiffener for a solar array is illustrated in Figure 3-1. In the packaged condition both the fiberglass and polyethylene tubes may be flattened and packaged with a packing factor of about 3. The inflation pressures required to erect most structures in a hard vacuum are usually only a fraction of a pound per square inch. Residual air, volatile liquids and solids, or controlled air inputs may be easily used to attain these pressures. In most cases, the erected structures would tend to retain their deployed configuration even though the inflation pressure was lost prior to rigidization, unless they were acted upon by unusual forces.

All of the pre-impregnated liquid resin systems are somewhat sticky and tend to block when one surface is folded on another. This situation may

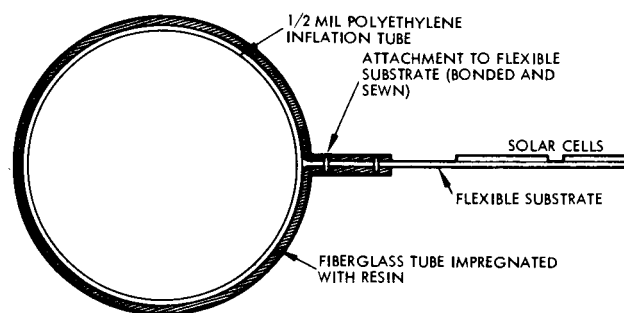


Figure 3-1. Cross Section of Rigidized Tube After Deployment

be eliminated by the use of parting films similar to the internal pressuring tubes. In some cases this tendency to stick may be utilized to control the manner and rate of deployment of the tube. The slow peeling of a spirally wound tube, either by initiating inflation at the outer tip or by the action of centrifugal force on a rotating satellite, would be most desirable compared to the sudden and erratic deployment that might occur in an unrestrained non-sticky system. A measure of the force required to unpeel the three prime rigidizing systems is given in the paragraph, Adhesion of Unrigidized Tubing.

A comparison of various rigidizing systems is given in Table 3-1. Of these systems, the first three, polyester, gelatin, and polyurethane, are all wet systems which are considered highly suitable for solar array use. These systems have been thoroughly tested for handling, storage, and curing properties and may be considered as developed systems. The remainder of the systems listed may be considered as partially developed systems that would require additional basic development to adapt them to use in the rigidization of solar arrays.

In addition to the systems listed in Table 3-1, the following systems have been proposed as having possibilities for very rapid curing:

- 1) A rapid curing epoxy in which the hardener is wiped on the pre-impregnated epoxy/fiberglass material from a separate reservoir during the movement of deployment.
- 2) A resin based on a low molecular weight polymer is adjusted to a high pH and impregnated into fiberglass. After erection, the action of acid fumes permeating the walls of the internal pressurizing tube cause a decrease in pH and a rapid cure (polymerization) of the resin.

The following factors common to all systems should be noted.

- 1) All systems will outgas to some extent during the rigidization process. However, the greatest outgassing will occur in the solvent release system (gelatin) in which the material released is water. The next greatest outgassing will take place from the polyurethane resin. Outgassing of the other systems will be dependent on the conditions of cure. The effect of outgassing on the performance of solar cells has been shown to be minor (see Outgassing Effect of Rigidizing Components on Solar Cells).
- 2) All pre-impregnated systems are catalyzed, except the gelatin and those listed specifically as noncatalyzed. The use of the catalyzed resin then results in the automatic rigidization under space conditions. At the same time the incorporation of the catalyst limits the storage life, however, the polyester and polyurethane systems are storable undeployed for at least 1 month.

- 3) All systems can be designed to have approximately the same tear and stretch resistance, since this would be a function of the fabric substrate.
- 4) All systems have good adhesive compatibility permitting attachment of the base of the tubes to the vehicle by established bonding procedures.
- 5) All pre-impregnated systems would be affected to some extent by the spinning. Spinning in the undeployed state would probably be less detrimental than spinning after deployment. Slow cure of the liquid impregnant would allow centrifugal forces to cause the liquid to "run" down to the extremities, thus resulting in a nonhomogeneous structure. However, testing of unrigidized gelatin, polyester, and polyurethane impregnated fabric has shown that only the gelatin system is significantly affected by this degree of centrifugal force. It is considered very possible to modify the gelatin formula to prevent the migration which did occur (see Effect of Centrifugal Force on Uncured Resins).

In summary, many systems exist for deploying and rigidizing structural members by the use of chemical rigidization. Most of the versatility of standard fiberglass laminates can be achieved using these systems. Three of the systems, gelatin, polyester, and polyurethane are considered to be ready for use with little further development.

Strength Properties of Space Rigidized Materials

The strength of space erected and cured flat laminates made from standard fiberglass cloths may be assumed to be approximately one half of that obtained from the same materials laminated under ideal conditions on earth. The designer therefore may use one half of the strength values given in such as standard references as MIL-HDBK-17 "Plastics for Flight Vehicles." The reduction in strength is due primarily to the lack of compaction (high porosity) of the space cured laminates.

Tests on Short Braided Tubing

In order to obtain a preliminary estimate the strength properties of circular tubes rigidized with the gelatin, polyester, and polyurethane resin system, braided fiberglass sleeving of various diameters was rigidized and tested (see Figures 3-2 through 3-6). The sleeving was obtained from the H. I. Thompson Company and is woven from type E fiberglass. The following types were used:

1/2-inch diameter, 0.020-inch wall	0.021 lb/ft
1-inch diameter, 0.015-inch wall	0.023 lb/ft
1-1/4-inch diameter, 0.015-inch wall	0.032 lb/ft

System	Unrigidized State					
	Length of Storage		Method of Packaging	Thermal Cycling	Vibration Effects	Specific Weight ₂ (0.020 inch approximate
	Room Temperature	-20 to +60° C				
Pre-impregnated polyester	1 to 3 months	-20° indefinite, 60° C for 30 days	Moisture resistant package	High temperature reduces storage life	Negligible	30
Pre-impregnated polyurethane resin	2 months	-20° indefinite, 60° C for 30 days	Must be kept in sealed container	High temperature reduces storage life	Negligible	32
Pre-impregnated gelatin	Indefinite	-20° indefinite, 60° C OK if in closed container	Closed container	No effect	Negligible	Approximately 65
Pre-impregnated heat curing epoxy	1 to 2 months	-20° indefinite, 60° C for 30 days	Moisture resistant package	High temperature reduces storage life	Negligible	27
Pre-impregnated one component urethane foam powder	Indefinite	No effect	Desiccated package	No effect	No effect	Not too applicable to flat sheets
Foam-in-place liquid urethane two-part system	Indefinite	No effect	Hermetic packaging	No effect	No effect	Not easily applicable to flat sheets
Pre-impregnated noncatalyzed systems	Indefinite	No effect	Moisture resistant packaging	No effect	No effect	30

TABLE 3-1. COMPARISON OF PROPERTIES OF SPACE-RIGIDIZED SYSTEMS

Activation Means	Cure Time, hours	Specific Weight oz. /yd ² (0.020 inch approximate)	Physical Properties (Approximate)		
			Flexural Strength, psi	Tensile Strength, psi	Tensile Modulus of Elasticity, psi
Ultraviolet radiation	1/3 to 4	30	15,000	18,000	1 x 10 ⁶
Water vapor introduced through walls of polyethylene tubes	2 to 16	30	10,000	18,000	5 x 10 ⁵
Loss of solvent by vacuum	4 to 24	35	10,000	15,000	5 x 10 ⁵
By infrared heat to 250° to 300° F	4 to 6	30	25,000	20,000	1.5 x 10 ⁶
By infrared heat 250° to 300° F	1 to 2	6 to 8 lb/ft ³	NA	NA	Compressive modulus 2-3 x 10 ³ ; compressive strength 10-25 psi
Self-activated	1/3 to 4	1 to 4 lb/ft ³	50 to 100 (strength of fabric is not included)	50 to 100 (strength of fabric is not included)	Compressive modulus 2-3 x 10 ³ ; compressive strength 10-25 psi
Dependent on system gas, or "wipe-on" catalysis	1/4	30	—	—	—

3

Rigidized State

Effects of Ultraviolet	Thermal Effects	Remarks
Fair to good	Not much up to 250° F	Assembly must be sun oriented for initial rigidization.
Good resistance	Not much up to 250° F	Because of vapor, catalyst system is mainly applicable to tubular type or sandwich structures; also requires special containers for water; must be sealed on ground and opened in space.
Good resistance	Not much up to 200° F	Very reliable, but has weight penalty and may have slight distortion due to shrinkage during cure.
Good resistance	Not much up to 250° F	Currently no easy means of applying heat and then reducing surface temperature; requires variable surface.
Fair to good	Good up to 250° F	Same drawback as above; most useful in rigidization of tubular members.
Good resistance	Good up to 160° F	May require development of special mixing, metering, and impregnation apparatus, and special vacuum operable resin system, therefore a weight penalty.
Dependent on system	Dependent on system	Gas catalysis systems have not worked well, so far, except urethane; catalyst "wipe on" probably only applicable to very thin wall systems (mechanically complicated).

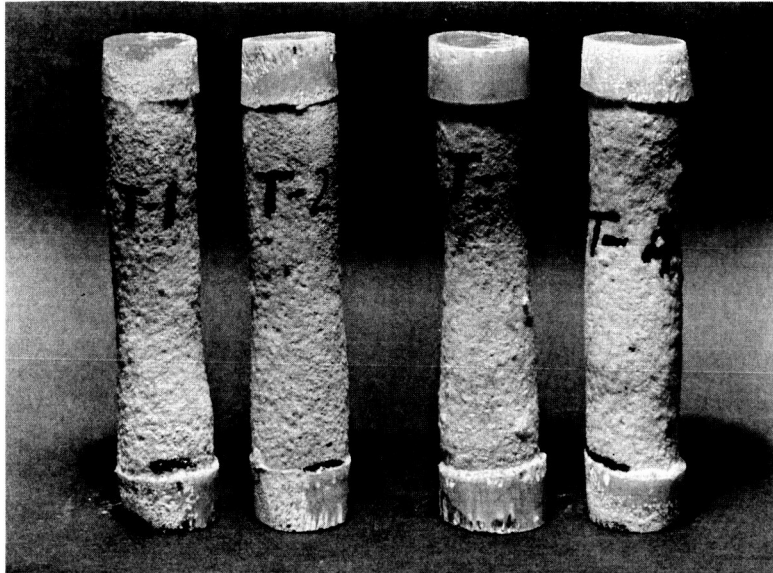


Figure 3-2. Tensile Test Specimens
Made from Braided Fiberglass
Sleeving Space-Rigidized
with Polyurethane

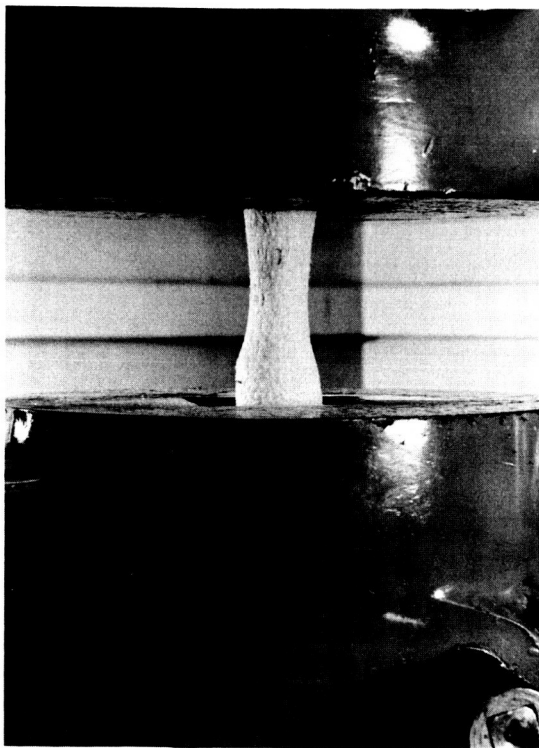


Figure 3-3. Elongation of Polyurethane Test Tube During Tensile Test

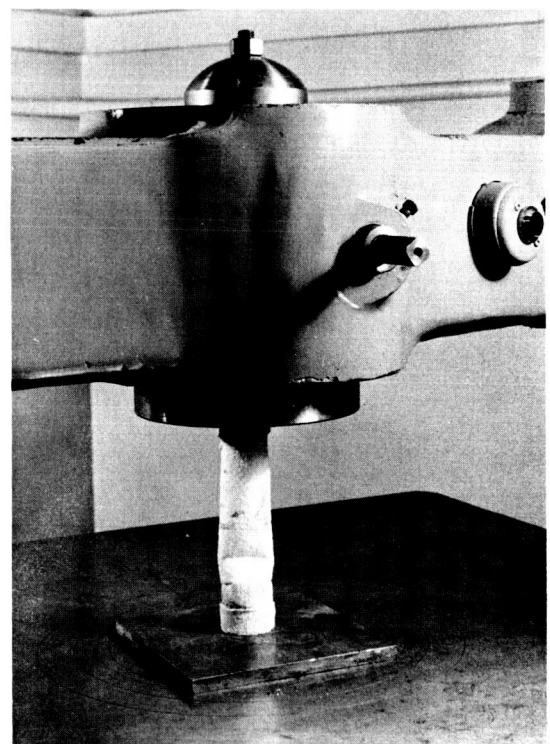


Figure 3-4. Failure of Polyurethane Tube During Compression Test



Figure 3-5. Flexural Specimen of Rigidized Tubing Fitted for Test as Cantilever Beam

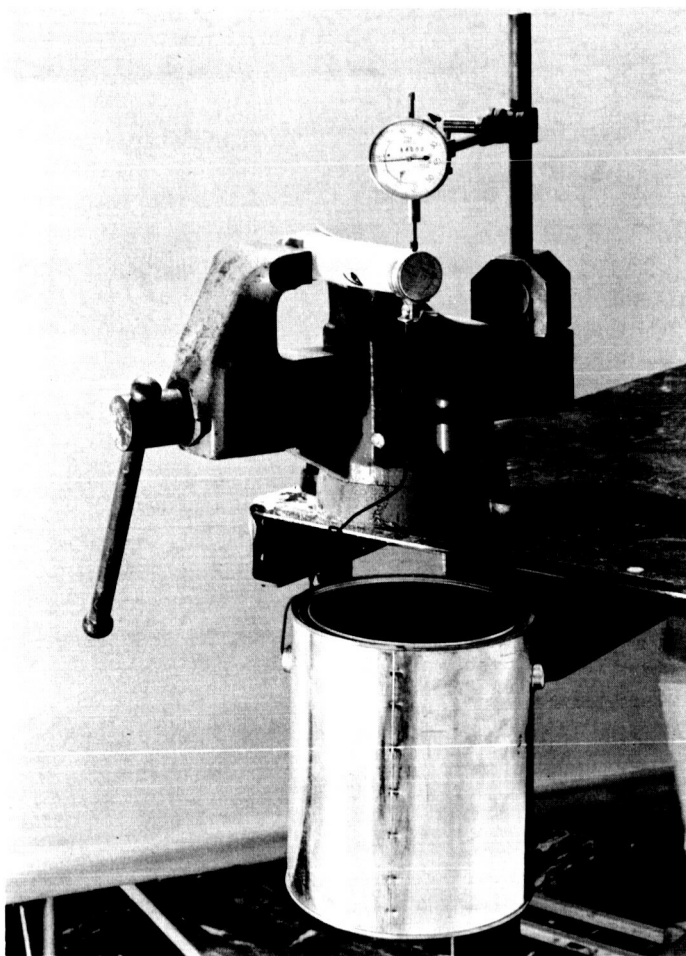


Figure 3-6. Setup for Flexural Testing of Short Tubes as Cantilever Beams Prior to Starting Test

The sleeves were chosen because they were convenient to test and readily available. The material does not represent the optimum strength which could be obtained from fiberglass tubes of equal weight, because the helical arrangement of the fibers is not optimum for the type of loading in the tests. All of the tests were performed by making specimens with a length to diameter ratio of four or greater and encapsulating the ends to preclude edge failures. The load deflection curve for a gelatin rigidized tube is shown in Figure 3-7.

The results of the flexural, tensile, and compressive tests of braided tubing are shown in Tables 3-2 and 3-3. The load carrying ability of the tubes is excellent, especially when it is considered that these tubes were all automatically erected and rigidized in a vacuum chamber. The results are therefore strongly indicative of what could be obtained by rigidizing techniques in space.

Test on Long Cloth Tubes

In order to obtain some quantitative information on the flexural properties of 6-foot tubes, several were made using different configurations and constructions. Tapered tubes were fabricated 2 inches in diameter at the base and 1 inch in diameter at the tip. They consisted of constructions using both 1 and 2 plies of style 181 cloth and 2 plies style 120 cloth. Straight tubes using 1/2-inch diameter, 1-inch diameter, and 1-1/3 inch-diameter braided cloth tubes were also prepared. All tubes were impregnated with polyester resin and laid over an inflated polyethylene tube used as a mandrel.

The flexural tests were performed by potting one end (the larger one in the case of tapered tubes) and clamping it in a vise parallel to the floor. A small cup was tied to the other end and then lead shot in 1/10-pound increments was added every 20 seconds. The amount of shot needed to break the tube was then determined. The results are shown in Table 3-4. A 1-inch diameter braided tube bent until it touched the floor but did not break. After the weight was removed, the tube sprang back but was permanently deformed with a deflection of approximately 22 degrees from its original parallel position.

The breaking loads for the tubes appear at first to be low. However, all the tubes except the braided gelatin tube previously mentioned failed in buckling at some wrinkle or other flaw in the tube. This buckling usually occurred at the grips where the moment arm was greatest. Such flaws can be eliminated by improved techniques, tubes could be obtained that would undoubtedly support much higher loads.

Outgassing Effect of Rigidizing Components

Three different chemical rigidization systems (gelatin-water, polyester resin, and polyurethanes) were considered for the inflatable support tubes for the deployable solar array system. All the systems, while differing

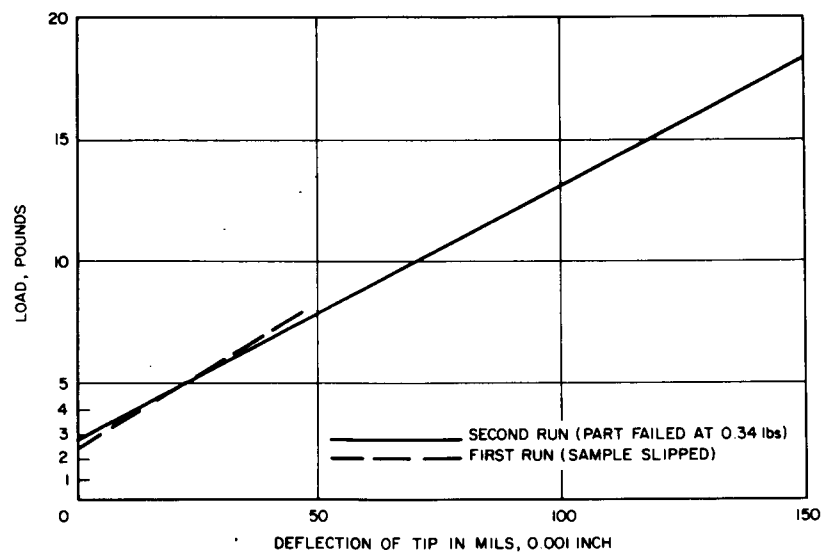


Figure 3-7. Load Deflection Curve for 1-inch-Diameter Braided Tube Impregnated with Gelatin

TABLE 3-2. FLEXURAL PROPERTIES OF IMPREGNATED BRAIDED TUBES

Type of Material	Approximate Tube Diameter, inches	Approximate Wall Thickness, inches	Span Length, inches	Specimen Number	Breaking Load, pounds	Remarks
Polyester-braided tube	1-3/16	0.015	5-27/32	F-1	—	Held at 20 pounds, applied at rate of 1 pound per minute
	1-1/4	0.015	5-21/32	F-2	—	Held at 21 pounds; applied at rate of 1 pound per 20 seconds; slipped in vice
	1-3/16	0.015	4-7/8	F-3	15	Load applied at rate of 1 pound per 20 seconds; failure induced prematurely by clamp holding 1 inch wide bar used to prevent specimen from slipping
	29/32	0.015	4-3/32	F-1	14	Load applied at rate of 1 pound per 20 seconds; 1 inch wide bar used to prevent specimen from slipping
	31/32	0.015	4-1/8	F-2	28	Load applied at rate of 1 pound per 20 seconds; 1 inch wide bar used to prevent specimen from slipping
Polyurethane braided tube	1-1/4	0.015	4-5/8	F-1	15	Load applied at rate of 1 pound per 20 seconds; 1 inch wide bar used to prevent specimen from slipping
	1-3/16	0.015	5-13/16	F-2	15-1/2	Load applied at rate of 1 pound per 20 seconds
	1-5/32	0.015	5-7/8	F-3	10	Load applied at rate of 1 pound per 10 seconds until a maximum of 10 pounds; specimen was held under 10-5/4 pounds (3/4 pound for weight of container) and buckled 5 minutes after start of test
	1-3/16	0.015	4-13/16	F-4	9	Load applied at rate of 1 pound per 20 seconds; failure induced prematurely by clamp holding 1 inch wide bar used to prevent specimen from slipping
	1	0.015	4	F-1	22	Load applied at rate of 1 pound per 20 seconds; 1 inch wide bar used to prevent specimen from slipping
Polyurethane braided tube	1	0.015	4	F-3	21	Load applied at rate of 1 pound per 20 seconds; 1 inch wide bar used to prevent specimen from slipping
	5/8	0.020	2-13/16	F-3	14-1/2	Load applied at rate of 1 pound per 20 seconds; 1 inch wide bar used to prevent specimen from slipping
	3/16	0.020	1-7/8	F-1	13	Load applied at rate of 1 pound per 20 seconds; 1 inch wide bar used to prevent specimen from slipping
	1-1/4*	0.015	5-1/2	F-1	23	Load applied at rate of 1 pound per 20 seconds
Gelatin-braided tube	1-1/16	0.015	5-1/8	F-1	34	Load applied at rate of 1 pound per 20 seconds; specimen tested twice, first time specimen slipped in vice at 18 pounds; test started a second time from beginning
	1/2*	0.020	4	F-1	19	Load applied at rate of 1 pound per 20 seconds

*Approximate outer diameter.

TABLE 3-3. TENSILE AND COMPRESSIVE PROPERTIES OF IMPREGNATED
BRAIDED TUBES

Type Braided Tube	Outer Diameter, inches	Breaking Tensile Load, pounds	Breaking Tensile Load, (average), pounds	Tensile Elongation, percent	Tensile Elongation, (average), percent	Compressive Strength, psi	Compressive Strength, (average), psi
Polyester	1-1/4	720 620 640	660	42 38 10	30	5800 7150 5730	5225
	1	1800 1760 1500 1450	1628	40 24 41 22	31.8	9200 4630 7620	7150
	1-1/4	1083 953 997 681	928	51 38 36	41.7	2750 2460 2150 4130	2872
Urethane	1	1910 1990 1915 1920	1934	43 26 35 44	37.0	7770 7350 6800 7900	7435
	1/2	3850 365 340	363	4 — 6	5	3430 4890 2960 5260	4135
	1-1/4	540 425	482	51 —	51	—	—
Gelatin	1	1175 940	1058	59 59	59	—	—
	1/2	700 700 450	617	— — —	—	—	—

TABLE 3-4. FLEXURAL TEST OF 6-FOOT POLYESTER TUBES

Construction of Tube	Breaking Load, pounds	Remarks
Tapered tube 2 to 1 inches, two plies No. 120 cloth	0.1	Load applied at rate of 0.1 pound per 20 seconds
Tapered tube 2 to 1 inches, one ply No. 181	0.7	Load applied at rate of 1 pound per 20 seconds
Tapered tube 2 to 1 inches, two plies No. 181	1.4	Load applied at rate of 0.1 pound per 20 seconds
Braided straight tube 1-inch diameter	Touched floor after 1.2-pound load but did not fail	Load applied at rate of 0.1 pound per 20 seconds; after load removed, tube deformation was 22 degrees from its original horizontal axis
Braided straight tube 1/2-inch diameter	0.3	Load applied at rate of 0.1 pound per 20 seconds

chemically, have the common characteristic of high volatile release in the period between initial exposure to the vacuum environment and final rigidization. It was therefore considered necessary that tests be made to determine if this outgassing would affect the solar cell output.

A test solar cell was mounted by heat conductive cement, on a small jacketed copper plate that could be maintained at approximately 32°F. The assembly was enclosed in a quartz-Vycor tube that was also connected to a liquid nitrogen trap and a mechanical and mercury diffusion pump. A resin-impregnated fiberglass sample, approximately 1 by 3 inches, was also contained in the lower half of the tube. (This size sample gave a ratio of fiberglass to cell area that would be many times the actual ratio in service.) The copper plate was approximately an inch above the fiberglass sample and inclined at a 45-degree angle to ensure impingement of the volatiles on the cell. A similar cell was mounted on the outside of the transparent chamber to be used as a comparison standard. Figure 3-8 illustrates the setup, showing the vacuum train, the Veeco vacuum gage and mechanical and mercury diffusion pumps, and the cell cooling pump and illumination equipment. Figure 3-9 is a closeup of the test chamber showing the fiberglass sample wrapped in cellophane (but not sealed), the test cell, and the standard cell mounted on the exterior of the test chamber.

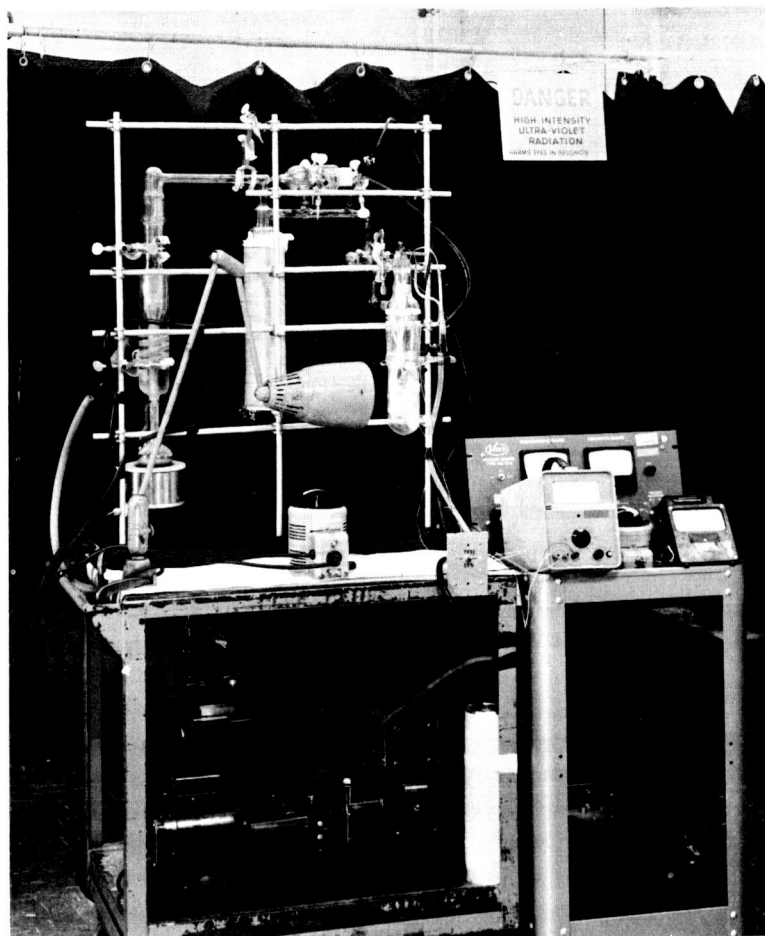


Figure 3-8. Vacuum Test Setup for Determining Effect of Rigidization Component Outgassing on Solar Cell Efficiency

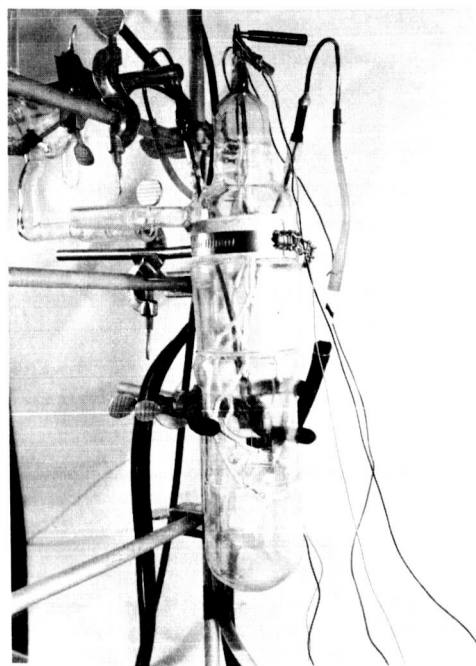


Figure 3-9. Closeup of Vacuum Test Chamber

Each solar cell was shunted with a 1.0-ohm precision resistance, and a Kintel Electronic Galvometer, Model 204a, was used to measure the output voltage during test. Illumination was furnished by a 150-watt incandescent bulb run at 100 ± 0.5 volt using a Variac for adjustment and a Sola constant voltage transformer to maintain a uniform voltage.

Test Method

- 1) Prior to establishing a vacuum in the chamber, the test solar cell was cooled to 32 to 35°F by circulating ice water through the mounting plate.
- 2) The voltage output of the test cell and the standard cell was then determined at the uniform illumination.
- 3) The vacuum was then drawn in the chamber and the temperature of the fabric sample and cell was monitored at small time intervals. The electrical output of each cell was also monitored to detect any changes. Each test was continued until rigidization was complete.

In no case was there any significant change in the output voltage of the test cells. The gelatin solution impregnated sample showed a considerable change in temperature, dropping to approximately 12°F as a result of the rapid evaporation of water. This temperature, however, soon rose above that of the solar cell so that condensation could have taken place.

Conclusions

On the basis of the tests run it may be concluded that there will be no significant effect on the solar cells from outgassing by any of the chemical systems.

Examples of typical test results are shown in Table 3-5.

Effect of Centrifugal Force on Uncured Resins

The effect of centrifugal force on the composition of resin-impregnated, unrigidized braided fiberglass sleeving was determined by whirling specimens under controlled conditions to simulate forces to which such materials will be subjected in the deployed state prior to rigidization.

Some tests were conducted in a standard laboratory centrifuge, while others were made using a small turntable. In all tests, the speed was either adjusted for a given radius, or visa versa, to simulate the centrifugal force experienced by an object rotating at a distance of 8 feet from the center of rotation at 40 rpm. After running the polyester tests on the turntable, it was found that the actual speed was somewhat higher than supposed. This resulted in a force approximately twice as great as desired. Since the polyester-impregnated sleeving withstood the tests without undue change in composition,

TABLE 3-5. TEST RESULTS

Time	Test Cell		Standard Cell, volts	Line Voltage	Sample Temperature, °F	Pressure, microns
	Temperature, °F	Volts				
Gelatin-Water Impregnant						
3:40 pm	37	0.00795	0.00640	100	62	>1000
3:44 pm	32	0.00800	0.00640	100	22	500
3:45 pm	32	0.00800	0.00635	100	17	225*
3:49 pm	30	0.00800	0.00635	100	12	225
3:53 pm	24	0.00785	0.00605	100	16	225
4:00 pm	24	0.00780	0.00605	100	20	225
4:15 pm	25	0.00775	0.00615	100	26	225
4:30 pm	27	0.00765	0.00615	100	49	225
4:45 pm	30	0.00760	0.00620	100	61	225
5:00 pm	25	0.00755	0.00620	100	74	400**
5:30 pm	25	0.00740	0.00620	100	74	500
9:10 pm	60	0.00765	0.00620	100	74	500
8:30 am	30	0.00755	0.00630	100	70	500
Polyester Resin Impregnant						
2:29 pm	25	0.00780	0.00645	100	60	>1000
2:32 pm	25	0.00790	0.00700	100	67	200
2:34 pm	25	0.00800	0.00700	100	69	125
2:40 pm	25	0.00800	0.00705	100	78	75
3:10 pm	25	0.00820	0.00705	100	89	33
3:45 pm	25	0.00805	0.00705	100	92	13
4:40 pm	25	0.00805	0.00700	100	91	15
5:00 pm	25	0.00805	0.00700	100	93	12
Polyurethane Resin Impregnant						
9:30 am	30	0.00830	0.00660	100	60	>1000
9:35 am	30	0.00845	0.00670	100	58	55
11:00 am	30	0.00765***	0.00600	100	65	15
11:30 am	30	0.00785	0.00605	100	73	15
12:00 n	30	0.00790	0.00610	100	86	15
1:30 pm	30	0.00795	0.00600	100	89	13
2:00 pm	30	0.00790	0.00610	100	90	13
3:30 pm	68	0.00790	0.00605	100	91	13
5:00 pm	68	0.00790	0.00605	100	92	13

*Pressure was limited to vapor pressure of water and slight leakage.

**Equipment leakage increased.

***Cooling line plugged, during adjustment illumination lamp was inadvertently moved.

Note: It should be noted that the data shown for the polyester and polyurethane samples include exposure to approximately one solar equivalent ultraviolet exposure. This then accounts for the higher temperatures reached by the samples.

the tests were not repeated. The urethane and gelatin tests were run at the correct speed.

The resin content of various portions of each test piece was determined by ignition in a muffle furnace. For those cases in which the impregnated braid was enclosed in polyethylene tubing, this was removed, washed and weighed prior to ignition to allow an accurate resin content to be calculated.

Polyester

The polyester formulation used consisted of 100 parts by weight (pbw) of Hetron 103, 2 pbw of Benzoyl Peroxide, 2 pbw of Benzoin, 2 pbw Cab-O-Sil and 3 to 5 pbw of acetone to improve the wetting action. The sleeving was impregnated by hand dipping. The excess resin was removed by passing the material through a hand washing machine roller assembly with the pressure adjusted to give material with a resin content of 40 to 45 percent. After air-drying for 30 minutes, coated sleeving was placed between thin sheets of polyethylene. Four-inch lengths, cut from the impregnated material, were cut into two lengthwise strips. One strip was retained as a control while the corresponding strip was whirled in either the centrifuge or the turntable.

One hour in the centrifuge at 140 rpm (equal to 40 rpm, 8-foot radius) resulted in no appreciable difference in composition. Five hours in the centrifuge caused changes in composition as high as 10.7 percent. These results were considered to be doubtful, since during the test, the sample was draped over the edge of a brass centrifuge cup which assumed a 45-degree angle during rotation. Thus about half of the material was supported laterally by the cup while the other was not.

Three runs were made on the turntable at a radius of 12 inches and what was thought to be 78 rpm was found, later, to be 170 rpm. The first run for 1 hour resulted in slight changes up to a maximum 1.4 percent. The second run for 5 hours gave maximum changes of 7 to 8 percent. A third test run in the full sunlight gave a maximum random variation of 0.4 percent which is negligible.

Gelatin

The gelatin formulation used consisted of 100 pbw of Swift's 6/20 gelatin, 200 pbw of water, 0.1 pbw Triton CF-21 wetting agent, 0.1 pbw Dowcide G, 7 parts Thiourea (liquidizer) and 4 pbw of Cab-O-Sil. The coating of the sleeving was accomplished in the same way as the coating of the polyester. Initial formulations that did not contain the Cab-O-Sil coated on glass sleeving were found to migrate excessively when subjected to centrifugal force. By the addition of the Cab-O-Sil and the reduction of the resin solids from 50 to 20 percent, this problem was completely eliminated.

Urethane

The urethane formulation consisted of 100 pbw of Wyandotte urethane resin PR-1502-E6, 0.5 pbw of trimethyl piperazine, 10 pbw of Toluene. Glass sleeving was impregnated in the same manner as with the polyester and gelatin. Impregnated sleeving was covered with thin polyethylene to exclude atmospheric moisture as much as possible. The rotation of test samples containing as much as 40 percent resin solids resulted in virtually no migration of resin.

Conclusions

From the results obtained, it appears that all three candidate resin systems can be utilized without fear of excessive resin migration prior to rigidization. The resin solids of the gelatin structures will have to be kept at or below 20 percent with the present composition.

Adhesion of Unrigidized Tubing

Long strips of 1-inch diameter glass sleeving impregnated with the standard formulations of polyester, gelatin, and urethane were wrapped about a 12-inch diameter drum. At least two complete turns of material were wrapped around the drum. After peeling away a 3/4-inch length, a small hook was attached to the end. Small weights (loops of wire) were carefully added to the hook until peeling started. Once started, the peeling process accelerated since the weight of the peeled material was added to the original weight. The weight in grams necessary to initiate peeling along with the unit weight were as follows:

	<u>Weight, grams</u>	<u>Grams per Lineal Inch</u>
Polyester	2.76	3.47
Urethane	1.71	3.53
Gelatin	5.30	3.99

Results show that the magnitude of the force required to initiate peeling is small as previously discussed; this force may be utilized to prevent erratic deployment. Special mechanisms will not be required to unfurl the impregnated tubing.

PHYSICAL PROPERTIES OF SUBSTRATE MATERIALS

Substrate materials are used in sheet form as platforms to which the solar cells are bonded. These substrates may be either flexible or rigid. The flexible substrates have the distinct advantage of compact packaging but they must be supported in space by some type of rigid frame. The rigid or self-supporting substrates are seen as being deployed by purely mechanical means. The inherent bulkiness and difficulty of packaging the rigid materials is increased by the necessity of using these materials in sandwich form. Flat sheets of the rigid materials are inefficient and excessively heavy because of their low stiffness compared to sandwich forms that utilize very thin face sheets and low density cores.

Desirable characteristics of all substrate materials may be listed as follows:

- 1) Electrically insulating surface
- 2) Resistance to damage from soldering and other manufacturing operations
- 3) Low elongation and high tensile strength
- 4) Stability in space environment particularly with respect to hard vacuum and ultraviolet radiation and extremes of temperature
- 5) Low absorptivity-to-emissivity ratio of the surface to prevent excessive temperatures due to solar radiation
- 6) Surface suitable for bonding

Flexible Substrate Materials

The rigorous requirements for substrate materials serve to eliminate most flexible sheet materials from serious consideration. Only two materials, a glass reinforced teflon, and polyamide film (H Film) are suitable, and both of these materials must have specially treated surfaces to assure good bonding.

Tests were conducted to determine the tensile strength of these two flexible substrates for deployable solar arrays. One material consists of TFE teflon on 1-mil glass fabric (EX 317-Taconic Plastics), the other a polyamide film coated on one side with FEP teflon (H Film - DuPont). Both were tested at room temperature and 300° F in an unetched and etched condition (etched per HP 4-130). Results are shown in Table 3-6.

The EX 317 tested contains a starch sizing on the cloth that acts as a lubricant to prevent fibers in the cloth from abrading one another. This sizing gives a tan color to the fabric. A "white" EX 317, which has no starch, is reported to have 10 to 15 percent less tensile strength than the regular EX 317.

The results of strength testing show that both materials are strong in tension and that they retain a large proportion of this strength at 300° F. Etching of the surface for bonding of TFE fiberglass material does not appear to be deleterious. It should be noted that the TFE fiberglass is highly anisotropic and care would be necessary to properly orient this material with respect to the loads in use. However, if the design permits the use of the highly directional material, it offers a considerable advantage in weight compared to the H film.

Rigid Substrate Materials

A great variety of face and core materials exists for use in sandwich-type structures. The use of sandwich configuration in rigid lightweight structures is commonplace in the aerospace industry. The choices of materials becomes more limited however when extreme lightness is required. The lightest honeycomb core materials in production have apparent densities of the order of 2 lb/ft³ for both the aluminum and fiberglass varieties. Rigid foams are available in lower densities but are difficult to work with and excessively fragile in densities lower than 1.5 lb/ft³. Similarly, it is very difficult to fabricate sandwich structures with face sheets thinner than 0.001 inch for aluminum and 0.003 inch for fiberglass. For instance, the rigid solar cell panels used on the Syncom and Comsat are approximately 1/4-inch thick and weigh about 0.27 lb/ft² of area including the weight of inserts and edge seals. These panels are considered to be close to the ultimate in lightness for conventional sandwich materials. The panels have 0.003-inch thick fiberglass-epoxy faces cured directly on a 2.0 lb/ft³ aluminum honeycomb without the use of separate adhesives.

The recent development of mylar honeycomb provides a new lightweight material for rigid sandwiches. Ordinarily unprotected mylar is not considered to be suitable for space use because of its rapid degradation by ultraviolet light. In a rigid sandwich, however, the honeycomb material would be protected by the faces. Coatings would be applied to the exposed surface for additional protection. The available properties of mylar honeycomb are compared to the conventional aluminum and fiberglass honeycomb in Table 3-7. Additional information on actual sandwiches is provided in Table 3-8 in which the properties of a typical lightweight honeycomb sandwich (fiberglass core and faces) are compared with an all-mylar honeycomb. The strength of the mylar honeycomb, although low, is probably quite adequate for this type of mission.

TABLE 3-6. TENSILE STRENGTH (ASTM D 882) OF
FLEXIBLE SUBSTRATE MATERIALS

Substrate Material	Specimen Direction	Substrate Condition	Test Temperature, ° F	Pounds per Inch (width)
EX 317 *(TFE on 0.001-inch glass cloth) Total thickness 0.0012 inch 0.012 lb/ft ²	Longitudinal	Unetched	Room temperature	31.1
			300	29.4
		Etched	Room temperature	34.0
			300	35.3
	Transverse	Unetched	Room temperature	4.1
			300	12.6
H-Film with FEP coating Total thickness 0.0055 inch 0.039 lb/ft ²	**Longitudinal	Unetched	Room temperature	42.1
			300	37.1
		Etched	Room temperature	54.7
			300	36.1

*Material tested contained starch sizing on the glass. Starch free or white material has 10 to 15 percent less breaking strength.

**Material tested not wide enough to cut specimens in transverse direction.

Type of Honeycomb	Density, lb/ft ³	Cell Size, inches	Thickness, inch	Flatwise Compression, psi		Flatwise Compressive Modulus, psi	Flexural Shear, psi		Flexural Shear Modulus, psi	
				Without Skins	With A-1 Skins		Length	Width	Length	Width
Heat resistant phenolic	2.2	3/8	0.500	100	122	10,000	120	70	9,000	4,000
Aluminum	2.0	3/16	0.500	140 (80-3 σ)	—	45,000 (24,000-3 σ)	125 (76-3 σ)	78 (46-3 σ)	26,500 (17,500-3 σ)	14,300 (9,000-3 σ)
Mylar type A	2.0	3/8	0.500	78	89	—	100	4,798	38	1,593
Mylar type A	1.0	3/4	0.500	19	26	—	15	1,586	8	770
Mylar type A	2.0	3/8	0.256	85	89	5,736	—	—	—	—
Mylar type A	1.0	3/4	0.256	21	33	1,282	—	—	—	—
Mylar type A	0.5	1-1/2	0.256	4	8	—	—	—	—	—

*These values reported by Hexcel Products, Inc.

TABLE 3-7. PHYSICAL PROPERTIES OF TYPES OF HONEYCOMB
SUITABLE FOR SUBSTRATE*

Type of Honeycomb and Facings	Apparent Density, lb/ft ³	Cell Size, inches	Thickness of Sandwich, inches	Flatwise Compressive at RT, psi		Flexural Core Shear at RT, psi			
				Individual	Average	Individual (Ribbon)	Average (Ribbon)	Individual Transverse	Average Transverse
Heat resistant phenolic honeycomb, 2.2 lb/ft ³ density with 0.0035-inch epoxy fiberglass faces	5.6	3/8	0.230	157 152 193	167.3	33.5 51.0 36.0	40.2	20.2 20.3 19.6	20.0
Mylar honeycomb, 0.5 lb/ft ³ density, with 0.002-inch mylar faces	1.9	1-1/2	0.600	10.4 16.5 11.0	12.6	2.76 1.41 10.50	4.89	2.68 3.42 3.60	3.23

TABLE 3-8. PHYSICAL PROPERTIES OF LOW DENSITY HONEYCOMB
SANDWICHES SUITABLE FOR SUBSTRATE

The heat resistant phenolic and mylar honeycomb were obtained from Hexcel. The former had a cell size of 3/8 inch and a thickness of 0.230 inch, the latter a cell size of 1-1/2 inch and a thickness of approximately 0.600 inch. Style 103 cloth impregnated with epoxy resin was used as facing material for the phenolic honeycomb, the resin in the cloth being used as the bonding agent. Mylar faces were bonded to the mylar honeycomb using epoxy resin as the bonding agent. Two-inch by 2-inch flatwise compression specimens and 3 by 8-inch flexural specimens (in both the ribbon and transverse directions) were cut from the epoxy-phenolic panel. Four inch by 4-inch compression specimens and 3 by 6-inch flexural specimens were cut from the mylar-mylar panel. All specimens were tested at room temperature.

THERMAL RADIATIVE PROPERTIES

Measurements have been made of the solar absorptance and infrared emittance of fiberglass laminates based on two types of polyester resin (triallyl cyanurate polyester and diallyl isophthalate polyester). In addition, the effect of ultraviolet radiation up to a total exposure of 1000 solar equivalent hours has been determined. The values obtained are summarized as follows:

	<u>Initial Absorptance</u>	<u>Absorptance After Ultraviolet</u>	<u>Infrared Emittance</u>
DAIP polyester	0.57	0.70	0.84
TAC polyester	0.46	0.65	0.84

Based on many previous tests, the emittance may be assumed to remain essentially unchanged during ultraviolet exposure. The exposure changed the color of both materials to a dark brown. Assuming the emittance to be constant, the α/e ratio of the DAIP polyester changed from 0.68 to 0.83 while that of the TAC polyester changed from 0.55 to 0.77.

No values are available for the absorptance and emittance of fiberglass composites based on either gelatin or urethane. The values will not be too far different from those obtained for the two polyesters, based on previous test of other fiberglass composites. It has been reported by Wright Field that gelatin has a resistance to ultraviolet similar to that of mylar. However, ultraviolet degradation could be greatly reduced by the incorporation of a small amount of opaque pigment.

No values of absorptance and emittance are available for mylar and H-Film. α/e ratios for these materials are probably comparable with those of other plastics (approximately 1). The resistance of ordinary mylar film to ultraviolet radiation is relatively poor. One-mil mylar exposed to 4.5 times solar intensity (2200-4000Å) under high vacuum turned to a dark brown color and disintegrated on handling. Mylar type W (Weatherable), currently only available in a 5-mil thickness, would probably be much better in this respect.

Data available on the ultraviolet resistance of teflon under vacuum are contradictory to some extent. One source shows the tensile strength reduced from 5000 to 2600 psi by 37 solar equivalent hours radiation. Another source reported very slight discoloration and no appreciable change in flexibility or elasticity as a result of 427 solar equivalent hours exposure. Teflon, in the form of a fiberglass reinforced film would be satisfactory as a substrate material.

Thermal control coatings can be considered as coatings for both substrates and structural elements of a deployable solar array. The polyester could not be coated since such coatings exclude ultraviolet radiation from the underlying material and the ultraviolet-induced cure could not take place. The thermal control coatings, besides controlling the temperature of underlying materials, would also provide protection from ultraviolet for prolonged periods. The Hughes Surveyor inorganic white paint is relatively stable to ultraviolet. A particular coating had an initial absorptance of 0.15, which increased to 0.17 after 50 solar equivalent hours, 0.18 after 200 solar equivalent hours and 0.19 after 1000 solar equivalent hours.

Thermal Radiative Properties of Teflon

0.002-inch teflon per MIL-P-22241

		<u>Solar Absorptance</u>	<u>Infrared Emittance</u>
Before ultraviolet:	Specimen 1	0.80	0.87
	Specimen 2	0.81	0.89
	Specimen 3	0.81	0.88
After 500 solar equivalent hours ultraviolet:	Specimen 1	0.83	0.89
	Specimen 2	0.83	0.92
	Specimen 3	0.85	0.90

Strength Properties of Glass to Substrate Bonds

Specimens were prepared in order to test the bonding strength between the candidate flexible substrate materials and glass when bonded with epoxy adhesive. This adhesive has been thoroughly tested at Hughes for the bonding of solar cells. Solar cells were simulated by using standard microscope slides.

The tensile shear specimens consisted of bonding each end of a 1 by 2-inch strip of H-film coated with FEP to a 1 by 3-inch glass microscope slide (see Figures 3-10 and 3-11). The substrate materials were previously chemically etched in a sodium-tetrahydrofuran bath to enable them to be bonded. Peel specimens consisted of bonding a sufficiently large piece of the substrate material to entire surface area of a microscope slide and allowing a 1-1/2-inch overhang of substrate (see Figures 3-12 and 3-13). The peel specimens were pulled at room temperature and at a 45-degree angle. Results of the tensile tests showed that in both cases the primary failure occurred in the substrate material rather than in the adhesive bond. The results of the peel test are reported in Table 3-9.

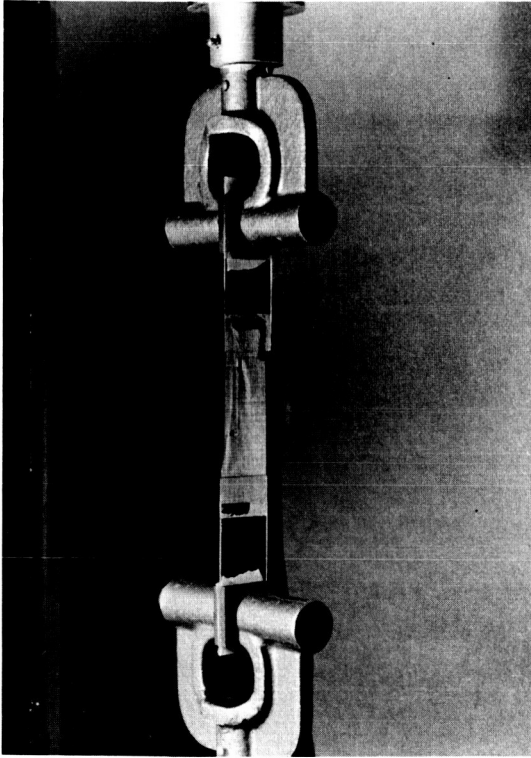


Figure 3-10. Tensile Shear Test of TFE Glass Cloth to Glass Specimen

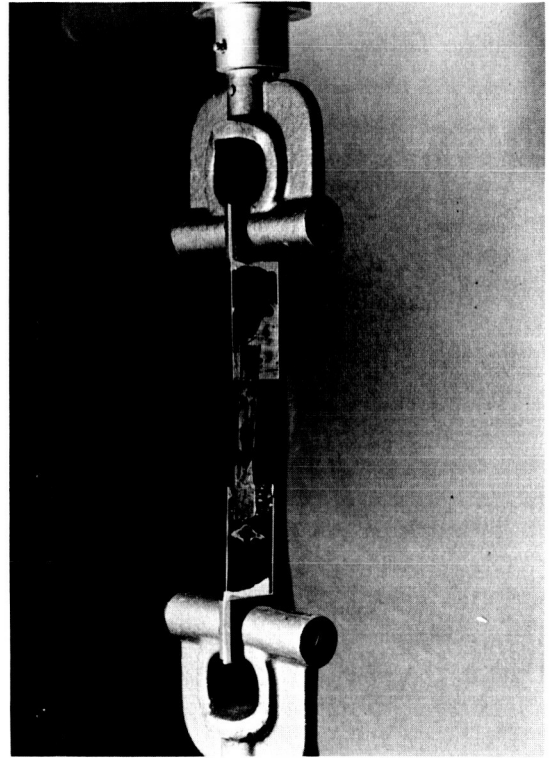


Figure 3-11. Tensile Shear Test of H Film (FEP Coated) to Glass Specimen

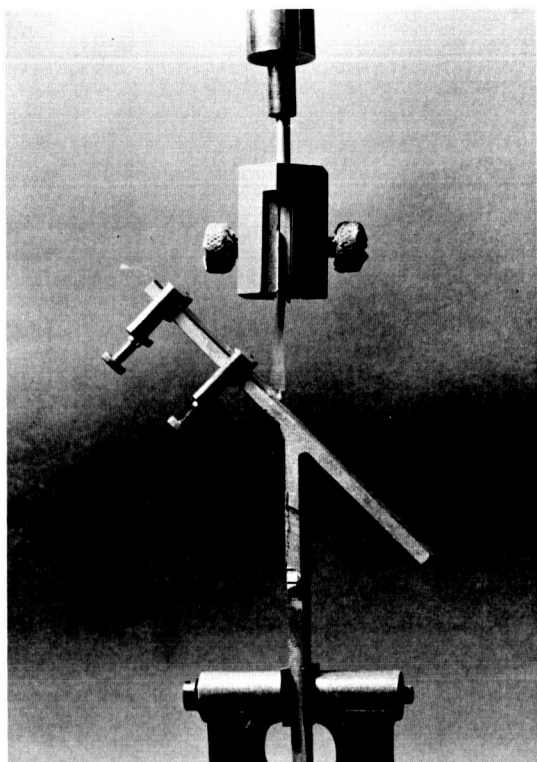


Figure 3-12. Peel Test of TFE Glass Cloth to Glass Specimen

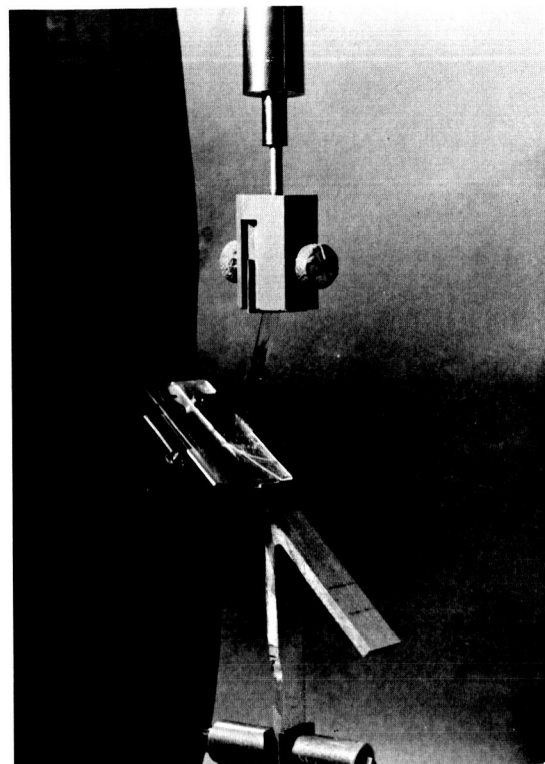


Figure 3-13. Peel Test of H Film (FEP Coated) to Glass Specimen

Type of Substrate Material	Tensile Shear at RT, psi	Type of Failure	Tensile Peel Strength, pounds at 45-degree angle, room temperature			
			Initial	High	Low	Average
H Film - FEP coated bonded to glass	8640	Substrate failed	0.4	0.6	0.5	0.6
EX 317 (TFE on 0.001-inch glass cloth) bonded to glass	11.2	Substrate sheared at bond line	0.5	0.5	0.5	0.5

TABLE 3-9. PHYSICAL PROPERTIES OF FLEXIBLE SUBSTRATE MATERIALS BONDED TO GLASS

4. WIRE INTERCONNECTION TESTS

The flexibility of the seven-cell assembly and the ability of the interconnecting wires to withstand the bending due to the rolled-up stowed configuration are key elements in the design of flexible deployed arrays. Many seven-cell assemblies have been fabricated, and they demonstrate the necessary flexibility for several bending operations. However, some amount of optimization and additional support data are desirable goals. A simplified theoretical analysis was conducted, followed by experimental laboratory tests on five different solar cell assemblies.

MECHANICAL ANALYSIS

Four different interconnection methods were studied:

- 1) No. 32 AWG copper wire loops perpendicular to the plane of the cells
- 2) No. 32 AWG copper wire loops parallel to the plane of the cells (Figure 4-1)
- 3) Coarse silver mesh (Exmet Corp. designation 5AG 14-1)(Figure 4-2)
- 4) Perforated copper foil 0.0008-inch thick (Figure 4-3)

The conclusions of the study are:

- 1) In all designs the stress is low enough (less than 1000 psi) to be insignificant for the small number of cycles to be encountered in service.
- 2) As a measure of flexibility, the reciprocal of the load necessary to deform the connection is used. This load is that which is applied when the cells are wrapped around a cylinder. The radius of the cylinder is immaterial for comparison purposes since it cancels out in the equation. With the subscripts 1 for wire loops perpendicular to the cells, 2 for wire loops parallel to the cells, 3 for

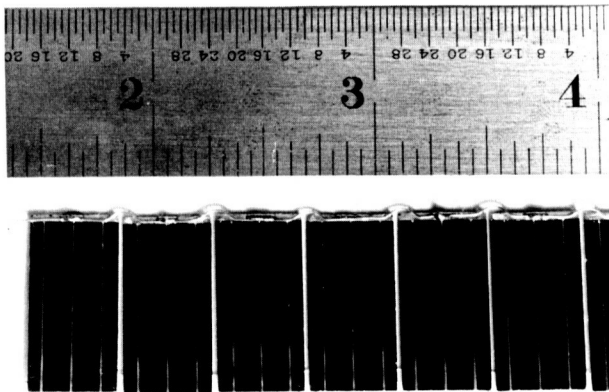


Figure 4-1. Cell Assembly -
Copper Wire Reversed Loops

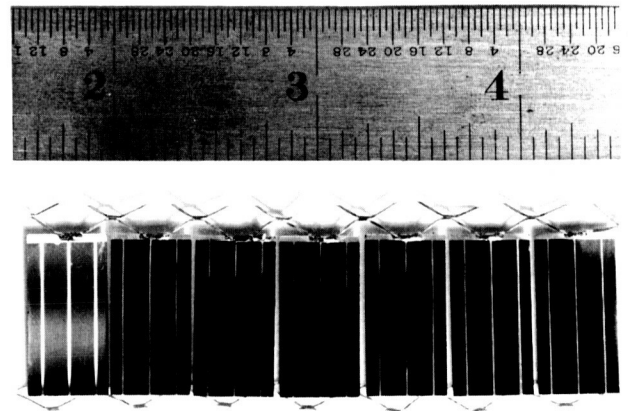


Figure 4-2. Cell Assembly -
Coarse Mesh

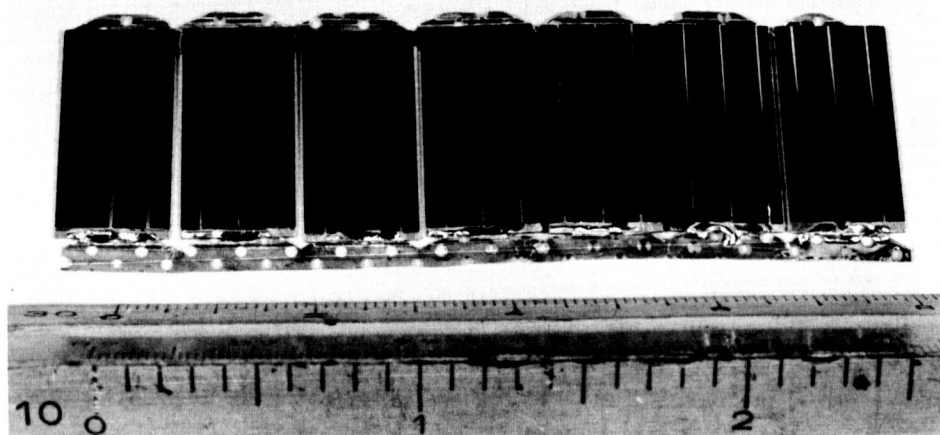


Figure 4-3. Cell Assembly - Copper Foil

the coarse mesh, and 4 for the copper foil, the ratio of the flexibilities, F , of the designs to the flexibility of the foil are:

$$\frac{F_1}{F_4} = 0.172, \quad \frac{F_2}{F_4} = 0.197, \quad \frac{F_3}{F_4} = 0.225$$

This indicates that if flexibility were the only design consideration, the foil would be the best followed by the coarse mesh, parallel loop, and perpendicular loop in that order.

- 3) The stress levels are in the same order; lowest in the foil and highest in the perpendicular loop but the stress is not high in any design considered.
- 4) The foil design is very sensitive to slight changes in geometry due to fabrication tolerances. Also, it will not yield the calculated results when exposed to any chance displacements other than those analyzed. The other designs are relatively insensitive to other displacements of the same order.
- 5) On the basis of the above, the coarse mesh appears to offer the most flexibility combined with the least variation of results.
- 6) The wire loops parallel to the plane of the solar cells were subsequently tested in lieu of the loops perpendicular to the plane of the cells.

BENDING TESTS

All assemblies used seven N/P silicon solar cells, 1 by 2 cm and 0.16 gram each, and 0.006-inch coverslips of clear Corning 0211 microsheet. The assemblies were bonded to a flexible teflon-impregnated fiberglass, 0.0012-inch thick. The combination was then bonded to a spring steel strip that subjected each assembly to a controlled bend around a 4-inch radius as shown in Figure 4-4. The five interconnection arrangements are listed below:

- 1) No. 32 AWG copper wire was formed into loops and soldered to the positive and negative contacts as shown in Figure 4-5.
- 2) Similar to 1) except the loops faced away from the coverslip to avoid interference as shown in Figure 4-1.
- 3) A coarse silver mesh (Exmet Corporation designation 5AG 14-1) was cut and formed to permit the parallel connection of the seven-cell assembly and also the series connection of the next assembly. This form of connection is termed a Z strip. Two such strips were soldered as shown in Figure 4-2.

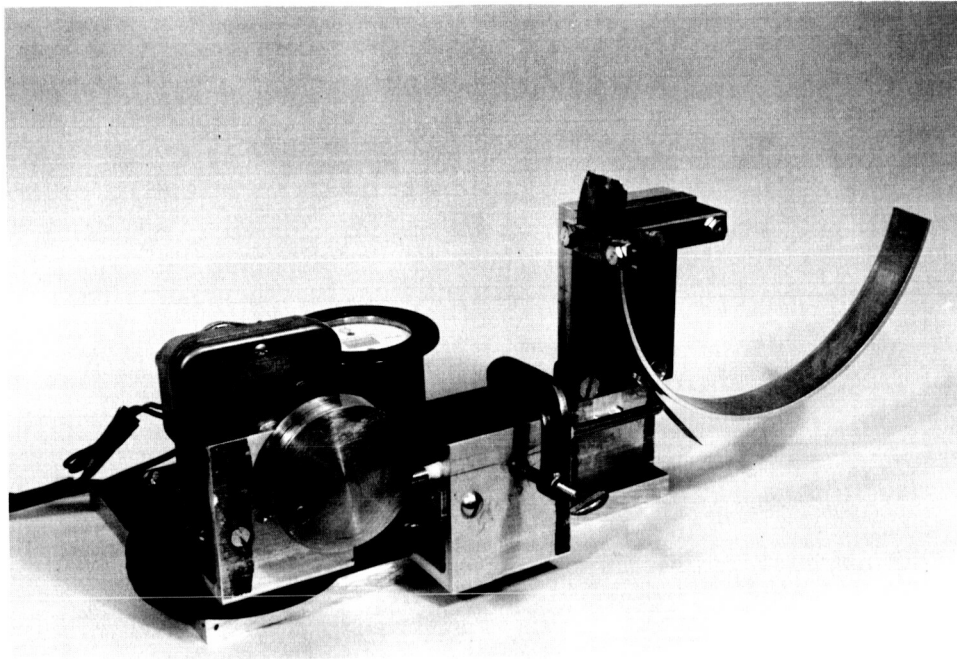


Figure 4-4. Cell Assembly Binding Test Apparatus

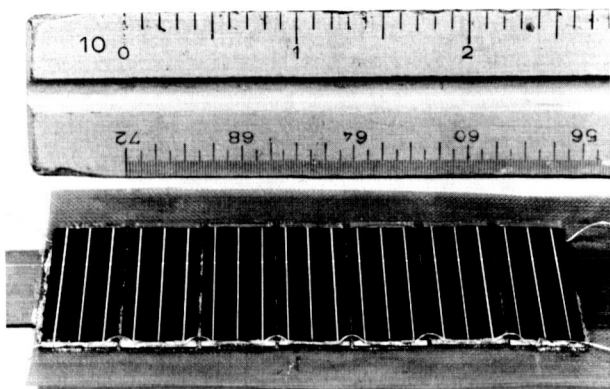


Figure 4-5. Cell Assembly -
Copper Wire

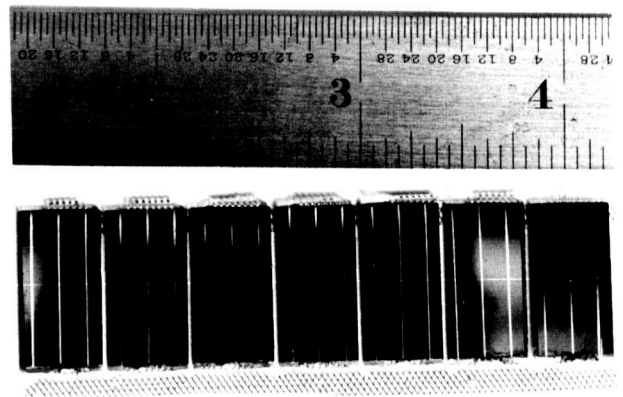


Figure 4-6. Cell Assembly -
Fine Mesh

- 4) A fine copper mesh (Exmet Corp. designation 3Cu5-5/o) was gold plated and formed into Z strips similar in function to 3) above. Two such strips were soldered as shown in Figure 4-6.
- 5) A perforated copper foil 0.0008-inch thick was cut to form Z strips with notches between cells to facilitate the bending. Two such strips were soldered as shown in Figure 4-3.

Each system was weighed to compute the weight of the interconnection and solder only. A gross evaluation of the superior interconnection method was determined by subjecting each assembly to continuous bending tests as described above. The data are shown in Table 4-1.

The coarse silver mesh lasted the greatest number of cycles without failure and the trend of the test results supports the theoretical analysis. It should be noted that systems 2, 3, or 4 could easily provide satisfactory cell assemblies since the number of bending cycles in the actual test and flight program should be no more than 10 to 20.

Type	32 AWG gage copper wire loops, facing in towards cell		32 AWG gage copper wire loops, facing outwards		Coarse silver mesh Z-strip (5 AG 14-1)		Fine copper mesh gold-plated Z-strips (3 Cu 5 - 5/o)		Copper foil, 0.0008-inch thick, perforated, Z-strips	
Weight of one strip and its solder, grams	0.06		0.06		0.142		0.145		0.135	
Handling	Good		Good		Poor - tends to stretch out of shape and catch on objects		Excellent		Fair - tends to crinkle easily	
Solderability	Good		Good		Good		Excellent		Fair - difficult to see solder joint	
Durability in flexing	Cycles	Failures	Cycles	Failures	Cycles	Failures	Cycles	Failures	Cycles	Failures
	4,530	1 top	30,700	0	71,000	0	13,340	0	1,310	0
	5,300	1 top	37,000	1 top-center of loop	78,000	1 top, 1 bottom	31,460	1 top	1,940	1 bottom
	6,920	3 tops							15,690	2 top, 1 bottom
	11,630	3 tops	47,700	2 top-center of loop						

TABLE 4-1. WIRE INTERCONNECTION EVALUATION

5. COMPARISON OF POLAR AND EQUATORIAL ORBITS

The purpose of this analysis is to compare the power producing potential of a 600-mile circular polar and equatorial orbit for a spin-stabilized satellite. The attitude of the satellite is assumed to be such that the spin axis is normal to both the orbit plane and the earth-satellite position vector, as shown in Figure 5-1. Thus the angular momentum vector $\bar{\zeta}$ is given by

$$\bar{\zeta} = \bar{R} \times \bar{V} \quad (5-1)$$

where \bar{R} is the earth-satellite position vector and \bar{V} is the spacecraft velocity vector.

It is further assumed that there will be no orbit stationkeeping and that after the spacecraft has been placed in its initial orbit, the orbit will vary according to the first order laws of orbital mechanics. The power produced by the solar cell panels mounted on such a satellite is a direct function of the solar incidence angle. The power output is thus directly proportional to $\cos \beta$ where β is the complement of the angle between the direction of sun's rays and the satellite spin axis (see Figure 5-2).

For an observer located on the earth, the sun appears to move along the ecliptic plane. Since the sun's rays are parallel, the direction of the sun can be represented by a position vector drawn from the sun's apparent position on the ecliptic plane through the center of the earth. Figures 5-3 and 5-4 show the earth and satellite orbit geometry. For an equatorial orbit, the value of β varies sinusoidally throughout the mission because the satellite moves in the equatorial plane whereas the sun appears to move in the ecliptic plane. For all other orbits, the oblateness of the earth sets up forces causing the orbit plane to precess about the equator. Thus, the change in the value of β for the polar orbit will be more complex than for the equatorial orbit. If orbit stationkeeping were to be employed and power output the only consideration, then an orbit plane coinciding with the ecliptic plane would be desirable.

The possibility of eclipses of the satellite by the earth's shadow must be considered. Figure 5-5 shows the simplified satellite eclipse geometry for a 600-mile circular orbit radius where the effect of the penumbra can

safely be neglected. If $\beta \geq \sin^{-1}(R_e/R_o)$, then there will be no eclipse during the orbit. Thus for the 600-mile orbit, R_o equals 1.15 earth radii so that if $\beta < 61.64$ degrees, there will be an eclipse of the satellite during some portion of the orbit.

An equation for $\sin \beta$ has been derived* as a function of the orbit parameters:

$$\begin{aligned} \sin \beta = & \left[\frac{\sin i}{2} (1 - \cos e) \right] \sin \left[(\dot{\psi} + \dot{\Omega})t + \psi_o + \Omega_o \right] \\ & - \left[\frac{\sin i}{2} (1 + \cos e) \right] \sin \left[(\dot{\psi} - \dot{\Omega})t + \psi_o - \Omega_o \right] \\ & + \left[\cos i \sin e \right] \sin \left[\dot{\psi} t + \psi_o \right] \end{aligned} \quad (5-2)$$

where

i = orbital inclination angle

e = angle between earth equatorial plane and ecliptic plane = 23 degrees 27 minutes

Ω = right ascension of ascending node

ψ = angle between sun-earth position vector and vector in direction of first point of Aires

t = time after injection into initial orbit, days

The subscript o denotes an initial orbit parameter, i. e., at injection. For simplicity, injection is assumed to occur along the vernal equinox so that ψ is zero. $\dot{\psi}$, the time rate of change of ψ , is assumed constant at its mean rate throughout the year, 0.986 degree per day. $\dot{\Omega}$ is the rate of precession of the orbit plane in degrees per day and for circular orbits is given by

$$\dot{\Omega} = - \frac{20.8158}{R^{7/2}} \times 10^{13} \cos i \quad (5-3)$$

where R is the orbit radius in kilometers.

*"Multiple Mission Advanced Syncom, Vol. I, Technical Development Plan," (NASA Contract 5-2797), SSD 31265P, p 4-12, 31 January 1964.

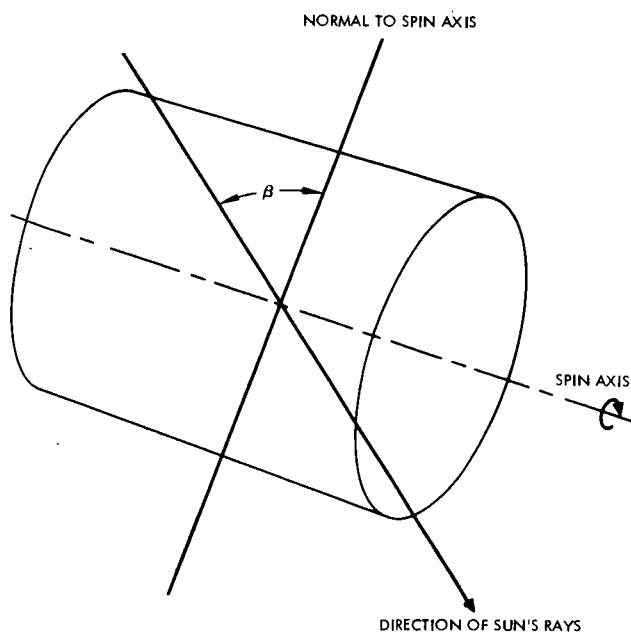
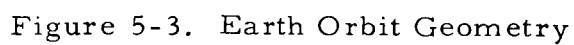


Figure 5-2. Satellite Geometry



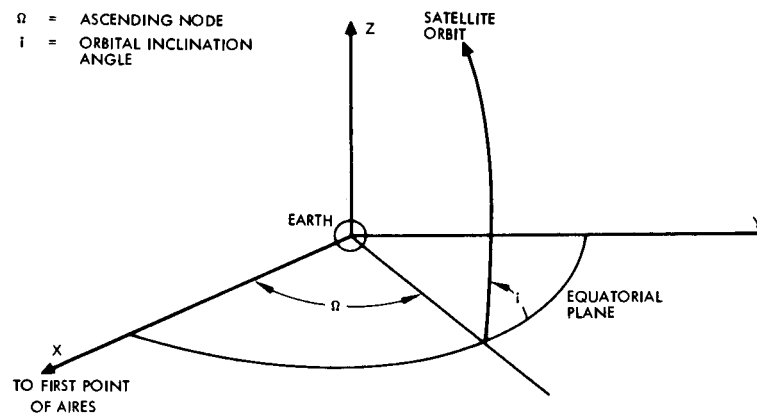


Figure 5-4. Satellite Orbit Geometry

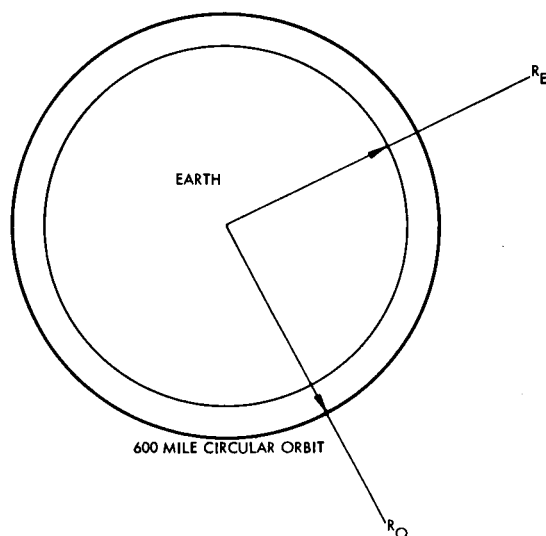


Figure 5-5. Satellite Eclipse Geometry

For an equatorial orbit, $i = 0$ degree and for a polar orbit $i = 90$ degrees. Thus the equations for $\sin \beta$ for the equatorial orbit ($\sin \beta_e$) and for the polar orbit ($\sin \beta_p$) thus become

$$\sin \beta_e = 0.398 \sin (0.986t) \quad (5-4)$$

$$\sin \beta_p = \left[0.0413 \sin(0.986t + \Omega_o) \right] - \left[0.9587 \sin(0.986t - \Omega_o) \right] \quad (5-5)$$

Equation 5-4 was evaluated at 0.1 year intervals and the average value of β defined by

$$\bar{\beta} = \frac{\int \beta dt}{\int dt} \quad (5-6)$$

was determined by numerical integration. The variation of β_e has a period of $1/2$ year with an average value of $\bar{\beta}_e$ equal to 16 degrees. The average value of $\cos \beta_e$ is thus 0.96. The minimum value of β_e is 0 degree and the maximum value is 23 degrees. Figure 5-6 shows the time history of $\cos \beta_e$ for one period.

Rewriting Equation 5-5 and expressing the $\cos \beta$ directly yields,

$$\cos \beta_p = \left[1 - \left[\cos(0.986t) \sin \Omega_o - (0.9174) \sin(0.986t) \cos \Omega_o \right]^2 \right]^{1/2} \quad (5-7)$$

Thus β_p depends on initial right ascension of the ascending node. Equation 5-7 was solved similarly to Equation 5-4 for several values of Ω_o . Figure 5-7 shows that the minimum value of β_p occurs at about $\Omega_o = 10$ degrees. At this point, the average value of β_p is equal to 43.1 and $\cos \beta_p$ is equal to 0.7301. The range of β_p is from 10.04 to 65.67 degrees and the period of the change of β_p is also $1/2$ year.

On the basis of the average values of $\cos \beta$, it is apparent that the power output of a satellite will be greater and the power variation smaller while in an equatorial orbit than in a polar orbit. In addition, the average values of β for both orbits show that satellite eclipses will occur about equally during both orbits. Although the eclipse durations will not all be equal, the difference will not significantly affect the required solar panel size* and therefore satellite eclipses can be neglected. Figure 5-8 shows the time history of β_p for one period.

*The required battery weight and thus the total spacecraft weight could be affected however.

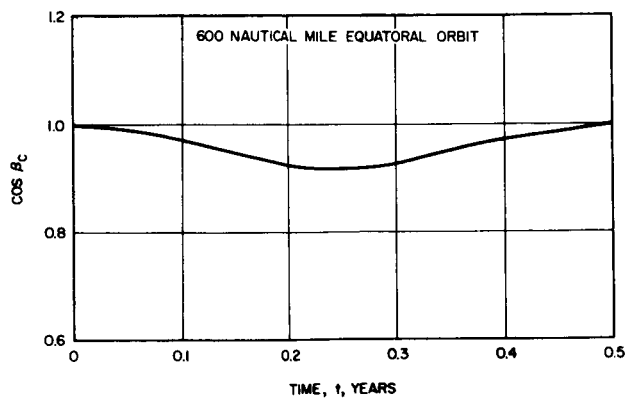


Figure 5-6. $\cos \beta_e$ versus Time After Injection

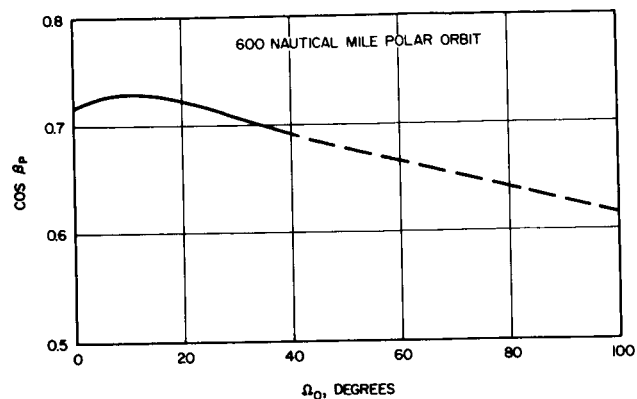


Figure 5-7. Average $\cos \beta_p$ Initial Right Ascension of Ascending Mode

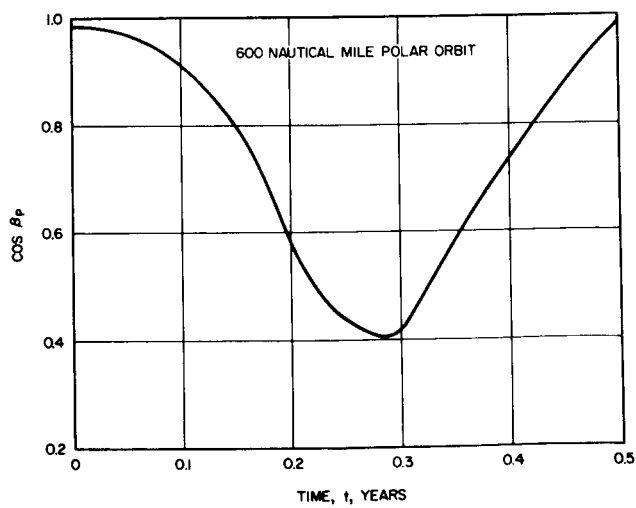


Figure 5-8. $\cos \beta_p$ Time After Injection for $\Omega_0 = 10$ degrees

It should be noted that many orbits other than the two mentioned offer advantages that may be realized if the proper inclination angle and altitude can be accommodated. An example of this is the twilight or 88-degree quasi polar orbit which precesses at the same rate as the earth about the sun.

EVALUATION OF SEMI-ORIENTED (1 DEGREE OF FREEDOM) ARRAYS

It is of interest to determine the relation between the average power output of a spinning satellite having extended solar panels and the angle, γ , that the panels make with the spin axis. Figure 5-9 shows the spinning satellite with the angle γ defined. For a given solar panel and space environment, the average power is proportional to the projected sunlit panel area (normal to the direction of the incident sunlight). This will vary as the satellite spins. The average of this area is defined by:

$$A_{avg} \equiv \frac{\int_0^{2\pi} A \, d\theta}{\int_0^{2\pi} d\theta} \quad (5-8)$$

θ is the angle through which the satellite has rotated at any instant of time. Once the relations between β , γ , and θ are known, it will be possible to determine the optimum angle to set a fixed panel at, since the average β can be calculated for any mission. It is also possible to then determine what advantage, if any, can be gained by varying γ in space during the mission.

The relationships between γ and β depend on the particular panel configuration studied. The deployable solar panel configuration, consisting of three flexible panels wrapped around the body of the satellite, was chosen for this study. A scale model was constructed (about 1/8 scale) with which γ and θ could be varied and accurately positioned, as shown in Figure 5-10. The model was mounted on a shaft so that it could spin freely. A circular position marker was also mounted on the shaft. The shaft was mounted on movable supports which could be positioned to simulate various β s. This setup is shown in Figure 5-11. Photographs were taken of the model from a distance of 50 feet. The camera was held fixed and the model moved to vary β from 0 to 60 degrees, γ from 0 to 75 degrees, and θ from 0 to 120 degrees. It is sufficient to vary θ from 0 to 120 degrees instead of from 0 to 360 degrees because of the symmetry of the model. The photographs were taken with a 35-mm camera using a 135-mm focal length lens. The negatives were enlarged 24 diameters.

The panel area recorded by the camera is equivalent to the component of the exposed panel area normal to the sun's rays. The maximum error

expected in the area measurement (perspective) due to the fact that the camera was 50 feet away and not at infinity is less than 3 percent at $\beta = 60$ degrees and decreases with smaller values of β . An additional panel, equal in area to the model panels, was mounted directly below the model, normal to the camera-model line. Thus, by employing this second area as a standard, the panel areas could be determined from each photograph, thereby obviating errors which might have entered due to the photographic developing and printing processes.

The panel areas on the photographs were measured with a planimeter. The values of Aavg were obtained by numerical integration for each value of β and γ and the results are shown in Table 5-1.

TABLE 5-1. REDUCED DATA

β , degrees	γ , degrees	Aavg, ft ²	Aavg (γ_{opt}) ft ² at γ_{opt}
0	0	16.44	16.44 at 0 degree
15	0	17.10	17.30 at 8.5 degrees
	5	17.18	
	10	17.26	
	15	16.90	
	20	16.40	
30	0	15.50	15.75 at 6 degrees
	10	15.64	
	20	14.91	
	30	14.06	
	40	13.10	
45	0	13.20	13.20 at 0 degree
	10	13.06	
	20	13.16	
	30	12.69	
	40	13.13	
60	0	9.38	~25.10 at 90 degrees
	15	10.03	
	30	12.56	
	45	18.09	
	60	22.50	
	75	24.50	
90	90	29.25	29.25 at 90 degrees

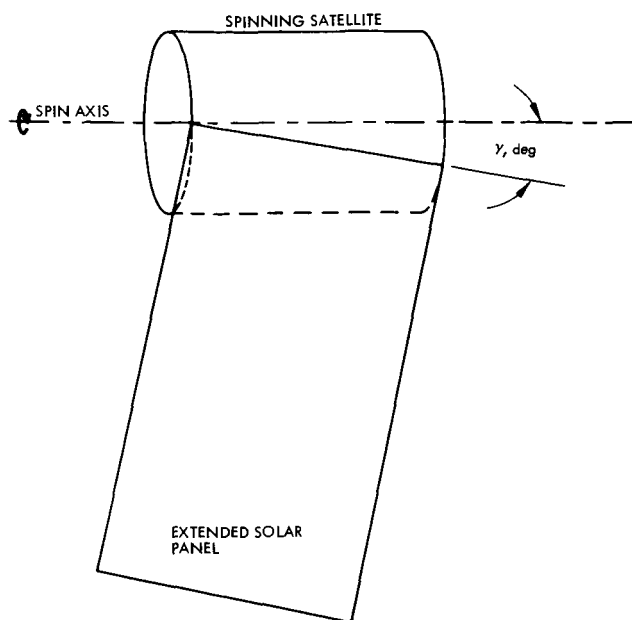


Figure 5-9. Spinning Satellite

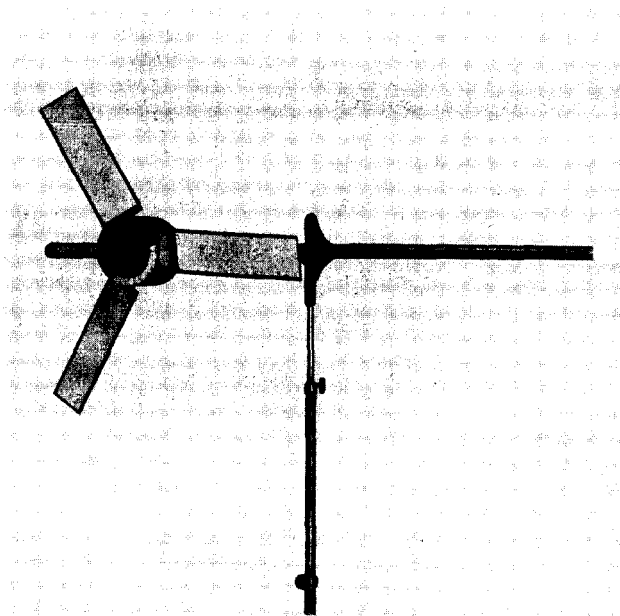


Figure 5-10. Deployable Solar Cell Array

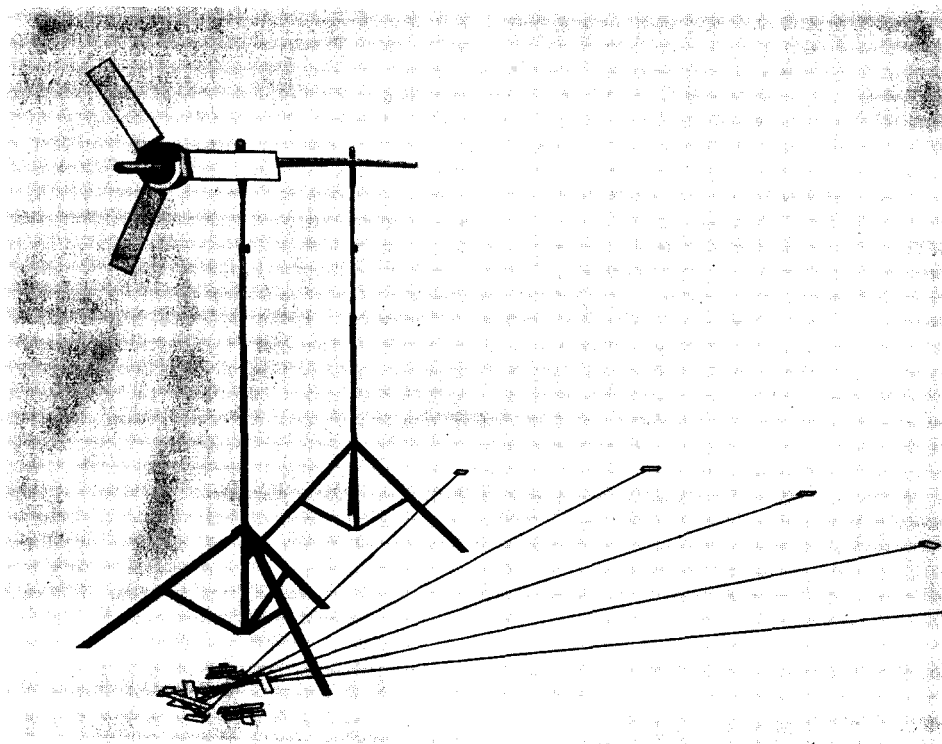


Figure 5-11. Deployable Solar Cell Array
Mounted on Movable Supports

The values of A_{avg} for $\beta = 0$ degree, $\gamma = 0$ degree, and $\beta = 90$ degrees and $\gamma = 90$ degrees were obtained graphically. The values of γ_{opt} and A_{avg} (γ_{opt}) were obtained by plotting A_{avg} versus γ for each value of β as shown in Figure 5-12. The curve for A_{avg} changes from a cosine function at $\beta = 0$ degree to a sine function at $\beta = 90$ degrees. At $\beta = 45$ degrees, the curve of A_{avg} versus γ is a straight line.

Figure 5-13 shows γ_{opt} (obtained from Figure 5-12) plotted against β . There are insufficient data to establish the exact shape of the curve between $\beta = 45$ degrees and $\beta = 60$ degrees so that portion is shown with dashed lines. The straight line at $\beta = 45$ degrees on Figure 5-12 accounts for the discontinuity of the curve of Figure 5-13 at that point and as Figure 5-12 indicates, the optimum γ is 90 degrees for β greater than 45 degrees. From $\beta = 45$ degrees to $\beta = 90$ degrees, the panels do not shadow each other so that a γ of 90 degrees will maximize the area normal to the sun.

The optimum angle at which fixed panels should be set can now be determined for any mission once the orbit is specified, since if the orbit is specified, β can be calculated. For example, the average $\bar{\beta}$ for an equatorial orbit was shown to be 16 degrees. Thus, for this orbit, fixed panels should be set at approximately $\gamma = 8$ degrees. Similarly, for a polar orbit where $\bar{\beta} = 43.1$ degrees, the optimum γ for panels which are fixed with respect to the satellite is approximately 0 degree. At any value of γ , the value of A_{avg} first increases and then decreases with increasing values of β . This is shown in Figure 5-14, where $A_{avg}(\gamma = 0)$ is plotted versus β . This phenomenon occurs because as β increases from 0, the effect of shadowing of the rear panels become less pronounced, and more total area is exposed to the sun. The component of the panel area normal to the sun is proportional to $\cos \beta$ and since the cosines of very small angles are very nearly equal to 1.0, the effect of exposing more panel areas predominates at small values of β . As β increases further, cosine β decreases rapidly and the total A_{avg} decreases.

It is also possible to determine the possible gain in power output which can be realized from varying γ in orbit to make it equal to γ_{opt} as β changes during the mission. Figure 5-15 shows the $A_{avg}(\gamma = \gamma_{opt})$ plotted against β . The exact shape of this curve is also not clearly defined between $\beta = 45$ degrees and $\beta = 60$ degrees, so this portion is shown with dashed lines. The algebraic difference between this curve and the curve of A_{avg} at the γ corresponding to the average β for this mission is a direct indication of the increase in power available at any value of β . Once the time history of β is established for a mission, the average power increase can be found for the entire mission by summing up the algebraic differences over the mission lifetime. Such an elaborate procedure is not always necessary. For the equatorial orbit, Figure 5-12 is used to derive the data shown in Table 5-2. The values of $A_{avg}(\gamma = 8$ degrees) are also shown in Figure 5-15. These curves coincide almost exactly from $\beta = 0$ to $\beta = 45$ degrees. For the equatorial orbit, β varies from 0 to 23 degrees and so for this orbit, the gain realized from varying γ is negligible.

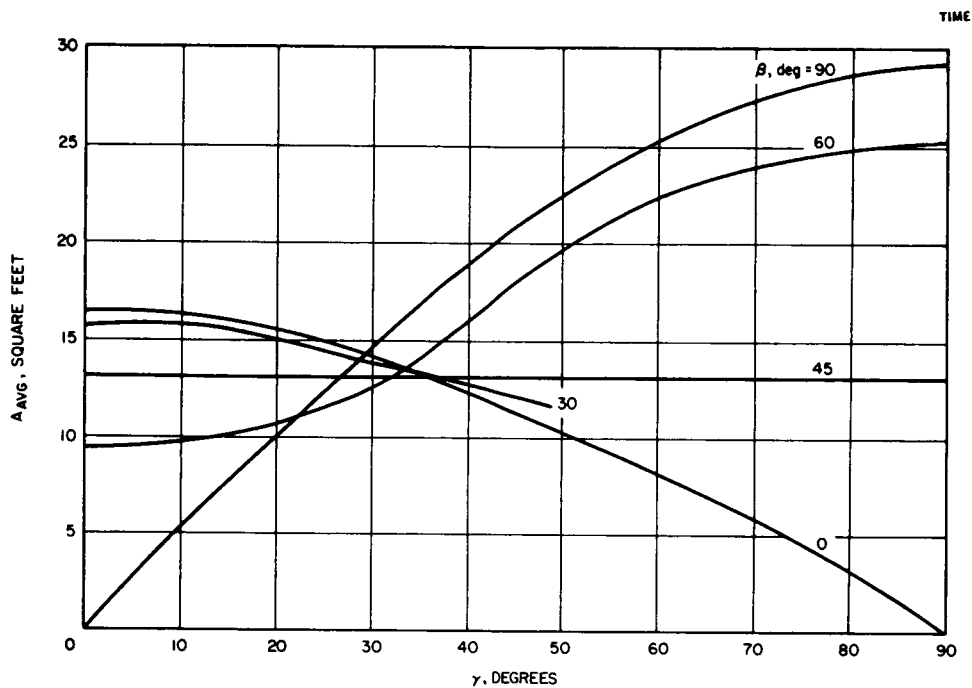


Figure 5-12. A_{avg} versus γ for Values of β

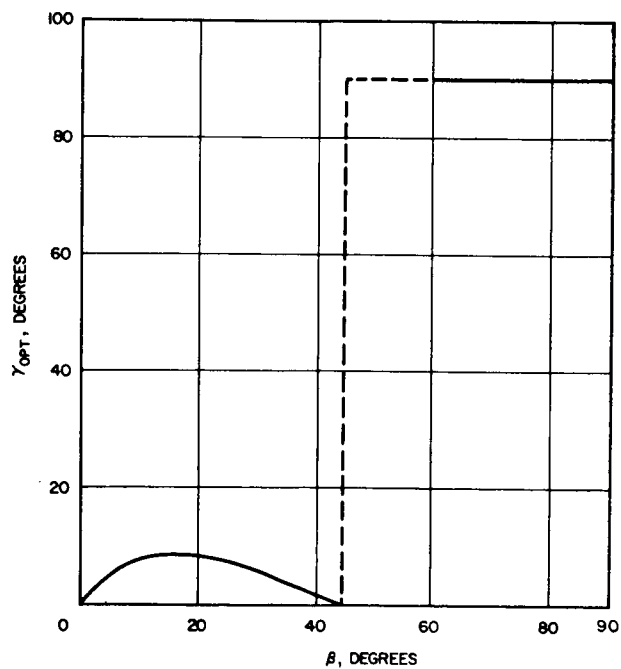


Figure 5-13. γ_{opt} versus β

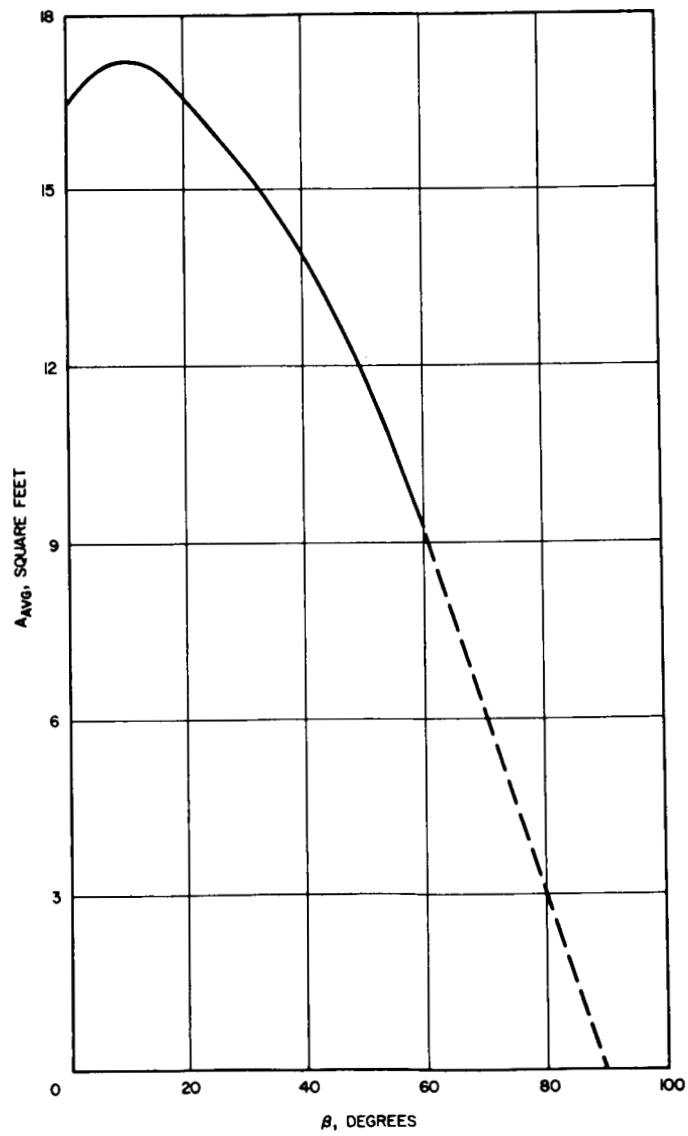


Figure 5-14. A_{avg} versus β for $\gamma = 0$

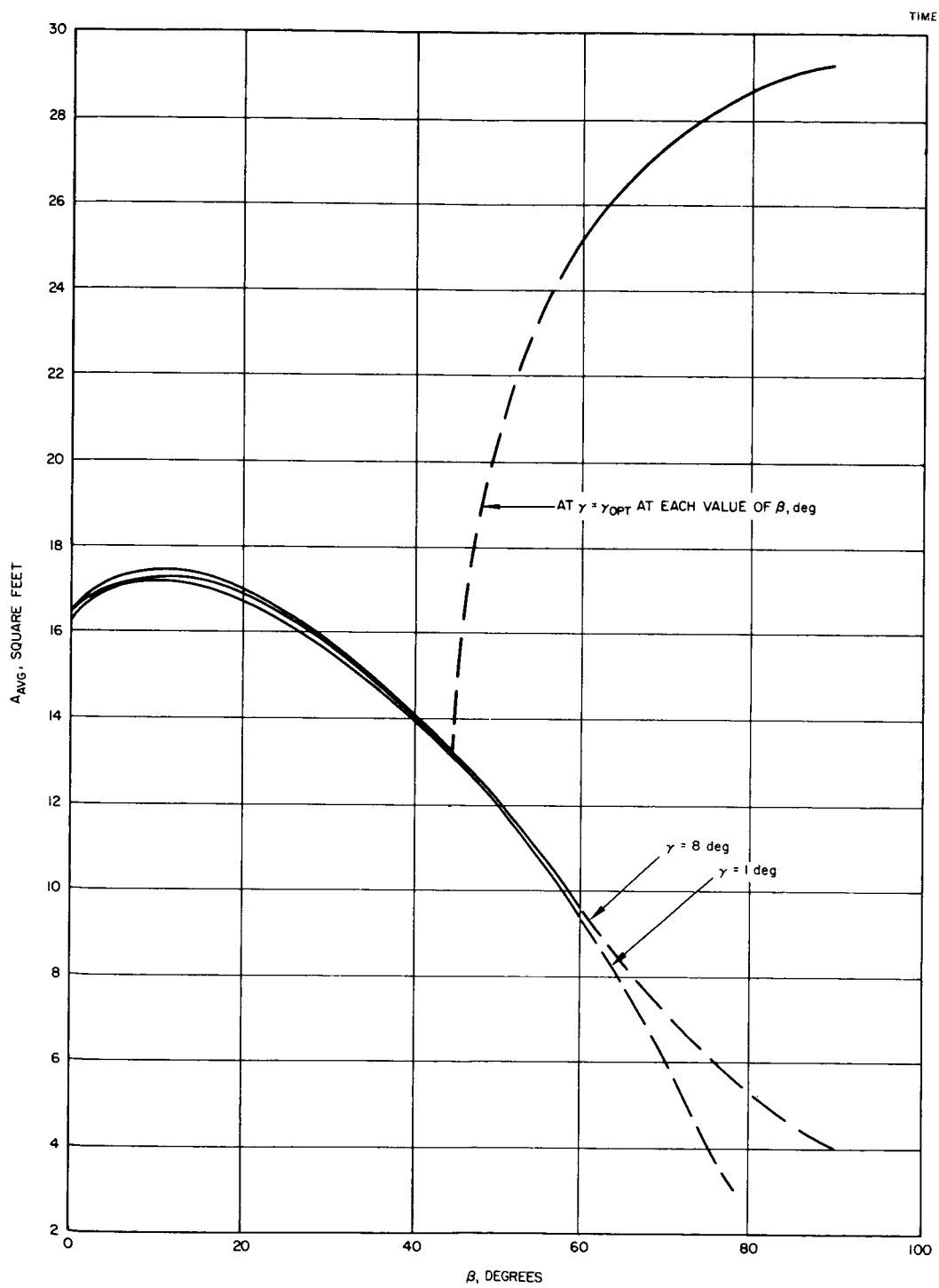


Figure 5-15. A_{avg} versus β for $\gamma = \gamma_{opt}$

TABLE 5-2. Aavg AT $\gamma = 8$ DEGREES FOR
VARIOUS β
Equatorial Orbit

β , degrees	Aavg ($\gamma = 8$ Degrees), ft^2
0	16.26
15	17.27
30	15.72
45	13.13
60	9.63
90	3.98

Figure 5-12 has also been used to derive the values shown in Table 5-3 for the polar orbit and the results plotted in Figure 5-15.

TABLE 5-3. Aavg AT $\gamma = 1$ DEGREE FOR
VARIOUS β
Polar Orbit

β , degrees	Aavg ($\gamma = 1$ Degree), ft^2
0	16.48
15	17.1
30	15.6
45	13.2
60	9.4
90	0.5

Whereas Aavg ($\gamma = \gamma_{\text{opt}}$) increases rapidly as β is increased above 45 degrees, Aavg ($\gamma = 8.0$ degrees) and Aavg ($\gamma = 1$ degree) continue to decrease to a minimum at $\beta = 90$ degrees. The range of β for the polar

orbit is from 10.4 to 65.6 degrees and at 65.6 degrees there is a considerable difference between $A_{avg} (\gamma = 1)$ and $A_{avg} (\gamma = \gamma_{opt})$. The following data was obtained from the curves using the time history of β , previously derived and is shown on Table 5-4.

TABLE 5-4. POLAR ORBIT

t, years	β , degrees	$A_{avg} (\gamma = \gamma_{opt}), \text{ft}^2$	$A_{avg} (\gamma = 1 \text{ degree}), \text{ft}^2$
0	10.04	17.44	17.19
0.1	23.36	16.70	16.43
0.2	53.49	22.82	11.20
0.3	65.67	26.50	7.66
0.4	42.27	13.75	13.60
0.5	10.04	17.44	17.19

The average value over a mission lifetime of $A_{avg} (\gamma = \gamma_{opt})$ is 19.44 square feet and the average value of $A_{avg} (\gamma = 1 \text{ degree})$ is 13.22 square feet. Thus, the percent gain in A_{avg} (and thus in the average power output) is 47 percent. That is, 47 percent more power can be obtained from the same panels if the panels are rotated in space so that γ equals γ_{opt} .

This study has shown that varying γ in space is definitely not warranted for an equatorial orbit, but can yield a considerable increase in power for a polar orbit. The results of this study can also be applied to any orbit, once the time histories of β or $\bar{\beta}$ have been calculated. The trend should be generally applicable, but it must be recognized that the numerical values presented are limited to the three-panel configuration. This potential gain in power output as the panels are rotated in the polar orbit must be compared against the additional cost and weight of the positioning mechanism to evaluate the net gain.

6. SYSTEM COMPARISON

COMPARISON CHART

The objective of the study is to give careful consideration to any deployment system showing promise for application to spinning satellites. This consideration should be sufficiently detailed so that the parameters of each system could be evaluated separately. This is especially desirable since no specific mission was assigned to the study. The system comparison chart, shown in Figure 2-5, was considered to be the most efficient and satisfactory manner in which to list the important parameters of each system studied. A definition of the headings follows:

- 1) System description – self-explanatory
- 2) Dimensions and ft³ – Appendix C contains the calculation of the stowed diameter and volume of the system using flexible panels wrapped around a cylinder.
- 3) Total weight, pounds – This includes all weight chargeable to the deployment system such as mounting brackets and hardware.
- 4) Deployed area, ft² – This is the total panel area including structural members such as support tubes and hinges, if used.
- 5) Projected area, ft² – This is the component of the deployed panel area on which solar cells are mounted which is perpendicular to the sun's rays. The sun is assumed to be perpendicular to the spin axis of the satellite ($\beta = 0$) and the panels are assumed to be parallel to the spin axis ($\gamma = 0$).
- 6) Array output watts – This is obtained by the following equation:

Array output = projected area (ft²) x cell packing factor

x panel efficiency x [1 - 0.005 (operating temperature
- 28°C)] x solar insolation (watts/ft²).

A packing factor of 0.89 was used as a result of cell layout drawings.

A panel efficiency of 10 percent (air mass 0 at 28°C) was used and assumes an initial efficiency for the solar cells sufficient to yield this value after final assembly.

The two headings above, 5) and 6), are further delineated to show the maximum, average, and minimum values. These are a result of the rotation of the spinning satellite.

- 7) $\frac{P_{\max} - P_{\min}}{P_{\text{ave}}}$ - This is the cyclic variation in power output obtained from the variation in 6) above.
- 8) Average panel operating temperature, °C - The calculation of the panel operating temperature is contained in Appendix B. The assumptions used in the calculations result in the maximum expected temperatures.
- 9) Watts per ft² - The average array output divided by the total deployed area.
- 10) Watts per pound - The average array output divided by the total weight.
- 11) Watts per ft³ stowed volume - The average array output divided by the total volume of the deployment system when in the stowed or launch configuration.
- 12), 13), 14) Estimates of reliability, cost, and growth potential are of a relative nature since sufficient details do not exist to allow more and accurate estimates.
- 15) Overall rating number - A rating system devised to weight some parameters more heavily than others. The three parameters used and their weighting factors are given below.

<u>Parameter</u>	<u>Weight Factor, W</u>
watts/lb	10
watts/ft ³	8
watts/ft ²	3

A rating is calculated for three parameters of each of the seven systems using the following equation:

$$R = W \left[1 + \frac{A - B}{B} \right]$$

where

R = rating

W = weighting factor

A = value of parameter

B = average value of parameter for seven systems

The summation of the three rating numbers for each system yields an overall rating number. Table 6-1 shows the values for the seven systems and the rating order.

The characteristics of the seven deployment systems, shown in Figure 2-5, are conservative in that they do not reflect the usual optimization procedures normal in the design of solar panels for a specific application. For example, the integration of the panel mounting with the spacecraft structure could result in considerable weight savings. If the actual spacecraft configuration is known and the effects of antennas and booms accounted for, it is then possible to optimize the length-to-width ratio of the solar panels. This length-to-width optimization yields significant increases in performance when flexible, rigidized solar panels are considered. Figure 2-11 shows the performance in watts per pound as the panel length is varied for two different panel widths.

The data were based on system 1. The fiberglass tube wall thickness was increased as the panels were progressively lengthened. This method is not an optimum design procedure and accounts for the decrease in the watts-per-pound curve as the panel is lengthened. The higher values of watts per pound for the wider 22-inch panel emphasize the importance of the correct panel aspect ratio and indicate that a panel wider than 22 inches may yield even greater performance. To be realistic, the optimization should be based on specific structural and electrical requirements.

CONCLUSIONS

The series of deployment systems utilizing flexible substrates show the highest watts per pound and watts per cubic foot with system 2, the highest at 9.2 and 393, respectively. The drum-stowed systems, 1 and 3, have comparable performance and have the advantage of mounting configurations not on the circumference of the spacecraft. The simple attachment of the drum systems is desirable for satellite checkout and assembly procedures. The inherent simplicity of the flexible systems is desirable when compared to the rigid panel deployment mechanisms.

Preliminary tests of rigidized fiberglass tubes as support members for the flexible panels have been very encouraging, especially since the tubes were erected and rigidized in a vacuum chamber. The tubes tested represented

TABLE 6-1. SYSTEM RATING METHOD

Weighting Factor = W

System Number	W = 10		W = 8		W = 3		Total Rating, R_T
	w/lb	Rating	w/ft ³	Rating	w/f ²	Rating	
1	8.0	11.1	140	6.6	1.90	2.2	19.9
2	9.2	12.8	383	18	2.45	2.9	33.7
3	8.6	11.9	192	9.0	2.09	2.5	23.4
4	7.7	10.7	158	7.4	3.32	3.9	22.0
5	6.7	9.3	132	6.2	2.93	3.4	18.9
6	5.4	7.5	126	5.9	2.28	2.7	16.1
7	5.1	7.1	61	2.9	2.95	3.5	13.5
Average	7.2	10.0	170	8.0	2.56	3.0	21.0

a first effort result and additional structural design effort on the fiberglass wall thickness, degree of tube taper, choice of cloth weight and weave, and the method of resin impregnation and tube erection should substantially increase tube performance.

Results of the interconnection wire bending test show clearly that more than one design; i.e., either the coarse mesh, fine mesh, or round wire, would be suitable for use on the flexible array designs. The coarse mesh was superior, having passed 71,000 cycles without failure. The only drawback to the coarse mesh is the tendency of the unconnected webs to become entangled during handling. It is believed that a mesh midway between the coarse and fine mesh evaluated would be the ideal size.

The results of the study of a spinning satellite with 1-degree-of-freedom of the solar panels showed that there is negligible gain from an equatorial orbit, but a polar orbit could yield a 47-percent increase in power with orientation of one axis. A thorough study of the tradeoffs involved when an orientation system is considered is necessary before such a design can be shown advantages.

7. RECOMMENDATIONS

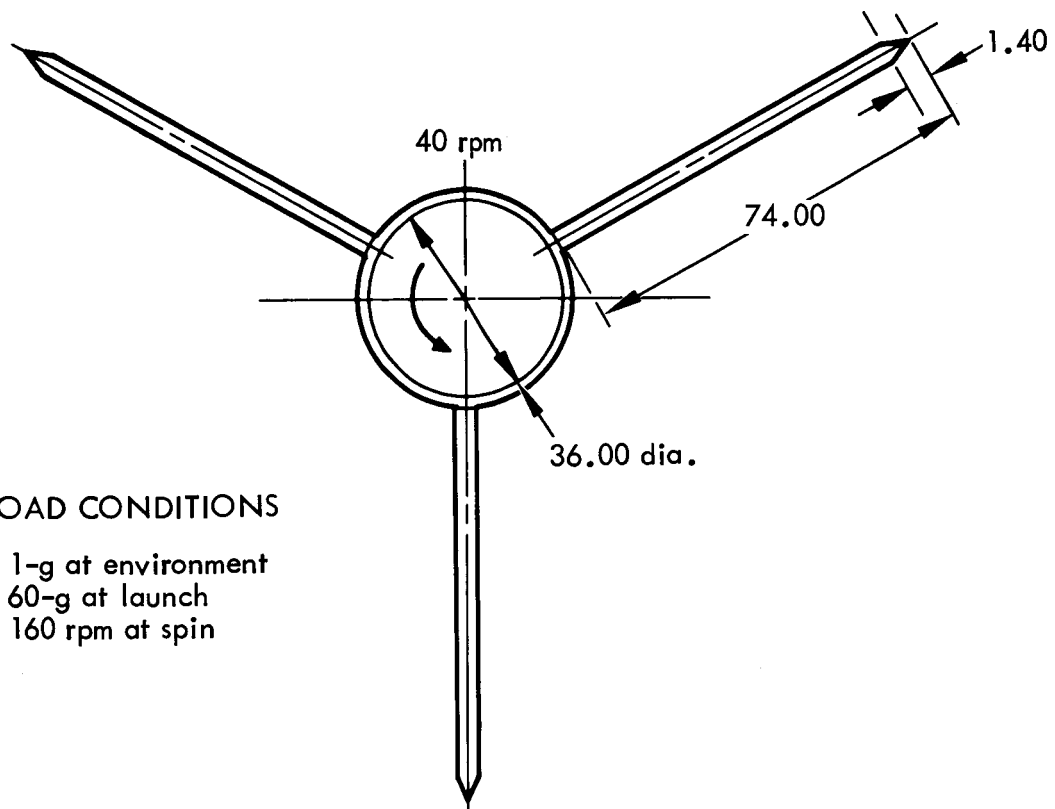
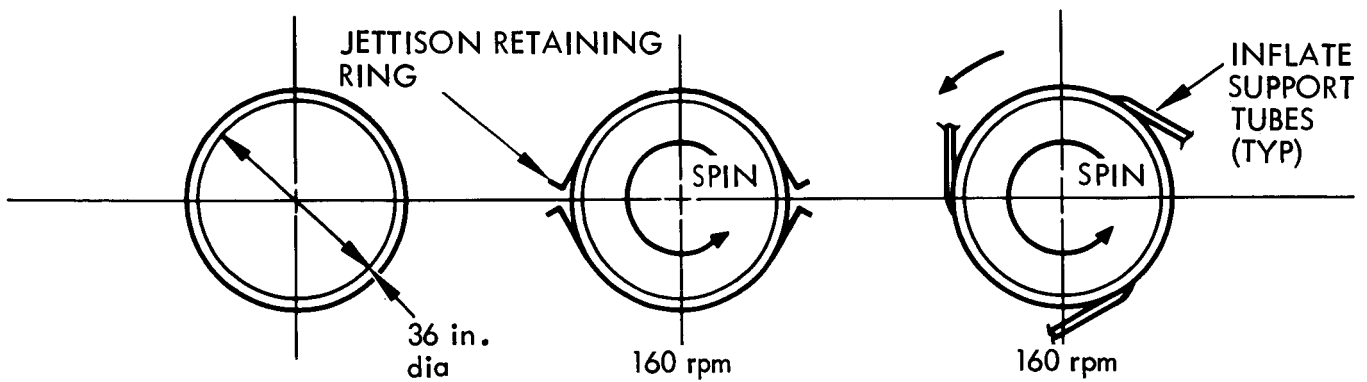
Based on the design results and tests conducted during this study, the following deployment system is recommended for further design optimization and fabrication of a proof-of-principle and flight model.

SYSTEM 3

Three flexible solar panels, each measuring 24 by 90 inches, attach to a common storage drum as shown in Figure 2-3b. The flexible substrate consists of 1 mil glass fabric impregnated with TFE teflon (EX317 - Taconic Plastics). The total thickness is approximately 0.0012 inch. The supporting fiberglass tubes are 1 inch in diameter and have 0.015-inch wall thickness impregnated with ultraviolet activated polyester resin. A total of 26,208, 1- by 2-cm solar cells are used, resulting in an average of 184 watts in a 600 equatorial orbit. This power is available when the sun's rays are normal to the spin axis, and the panel temperature at this time is 43°C. The maximum decrease in power output due to the change of the sun-spin axis angle is 8 percent. The total weight is estimated to be 21.5 pounds and the stowed volume to be 0.956 cubic foot. These values result in a performance of 8.6 w/lb and 192 w/ft³.

APPENDIX A. STRUCTURAL ANALYSIS

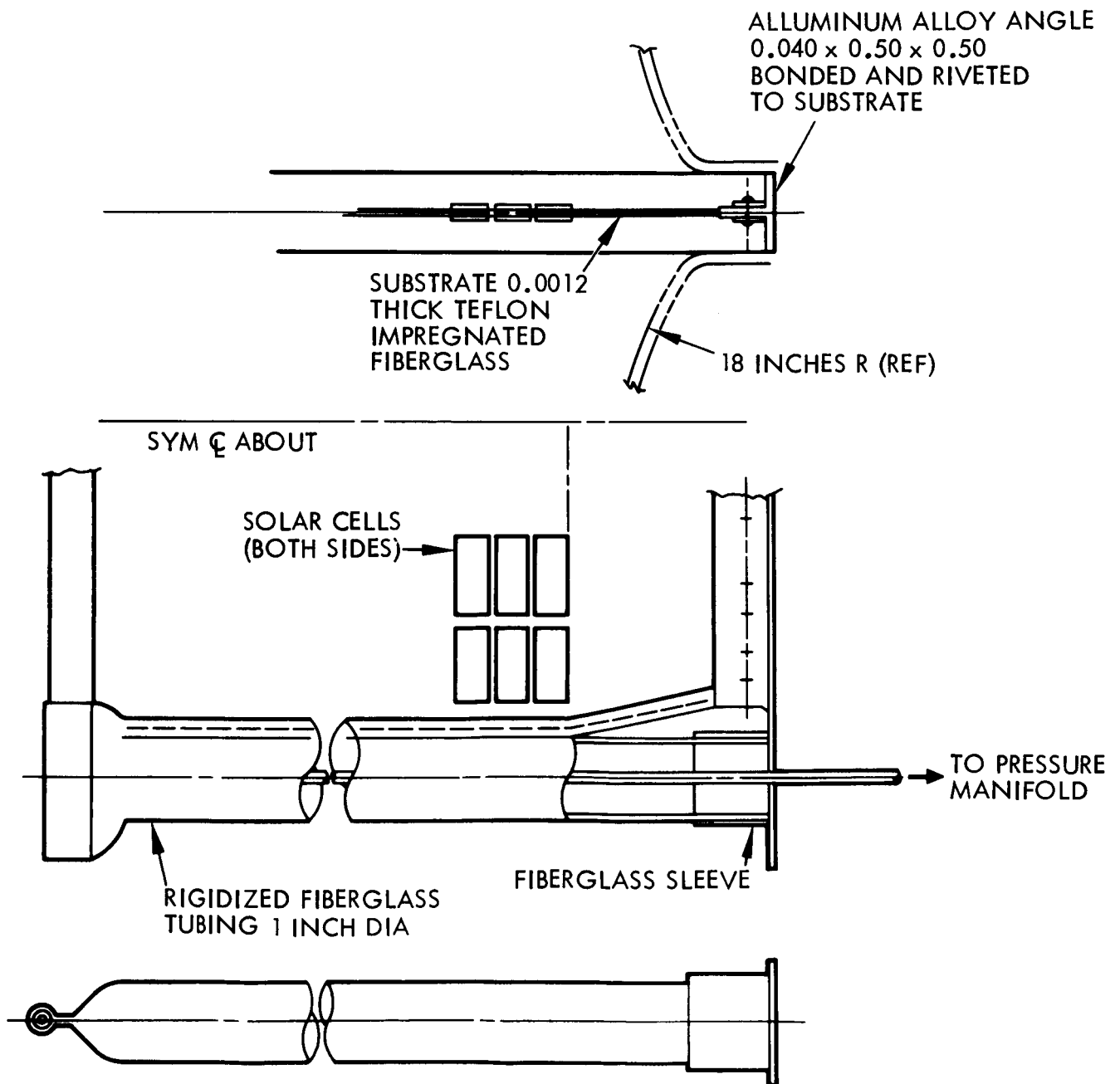
THREE FLEXIBLE PANELS ON 36 INCH DIAMETER (REFERENCE DRAWING NO. X 282024)



LOAD CONDITIONS

- 1) 1-g at environment
60-g at launch
- 2) 160 rpm at spin

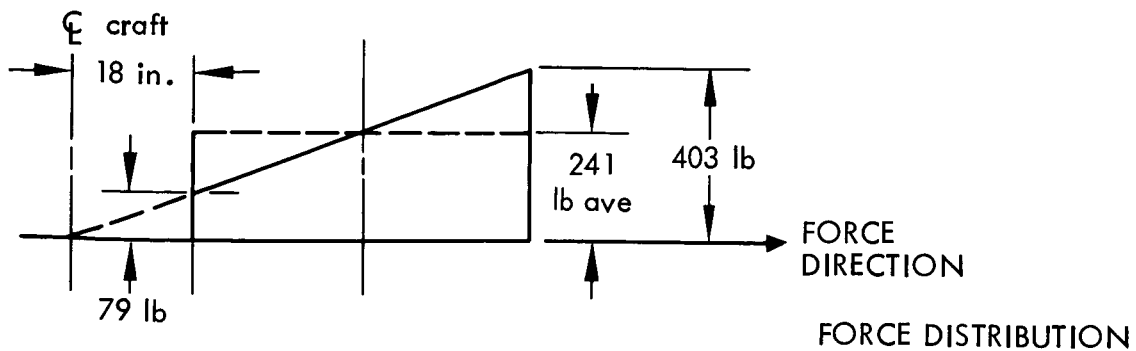
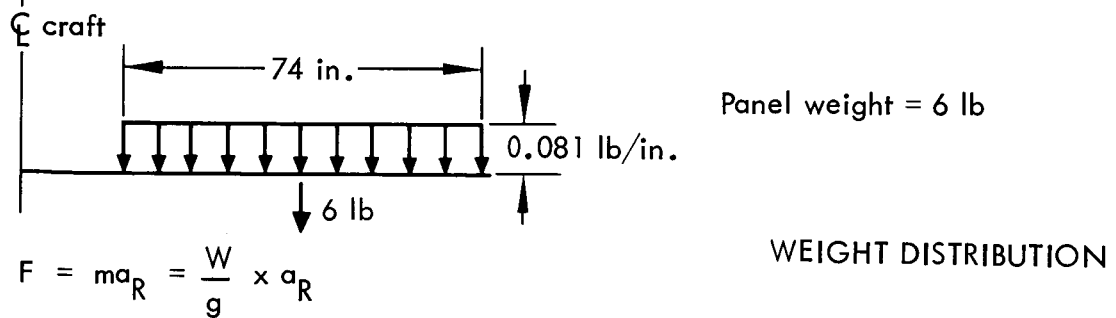
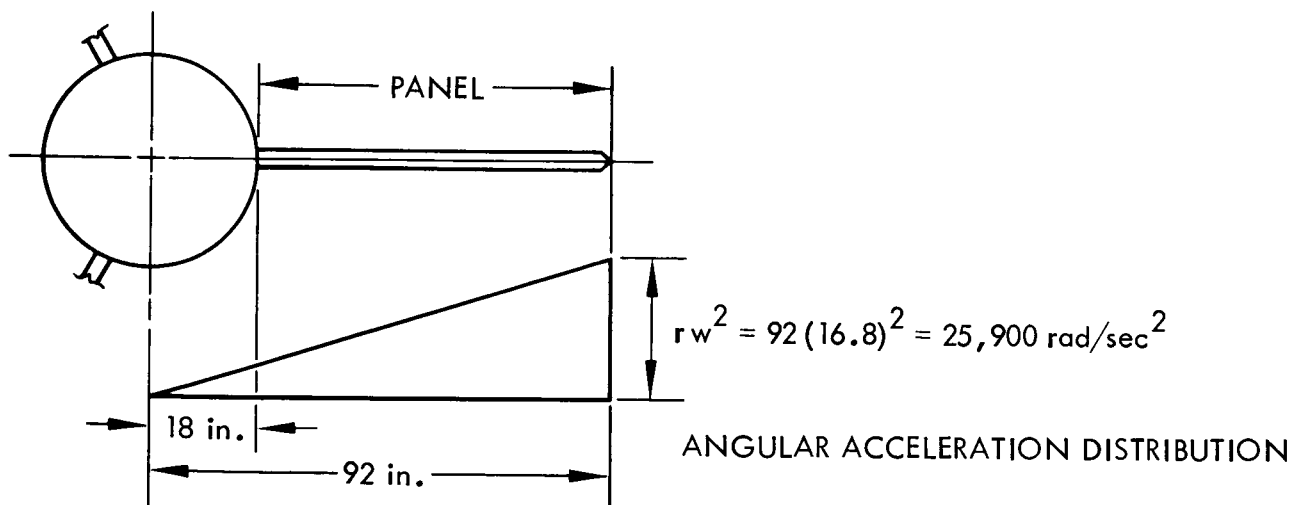
THREE FLEXIBLE PANELS ON 36-INCH DIAMETER



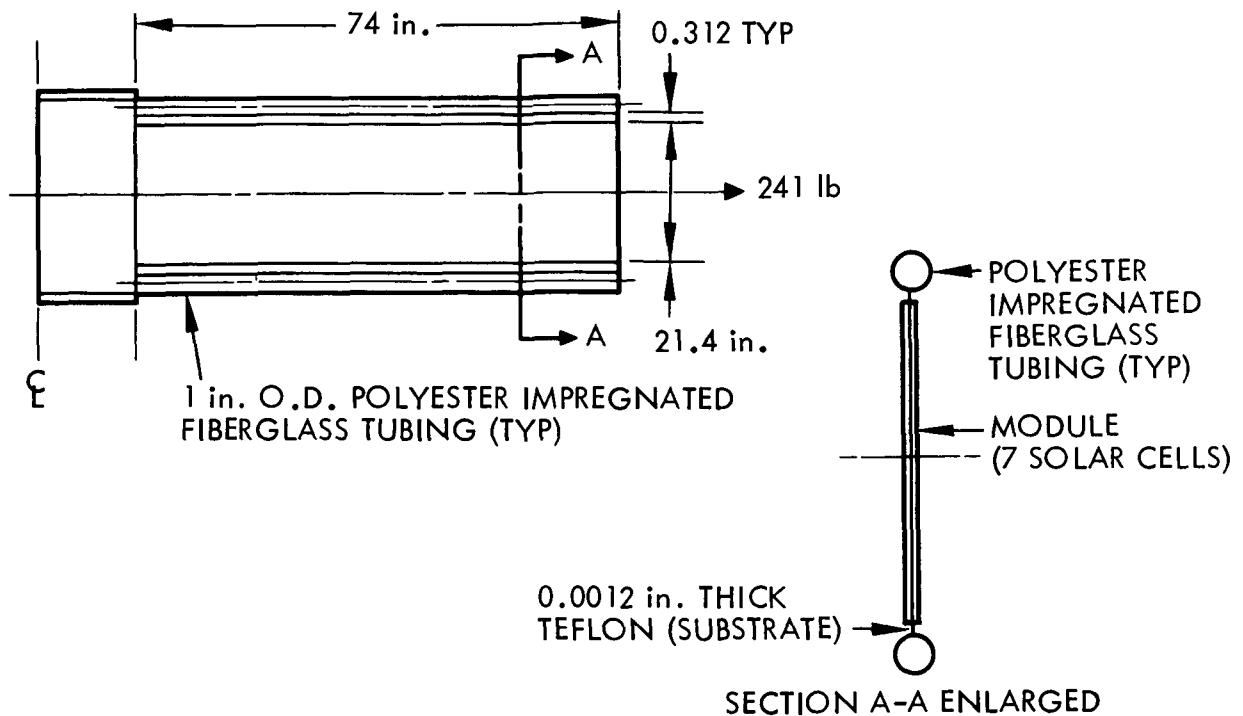
PANEL LOADINGS DUE TO NORMAL OR RADIAL ACCELERATIONS

Angular velocity, $w = 160 \text{ rpm} = \frac{160 \times 2\pi}{60} = 16.8 \text{ rad/sec.}$

The radial acceleration, $A_R = r w^2$ and varies linearly from the axis of rotation of the spacecraft to the tip of the panel.



PANEL-SUBSTRATE



The substrate is in tension

Assuming that the load of 241 pounds is equally resisted by the substrate along its width of 21.4 inches,

$$\text{The running tension load} = \frac{241}{21.4} = 11.25 \text{ lb/in.}$$

$$\text{Tension stress of substrate, } f_t = \frac{11.25}{0.0012} = 9400 \text{ psi}$$

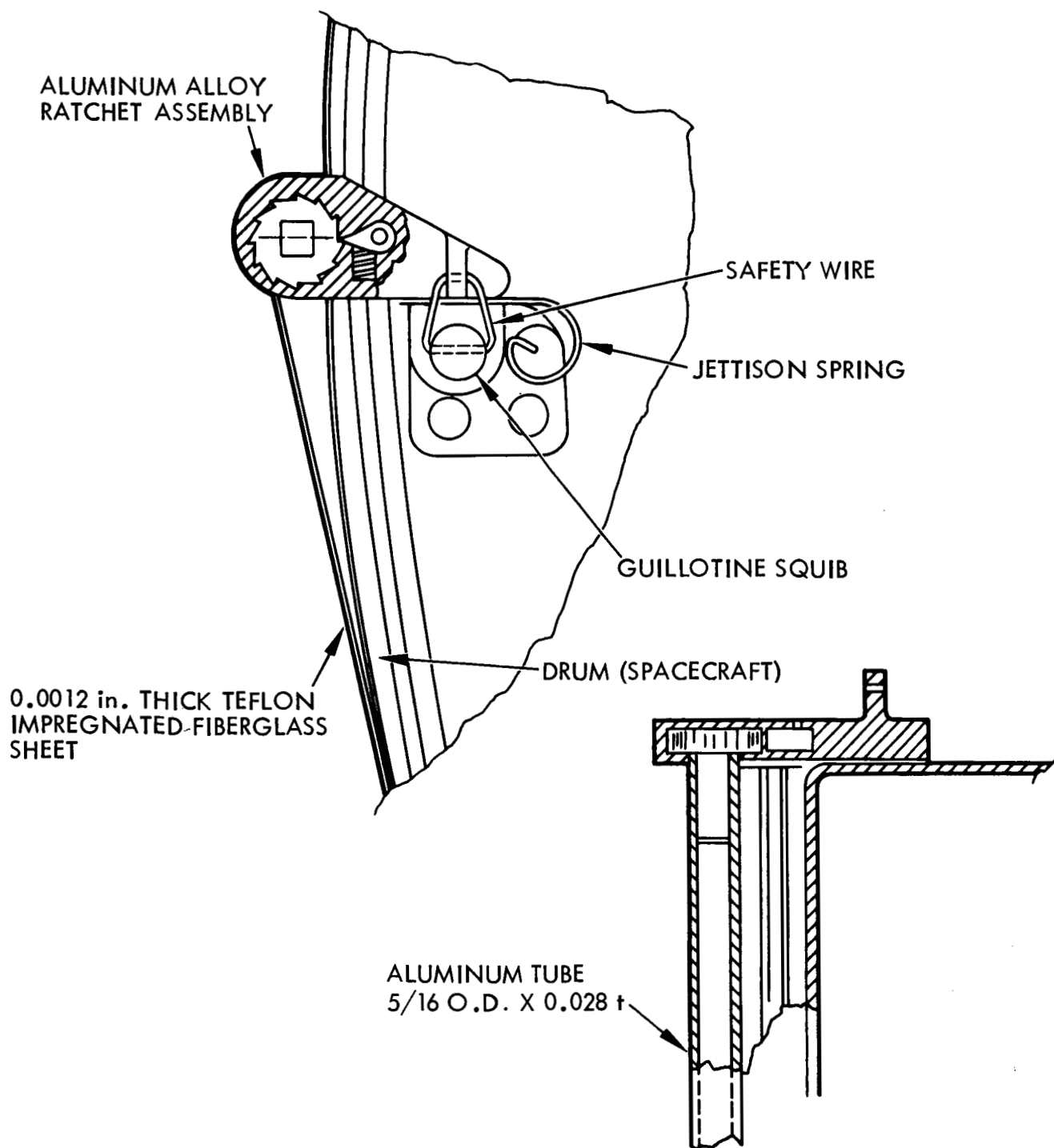
Tension allowable of EX317 TFE on 0.001 in. glass cloth substrate, F_{tu}

$$* F_{tu} = 29.4 \text{ lb/in. at } 300^\circ\text{F unetched (longitudinal)}$$

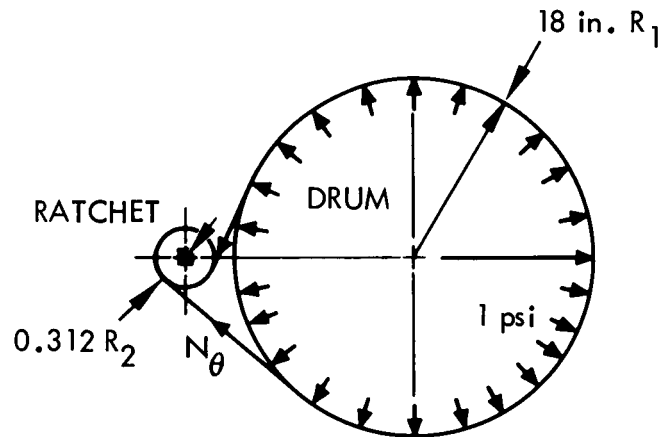
$$(\text{Margin of Safety} = MS = \frac{29.4}{11.25} - 1 = 1.61)$$

* From Table 3-1, Section 3.

RATCHET ASSEMBLY



HOOP RETAINING-SOLAR PANEL



The tension force, N_{θ} , applied on the substrate teflon for an equivalent of 1 psi external pressure applied on the drum is equal to:

$$N_{\theta} = pR = 1 \times 18 = 18 \text{ lb/in.}$$

The total force, F , exerted on a 21.38 inch width of substrate wrapped around the drum is:

$$F = T_x W = 18 (21.38) = 384 \text{ pounds}$$

The torque applied at the ratchet to pull an 18 lb/in. load on the teflon (substrate) is:

$$T = F \times R = 384 (0.3125) = 120 \text{ in.}/\text{lb}$$

Substrate Margin of Safety

$$M S (\text{tension}) = \frac{29.4}{18} - 1 = 0.63$$

TUBE ANALYSIS

In normal operation, centrifugal force loads are carried by the substrate. The following assumes the load to be carried by the rigidized fiberglass tubes.

1 inch diameter $t = 0.015$ Polyester fiberglass

$$A = \pi (1) (0.015) = 0.047 \text{ in.}^2$$

$$f_t = \frac{P}{A} = \frac{241}{2(0.047)} = 2560 \text{ psi}$$

$$*F_{tu} = \frac{1628 \text{ lb}}{0.047} = 34,500 \text{ psi}$$

Margin of Safety

$$MS (\text{tension}) = \frac{34500}{2560} - 1 = 12.5$$

* From Table 3-2, Section 3

APPENDIX B. SOLAR ARRAY THERMAL ANALYSIS

The direct sunlight absorbed by the array is

$$Q_s = S A_p \bar{\alpha}$$

where

S = solar constant, $442 \frac{\text{Btu}}{\text{hr ft}^2}$

A_p = average projected area receiving sunlight, ft^2

$\bar{\alpha} = \alpha_s f + \alpha (1-f)$, array solar absorptivity

α_s = solar cell absorptivity, 0.82

α = absorptivity of the spaces between solar cells, 0.40

f = packing factor, 0.895

The reflected sunlight, or albedo, absorbed by the array is

$$Q_a = F_a A_a S a \bar{\alpha}$$

where

F_a = shape factor for albedo input

A_a = characteristic area of array for earth's albedo, ft^2

a = earth's average reflectivity, 0.40

The earth's infrared radiation input to the array is

$$Q_r = F_r A_r I_e$$

where

F_r = shape factor for infrared input

A_r = characteristic area of array for earth's infrared radiation, ft^2

I = average intensity of earth's infrared radiation, 66.4 Btu/hr ft^2

e = surface emittance or infrared absorptivity of array, 0.82

The total heat input is equal to the heat radiated out to space plus the electrical power output. The transient heat storage term can be neglected for the maximum temperature calculation because steady-state equilibrium is achieved due to the low-heat capacity of the array. The steady-state heat balance is

$$Q_s + Q_a + Q_r = \sigma e A F T^4 + P$$

where

σ = Stefan-Boltzmann constant, $0.171 \cdot 10^{-8} \text{ Btu/hr ft}^2 \text{ } ^\circ\text{R}^4$

A = total array surface, ft^2

F = average array view factor to space

T = array temperature, $^\circ\text{R}$

P = electrical output, (3.41 Btu/w-hr) (watts output)

The electrical output was assumed to be 10 percent of the direct sunlight input. Therefore

$$P = 0.10 Q_s$$

For simplicity in the analysis the following approximations were made:

$$A_p = A_a = A_r \quad \text{and} \quad F_a = F_r = 1.0$$

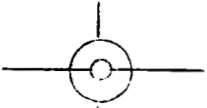
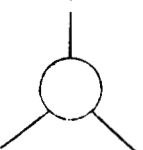
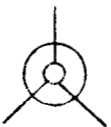
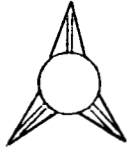

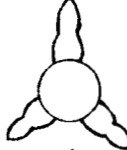
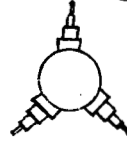
Substituting values into the heat balance equations above gives the array temperature

$$T = 100^\circ\text{R} \left[\frac{3600 A_p}{A F} \right]^{1/4}$$

Scale models of the systems 3 and 4 were used to determine (with a Form Factometer) the values of the average view factor, F , for the radiation out from the surface of the system. The values of F are 0.97 and 0.94 for systems 3 and 4, respectively.

The temperatures for the seven different systems are shown in Table B-1 below.

TABLE B-1. TEMPERATURES FOR SYSTEMS 1 THROUGH 7

System	$\frac{A_p^*}{AF}$	$T = 100^\circ R \left[\frac{3600 A_p}{AF} \right]^{1/4}$
1 	$\frac{17.88}{56.7 (0.94)}$	$590^\circ R = 130^\circ F = 54^\circ C$
2 	$\frac{17.07}{60.8 (0.97)}$	$570^\circ R = 110^\circ F = 43^\circ C$
3 	$\frac{17.07}{60.8 (0.97)}$	$570^\circ R$ same as system 2
4 	$\frac{9.18}{28.2 (0.97)}$	$590^\circ R$ same as system 1
5 	$\frac{16.12}{57.75 (0.97)}$	$568^\circ R = 108^\circ F = 42^\circ C$
6 	$\frac{13.2}{53.7 (0.97)}$	$550^\circ R = 90^\circ F = 32^\circ C$
7 	$\frac{16.35}{58.5 (0.97)}$	$568^\circ R$ same as system 5

*The average values of A_p were calculated graphically for the sunlight direction perpendicular to the spin axis.

APPENDIX C. CALCULATION OF STOWED DIAMETER OF ANY NUMBER OF FLEXIBLE PANELS ROLLED AROUND A CYLINDER

This calculation was originally derived for four panels and then extended to N panels. It is assumed that all the panels have the same total length, L, and thickness (this includes cells, substrate and cushion). These quantities are then defined:

n = number of $1/N$ turns each of the N panels makes when wrapped around the inner cylinder (of radius R_i)

ℓ = length of each $1/N^{\text{th}}$ turn

The total radius at each one-quarter turn (inner cylinder plus layers) as the layers are wrapped and the length of each quarter turn, ℓ , were calculated. These ℓ s are then summed up to equal the total panel length L

$$L = (2nR_i + n^2 \Delta) \pi / N \quad (\text{C-1})$$

Similarly, the total overall radius is found to be

$$R_n = R_i + n \Delta \quad (\text{C-2})$$

Equations C-1 and C-2 are combined to eliminate n, yielding

$$R_n = \left[R_i^2 + NL \Delta / \pi \right]^{1/2} \quad (\text{C-3})$$

and

$$n = \frac{R_n - R_i}{\Delta} \quad (\text{C-4})$$

Equation C-3 is used to determine the outer radius of a stowed, flexible configuration.

EXAMPLE

Three flexible panels $\therefore N = 3$

Inner radius = 18 inches = R_i

Panel length = 74 inches = L

$$\Delta = 0.150 \text{ inch}$$

$$R_n = \sqrt{324 + 10.6} = 18.3 \text{ inches}$$

If the panel width is 22.8 inches, the

$$\text{stowed volume} = \frac{((18.3)^2 - (18)^2) (22.8) \pi}{1728} = 0.438 \text{ ft}^3$$